Interactions of the Antimicrobial Peptide NKCS with the Cytoplasmic Membrane of *Escherichia coli*

Dissertation zur Erlangung des Doktorgrades
der Fakultät für Mathematik, Informatik und Naturwissenschaften
der Universität Hamburg

vorgelegt von
Agnieszka Rzeszutek

2011

Tag der Annahme der Dissertation: 22.03.2011
Tag der Disputation: 29.04.2011

Gutachter der Arbeit :
Prof. Dr. Regine Willumeit
Prof. Dr. Ulrich Hahn

Abstract

The antimicrobial peptides are considered as an alternative for the traditional drugs which have become insufficient in the fight with multidrug resistant pathogens. The main advantage of this class of antibiotics is that they interact directly with the lipids of the cytoplasmic membrane without the exploitation of any receptors.

The peptide NKCS is very active against both Gram-positive and Gram-negative bacteria and does not show toxicity toward human erythrocytes. The mechanism involved in the suppression of bacterial growth was studied using *Escherichia coli* as a model Gram-negative bacterium. The peptide was divided into two parts. The new derivatives, namely NKCS-[K17] and NKCS-[15-27] corresponded to the N-terminal part along with the kink region and the C-terminal fragment, respectively. These three peptides were applied for the biophysical studies. The interactions between the peptides and phosphatidylethanolamine (PE, the main phospholipid constituent of *E. coli* cytoplasmic membrane) were investigated with the Small Angle X-rays Scattering (SAXS) technique. Differential Scanning Calorimetry (DSC) was employed to study the influence of peptides on the phase behavior of the binary lipid system POPE/POPG (7/3). Finally, the secondary structure and the orientation of peptides upon the association with POPE/POPG (7/3) membrane were determined with the Fourier Transform Infrared (FTIR) spectroscopy. Based on the obtained results, the model of interactions between NKCS and the *E. coli* cytoplasmic membrane was built. The peptide displays a high affinity to the negatively charged phosphatidylglycerol (PG). Upon the membrane binding, NKCS induces the migration of PG lipids to the sites of association and the domains of POPG-NKCS and POPE with the remaining PG and peptide are formed. The interactions with the zwitterionic PE are possible. In this case the peptide induces the positive curvature within the membrane, stabilizing the bilayer structure and inhibiting the formation of non-lamellar inverse hexagonal phase. Since this phase is crucial for the cell division process, the inhibition of it prevents the bacterial cells division and growth. NKCS does not adopt a fully transmembrane orientation upon the membrane interactions. Only the N-terminus is embedded into the bilayer at the angle of 30°, whereas the C-terminal fragment stays on the membrane surface, where it can interact with the lipid head groups.

Zusammenfassung

Antimikrobielle Peptide könnten eine Alternative zu herkömmlichen Antibiotika werden, deren Effektivität durch die Ausbildung multiresistenter Keime deutlich herabgesetzt wird. Der Vorteil der antimikrobiellen Peptide liegt im Wirkmechanismus: durch die rezeptor-unabhängige direkte Interaktion mit den Lipiden der Zellmembran ist eine Ausprägung von Resistenzen deutlich schwieriger, wenn nicht gar unmöglich.

Das Peptid NKCS zeigt eine hohe Aktivität sowohl gegen Gram-positive, als auch Gram-negative Bakterien. Darüber hinaus werden humane Erythrocyten nicht angegriffen. *Escherichia coli* wurde als Gram-negativer Modellorganismus genutzt, um den Mechanismus der antibakteriellen Aktivität zu untersuchen. Zwei verkürzte Derivate von NKCS wurden hergestellt: 1. NKCS-[K17], bestehend aus dem N-terminalen Teil und der Knick-Region und 2. NKCS-[15-27] als C-terminales Fragment. Diese drei Peptide wurden in biophysikalischen Experimenten untersucht. Die Interaktion der Peptide mit Phosphatidyl-Ethanolamin (PE) als Hauptbestandteil der Zellmembran von *E. coli* wurde mittels Kleinwinkel-Röntgenstreuung (SAXS) analysiert. Die dynamische Differenzkalorimetrie (DSC) wurde herangezogen, um den Einfluss der Peptide auf das Phasenverhalten im binären Lipidsystem POPE/POPG (7/3) zu untersuchen. Die Sekundärstruktur und die Orientierung der Peptide in Kontakt zur POPE/POPG (7/3) Membran wurde mit Hilfe der Fourier-Transform-Infrarotspektroskopie (FTIR) analysiert. Auf der Grundlage der experimentellen Daten wurde ein Modell entwickelt, das die Wechselwirkung zwischen NKCS und der Zellmembran von *E. coli* beschreibt. Das Peptid zeigt eine hohe Affinität zum negativ geladenen Phosphatidylglycerol (PG). Die Bindung von NKCS induziert eine Relokalisierung der PG-Lipide, was zu einer Domänenbildung führt. Die entstehenden Domänen bestehen aus 1. POPG-NKCS und 2. POPE mit ungebundenem POPG. Das Peptid kann auch mit dem zwitterionischen PE wechselwirken. Dabei wird eine positive Krümmung der Membran induziert, die die Lipiddoppelschicht stabilisiert und den Phasenübergang zur nicht lamellaren inversen hexagonalen Phase verhindert. Diese Phase ist essentiell für den Zellteilungsprozeß, daher können die Bakterien sich nicht mehr vermehren. NKCS ist kein Membran-durchspannendes Peptid. Der N-terminale Bereich dringt in einem Winkel von etwa 30° in die Lipiddoppelschicht ein, wohingegen der C-terminale Bereich auf der Membranoberfläche liegt. Dort ist eine Wechselwirkung mit den Kopfgruppen der Lipide möglich.

Contents

1 Introduction*

1.1 Antimicrobial peptides

The contemporary health care is facing an alarming increase of resistance of pathogenic bacteria to antibiotic therapies [1, 2]. The studies show, that the development of the methicillin and vancomycin resistance in hospitals follows an exponential behavior while on the other hand the number of new antibiotics decreased significantly during the last 20 years [3, 4]. For this reason a worldwide effort is made to acquire potent alternatives for conventional antibiotics. Since nature has always been giving the best solutions, the naturally occurring antimicrobial peptides (AMPs) arose as promising candidates [5-7].

AMPs constitute a component of the innate immune system of all higher organisms [8-11]. They can act as immunomodulators or by direct killing of invading pathogens [12, 13]. Moreover they can be also produced by bacteria to fight other prokaryotes present in the same environmental niche [14]. AMPs were found very active against the broad spectrum of Gram-positive and Gram-negative bacteria, fungi, parasites, viruses and some of them display an activity also against tumor cells [15, 16]. They present various structures and it is very difficult to categorize them only on the basis of their secondary conformation [5, 17]. In general they can be characterized as short (12-50 amino acids), positively charged and

---

* Introduction constitutes a part of the book chapter: A. Rzeszutek, R. Willumeit, Antimicrobial peptides and their interactions with model membranes, in: A. Iglic (Ed.), Advances in Planar Lipid Bilayers and Liposomes, Chapter 6, vol. 12, Academic Press, 2010, pp. 147-165. Reprinted with permission from Elsevier.

amphipathic peptides. The two last features are considered to be crucial for the antimicrobial activity of AMPs.

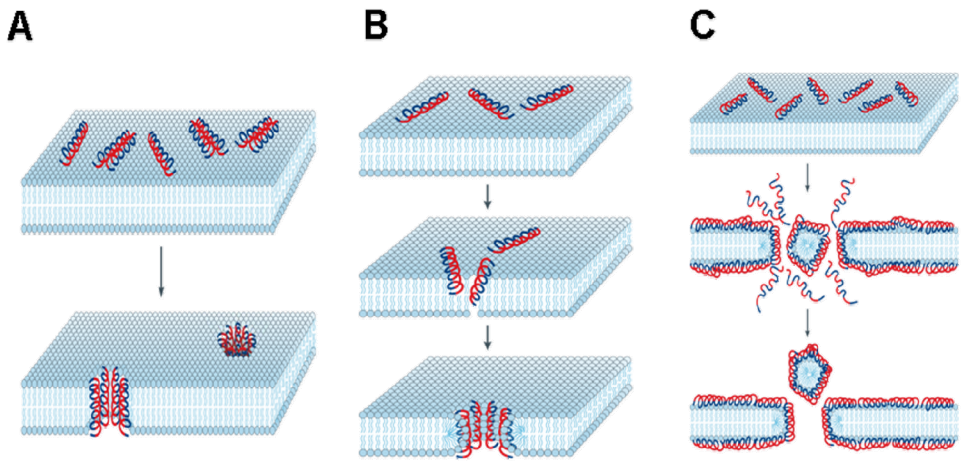

Figure 1.1. The model mechanisms of interactions between antimicrobial peptides and membrane bilayer: (A) barrel stave, (B) toroidal, (C) carpet model. Reprinted from ref. [18], copyright 2005, with permission from Macmillan Publishers Ltd.

Although hundreds of peptides have been identified, the mechanism of action has been deeply investigated only for few of them. Most of AMPs act by direct physical interaction with phospholipids present in a cytoplasmic membrane of pathogens without exploitation of any receptors [19]. The accumulation of peptides on the surface of target bacterial cell occurs via electrostatic interaction between positively charged AMPs and negatively charged residues of lipopolysaccharide in Gram-negative bacteria or teichoic and lipoteichoic acids in Gram-positive bacteria. In Gram-negative microorganisms the peptides pass the outer membrane using the "self-promoted uptake" system and interact with the phospholipids of the cytoplasmic membrane [20]. Several models have been developed to describe these interactions followed by the disruption of lipid bilayer, namely barrel-stave, toroidal pore and carpet models [9, 18] (Fig. 1.1). Upon the peptide-membrane interaction the amphipathic structure of AMPs, where the polar amino acid residues are localized on one side and the hydrophobic residues on the other side of a peptide, is very meaningful. The cytoplasmic

membrane of bacteria is enriched in negatively charged lipids and the peptide-membrane association is possible due to the attractive forces between the anionic lipid head groups and cationic side chains of AMPs. On the other hand, the interaction of peptides with the nonpolar interior of the bilayer is enabled by the hydrophobic side of AMPs. Although the peptide-membrane interactions at a high peptide:lipid molar ratio eventually lead to the membrane lysis, the intracellular activity of AMPs cannot be excluded [18, 21].

Currently several drugs based on AMPs are at the stage of preclinical or clinical studies [22]. Most of them are addressed to the topical applications where they can be used to fight surface infections. The systemic applications are limited due to the complex mechanism of peptides activity. Although the mode of action is thoroughly studied in the case of prokaryotic or simple eukaryotic organisms, the effect of AMPs on the higher organisms can be more complicated. One of the examples is the antimicrobial peptide LL-37 isolated from human cells [23]. LL-37 can translocate through the membrane to the nucleus carrying additionally a passenger molecule [24, 25]. Such behavior indicates that very subtle mechanisms of toxicity related to a systemic application, e.g. induction of apoptosis, should be also considered. Another limitation associated with a systemic application of AMPs is their weak stability in the presence of proteases. To omit this problem several solutions have been suggested: substitution of L-amino acids with D-amino acids, chemical modification of peptides, use of peptidomimetics with nonpeptidic backbones and development of delivery systems (e.g. employment of liposomes) [26].

1.2 Cytoplasmic membrane and phase behavior of lipids

The cytoplasmic membrane plays a very important role as a permeability barrier of a cell. It is composed mainly of lipids and proteins. The mass ratio of these two components can vary from 4:1 to 1:4 in different organisms [27]. The cytoplasmic membrane is a very dynamic and fluid structure. In the famous “fluid mosaic model” presented in 1972 by S. J. Singer and G. Nicolson [28], the membrane was shown as a two-dimensional solution of lipids and proteins. It is important to underline however, that the role of lipids is not limited only to support the proteins, but they are also involved in many biological functions [29, 30].

Table 1.1. The difference in the lipid composition between human red blood cells [31] and the inner membrane of *Escherichia coli* [32] and *Bacillus subtilis* [33]. PC, phosphatidylcholine; SM, sphingomyelin; PE, phosphatidylethanolamine; PS, phosphatidylserine; PI, phosphatidylinositol; PA, phosphatidic acid; PG, phosphatidylglycerol; CL, cardiolipin.

Membrane	**Lipid, %**							
	PC	**SM**	**PE**	**PS**	**PI**	**PA**	**PG**	**CL**
Erythrocyte – outer leaflet	44.8	42.1	11.1	-	-	-	-	-
Erythrocyte – inner leaflet	14.0	9.1	43.9	29.6	1.2	2.2	-	-
E. coli	-	-	69.0	-	-	-	19.0	6.5
B. subtilis	-	-	12.0	-	-	-	70.0	4.0

The various membranes, which can be found in the nature, are characterized by a very divergent lipid composition. Bacterial cells are composed of phosphatidylethanolamine as well as negatively charged phosphatidylglycerol and cardiolipin (Table 1.1). In contrast, human erythrocytes contain a high percentage of zwitterionic phosphatidylcholine, sphingomyelin and phosphatidylethanolamine. Interestingly, the lipid composition varies not only between species, but also between the cells of the same organism or even between different organelles of the same cell [34]. In addition to head groups, there is also a great diversity of hydrocarbon chain composition of lipid membranes. They differ in the length and saturation of acyl chains. Table 1.2 presents the fatty acids of *E. coli* grown at different temperatures. The lipid composition of the cells depends on such variables as temperature, pressure, pH or growth medium composition.

The phospholipids constitute the major class of lipids present in a cytoplasmic membrane. The most interesting feature of these molecules, which also decides about the functionality of membrane, is an ability to adopt different polymorphic structures [35]. Under the physiological conditions the membrane exists in a lamellar liquid crystalline phase (L_α). The phospholipids are organized in a lattice, which is represented by the bilayer with the hydrophobic core (Fig. 1.2). The acyl chains are disordered and fluid. Moreover, there is no order in the lattice and the head groups are randomly organized. Lipids in this state are able to

Table 1.2. The composition of fatty acids of *E. coli* cells cultured at different temperatures [36]. Additionally to the growth temperature, the fatty acid composition depends also on the growth stage and growth medium.

Fatty acid	**%**			
	10°C	**20**°C	**30**°C	**40**°C
Myristic acid (14:0)	4	4	4	8
Palmitic acid (16:0)	18	25	29	48
Palmitoleic acid (16:1)	26	24	23	9
Oleic acid (18:1)	38	34	30	12
Hydroxymyristic acid	13	10	10	8
Ratio of unsaturated to saturated	2.9	2.0	1.6	0.38

rather fast lateral diffusion. The fluidity of the membrane decides about many processes, for example the transport and the activity of enzymes [37, 38]. It depends on the membrane composition and can be regulated by the organisms in the response to the environmental changes. In bacterial cells the viscosity of membrane increases proportionally to the amount of phospholipids with the long and saturated acyl chains. Such phospholipids favor a rigid state in which the hydrocarbon chains interact with each other. Such structure is known as a lamellar gel phase (L_β). In addition to the high order in the hydrophobic core, this phase is

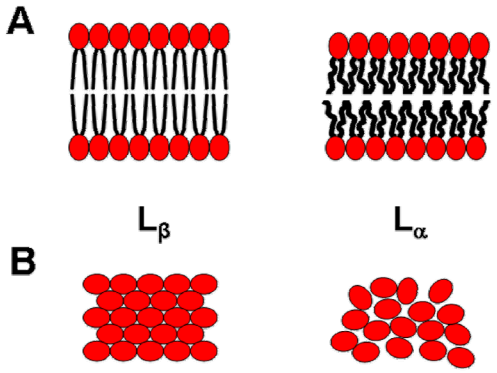

Figure 1.2. The lipid bilayer in a gel (L_β) and liquid crystalline (L_α) phase; view from the side (A) and from the top (B). Reprinted from ref. [39], copyright 2010, with permission from Elsevier.

also characterized by the crystalline order of the head groups, which are arranged in a triangular lattice. In animals the fluidity of membrane is modulated additionally by cholesterol [40, 41]. Although the sterol, namely lanosterol, is present also in the membranes of some prokaryotic organisms, it has very little influence on the membrane fluidity [42-45].

The other two lipid phases, which can be formed within the biological membranes, are non-lamellar structures: inverse hexagonal phase and three-dimensional cubic phases (Fig. 1.3). These forms appear in a very short time scale in living systems, e.g. during the cell division or fusion processes [46]. In the inverse hexagonal phase (H_{II}) lipids form elongated cylindrical structures with the acyl chains directed to the outside [47]. To avoid the contact with water these tubular structures arrange themselves in two-dimensional hexagonal crystals. The cubic phases formed by membrane lipids are mostly bicontinuous, which means that they consist of two coexisting water regions separated by a single lipid bilayer [48]. Although many types of cubic phases have been identified and described, only two of them are relevant for biological systems as they can exist in the excess of water [49]. These phases are

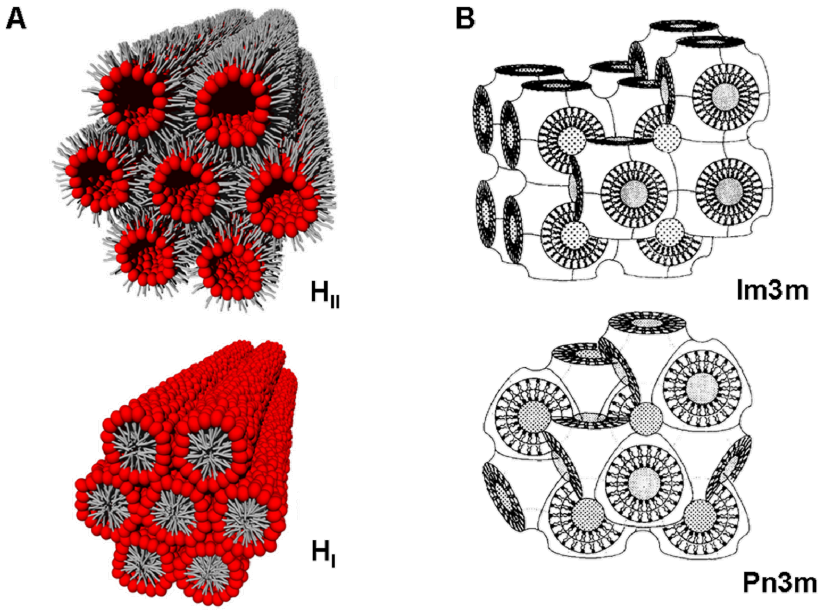

Figure 1.3. Inverse hexagonal (H_{II}) and normal hexagonal (H_I) phases. Reprinted from ref. [47], copyright 2009, with permission. (B) Cubic structures formed in biological systems. Reprinted from [48], copyright 1991, with permission from Elsevier.

characterized by Pn3m and Im3m space groups and are known also as Q^{224} and Q^{227}, respectively [50, 51]. The normal hexagonal phase (H_I) can be formed by the detergents and single chain phospholipids in artificial mixtures, however usually it is not adopted by biologically relevant molecules.

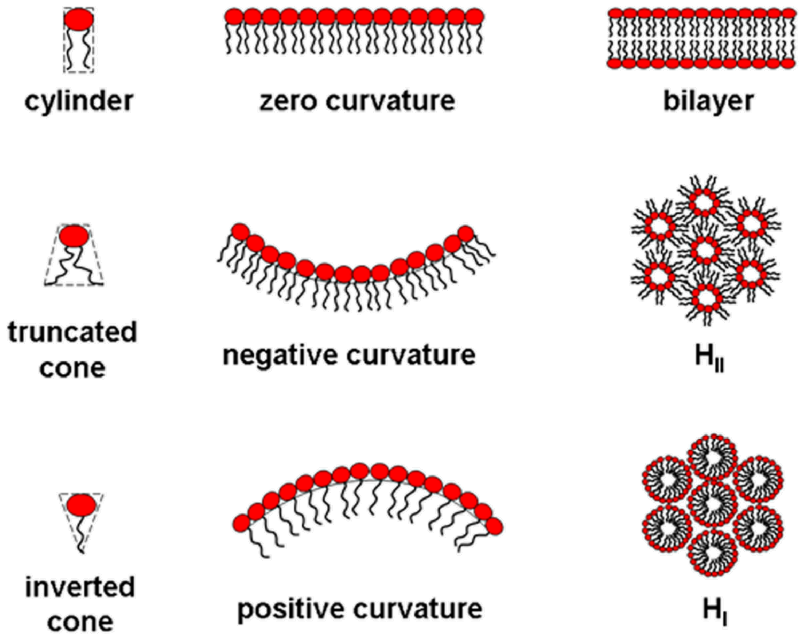

Figure 1.4. The relationship between the molecular shape of lipids and polymorphic structures. Reprinted from ref. [39], copyright 2010, with permission from Elsevier.

The ability of membrane to adopt one of these structures depends strongly on the type of lipids and their molecular shape [52, 53]. When an area occupied by a lipid head group is the same as a cross-sectional area of acyl chains, the lipid can be envisioned as a cylinder (Fig. 1.4). Such lipids favor planar bilayers and stabilize the lamellar phase. This group includes phosphatidylcholine, phosphatidylglycerol, phosphatidylserine, phosphatidylinositol, phosphatidic acid, cardiolipin, sphingomyelin. The lipids with a small head group and much larger area of acyl chains can be shown as a truncated cone. They have a very strong tendency to induce a negative membrane curvature. This feature imposes the formation of non-lamellar

structures: an inverse hexagonal phase, cubic phases or inverted micelles. This class is represented by phosphatidylethanolamine - the most prominent bacterial phospholipid. The third group comprises the molecules resembling an inverted cone – they are characterized by a relatively big head group and a small acyl chain volume. The detergents and single chain lysophospholipids can be assigned here. These molecules favor a positive curvature and tend to form a normal hexagonal phase or micelles. It is important to underline however, that the presentation of lipids in a molecular shape of truncated or inverted cone is an approximation. The lipid molecules are asymmetric with respect to the axis perpendicular to the monolayer surface and consequently can be characterized as anisotropic. The geometry of inverted or truncated cone can be assigned to isotropic molecules, favoring spherical or inverted spherical micellar shapes, respectively. In case of highly anisotropic elongated aggregates, typical for normal or inverted hexagonal phases, the anisotropy of molecules should be taken into account and the lipids should be considered as wedge shaped [54, 55].

The ratio of lamellar and non-lamellar prone lipids in a cytoplasmic membrane is crucial for many processes. It decides about the membrane permeability, transport, cell division and fusion, folding and functionality of membrane proteins [46, 56-59].

Since an activity of antimicrobial peptides requires interactions with a cytoplasmic membrane, the AMPs must influence the structure of phospholipid bilayer. The peptide-membrane association includes the changes in the curvature stress and the formation of non-lamellar phases. This can be directly linked to the mechanism of interactions [60].

The AMPs, upon the binding to the lipid bilayers, very often shift the temperature of the inverse hexagonal phase transition (T_H). The decrease of T_H is correlated with the promotion of a negative curvature, which consists in the bending of the bilayer around the lipid head groups. The peptides which affect the membrane in such a way can be considered as the catalysts of non-lamellar structures. It is suggested that this type of interaction can lead to the creation of transient non-bilayer intermediates and allows for the translocation of a peptide across the membrane, as in the case of polyphemusins [61]. On the other hand, the formation of non-lamellar phases supports the supramolecular reorganization of a bilayer and eventually brings to the perturbation of membrane integrity. The peptides inducing a negative membrane curvature include e.g. alamethicin, which at low concentrations decreases T_H of dioleoylphosphoethanolamine [62], nisin [63] and gramicidin A [64, 65].

The second group of peptides modulating the membrane curvature comprises the AMPs able to shift T_H to higher values. These peptides promote the positive curvature strain within a lipid bilayer and inhibit the formation of non-lamellar structures. The positive curvature leads to building a toroidal pore across the membrane. Such behavior was observed for magainin-2 [66], LL-37 [67], δ-lysin [68]. Very often the high concentrations of AMPs cause the micellarization of a lipid bilayer, which in fact can be considered as an extreme example of a positive curvature [60, 69].

1.3 NK-lysin, NK-2 and NKCS

NK-lysin is a polypeptide isolated from natural killer [46] cells found in a porcine small intestine [70]. It belongs to the family of SAPOSIN-like proteins (SAPLIPs), which comprise structurally conserved, but functionally diverse group of small (8 - 9 Da) polypeptides [71, 72]. NK-lysin displays a cytotoxic and antimicrobial activity – it kills the cells involving the lytic mode of action. It is composed of 78 amino acids organized in five α-helices [73]. The detailed studies of structure-function dependence revealed that the membranolytic activity can be caused in particular by the third and forth α-helices. This fragment, embracing 27 amino acids (39 – 65 residues of NK-lysin), was synthesized with three substitutions and named NK-2 [74].

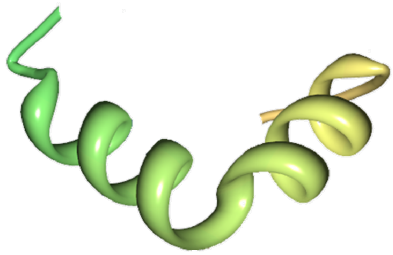

Figure 1.5. Structure model of peptide NK-2 extracted from the NMR structure of NK-lysin deposited at the PDB (1NKL). Reprinted from ref. [39], copyright 2010, with permission from Elsevier.

NK-2 exhibits a very good activity against Gram-positive and Gram-negative bacteria, pathologic fungus *Candida albicans*, protozoan parasite *Trypanosoma cruzi* and malaria parasite *Plasmodium falciparum* [74-76]. The studies revealed that NK-2 selectively kills several cancer cell lines [77]. Moreover, the peptide is non-toxic toward human cells, what makes it a good candidate for therapeutic applications [74, 77, 78]. NK-2 is randomly coiled in aqueous solutions, but adopts amphipathic α-helical structure in a hydrophobic environment [74]. The 3D structure of NK-lysin region corresponding to NK-2 allows to assume that the peptide does not resemble a rigid α-helical rod, but rather presents a helix-hinge-helix fold [78] (Fig. 1.5).

NKCS is an analog of NK-2, derived by the substitution of cysteine at the position 7 by serine [79]. This modification was dedicated to enhance the stability of the peptide. The presence of thiol group in cysteine was connected with the high susceptibility to an oxidation and formation of disulfide bridges. NK-2 dimers were found as a result of peptide aging and appeared inactive (detected by mass spectrometry, [80]). The amino acid serine was chosen to keep the same net charge (+10), to minimize possible conformational changes and to maintain the hydrophobicity of the peptide. NKCS displays an activity comparable to NK-2 – it is very active against Gram-positive and Gram-negative bacteria and does not display toxic activity against human cells [79, 81].

2 Scope of the work

The main objective of this work was to solve the mechanism involved in the inhibition of the growth of *Escherichia coli*, caused by an antibiotic peptide NKCS. The presented work comprises:

1. Determination of general antibacterial activity of NKCS and its derivatives against Gram-positive (*Bacillus subtilis*, *Staphylococcus carnosus*) and Gram-negative (*Escherichia coli*) strains of bacteria.

2. Analysis of peptides amphipathicity.

3. Investigation of toxicity of NKCS-derived peptides toward human erythrocytes.

4. Studies of the interactions of NKCS and its two derivatives NKCS-[K17] and NKCS-[15-27], representing respectively the N- and C-terminal fragments of the parental peptide, with the artificial systems mimicking the cytoplasmic membrane of *E. coli*:
   - Interactions with single lipid membranes comprising three phosphatidylethanolamine lipids with different acyl chains (POPE, DiPoPE and DOPE-trans).
   - Interactions with lipid mixture directly reflecting *E. coli* membrane composition (POPE and POPG at the molar ratio 7:3).

5. Determination of the secondary structure and orientation of NKCS upon interactions with POPE/POPG (7/3) bilayers.

6. The proposed mode of action.

3 Materials and Methods

3.1 Reagents and solutions

3.1.1. Chemicals

BD BBL™ Agar, Grade A	Becton Dickinson, Heidelberg, Germany
BD BBL™ Trypticase™ Soy Broth	Becton Dickinson, Heidelberg, Germany
BD Bacto™ Peptone	Becton Dickinson, Heidelberg, Germany
BD Bacto™ Tryptone	Becton Dickinson, Heidelberg, Germany
BD Bacto™ Yeast Extract	Becton Dickinson, Heidelberg, Germany
BD Difco™ Casein Digest	Becton Dickinson, Heidelberg, Germany
Chloroform	Merck, Darmstadt, Germany
Disodium hydrogen phosphate (Na_2HPO_4)	Sigma Aldrich, Schnelldorf, Germany
Glucose	Sigma Aldrich, Schnelldorf, Germany
Meat extract	Merck, Darmstadt, Germany
Methanol	Merck, Darmstadt, Germany
Morpholinoethanesulphonic acid (MES)	Merck, Darmstadt, Germany
Potassium chloride (KCl)	Merck, Darmstadt, Germany
Sodium chloride (NaCl)	Merck, Darmstadt, Germany
Sodium dihydrogen phosphate (NaH_2PO_4)	Merck, Darmstadt, Germany

All used reagents were analytical grade chemicals.

3.1.2. Buffers

Morpholinoethanesulphonic buffer (MES)

- 4.3 g of morpholinoethanesulphonic acid
- 8.2 g of NaCl
- add 1 L of double distilled H_2O
- pH 5.5

Phosphate buffered saline (PBS)

- 8 g of NaCl
- 0.2 g of KCl
- 1.44 g of Na_2HPO_4
- add 1 L of double distilled H_2O
- pH 7.4

Sodium phosphate buffer (NaP)

- 10 mM Na_2HPO_4
- 10 mM NaH_2PO_4
- the final buffer was obtained by mixing both solutions in a ratio giving pH 7.0

MES and PBS were sterilized in an autoclave for 25 minutes at 121°C.

3.2 Peptides

The peptide NKCS and all its derivatives were synthesized with amidated C-terminus by Biosyntan, Berlin, Germany. The purity of 95% was guaranteed by analytical RP-HPLC (Lichrospher 100 RP 18, 5 μm columns, Merck, Darmstadt, Germany) and MALDI-TOF (Bruker Daltonik GmbH, Bremen, Germany) performed by the company.

Melittin was obtained from Sigma Aldrich, Schnelldorf, Germany.

The peptides were stored at -20°C. Directly before an experiment they were dissolved in double distilled water to the final concentration of 1 mM. The solutions were stored at -20°C between measurements.

3.3 Lipids

Phospholipids POPE, DiPoPE, DOPE-trans and POPG were purchased from Avanti Polar Lipids, Alabaster, USA. They were stored airtight at -20°C.

The most important physicochemical properties of lipids used for the experiments are presented in Table 3.1 [82-86].

3.3.1. Multilamellar Vesicles (MLV)

Phospholipids POPE, DiPOPE, DOPE-trans and POPG were dissolved in chloroform/methanol (4/1, v/v). POPE and POPG were mixed to obtain the final molar ratio 7:3. The organic solvent was removed by a constant nitrogen stream and the resulting lipid film was dried overnight in vacuum at 40°C. Shortly before the experiments, the lipid films were hydrated with sodium phosphate buffer (10 mM, pH 7.0) and incubated for 2 hours. The temperature of incubation was chosen individually for each lipid following the rule that it should be higher than the temperature of acyl chain melting. According to this principle POPE, DiPOPE, and POPE/POPG (7/3) were incubated at 30°C, whereas DOPE-trans at 40°C. During the incubation the lipid suspensions were vortexed every 30 minutes for 1 min. The samples were cooled down to the room temperature and equilibrated for 30 minutes. This procedure resulted in the formation of multilamellar vesicles (MLV).

Table 3.1. The physicochemical features of lipids used in this work.

	Name	Acyl chain composition	MW (Da)	Phase transition	T (°C)	Buffer	Ref.
POPE	1-palmitoyl-2-oleoyl-sn-glycero-3-phosphoethanolamine	16:0-18:1	718.0	$L_\beta \rightarrow L_\alpha$	25.1	10 mM NaP, pH 7.4	[86]
				$L_\alpha \rightarrow H_{II}$	66.4	10 mM NaP, pH 7.4	[86]
DiPoPE	1,2-dipalmitoleoyl-sn-glycero-3-phosphoethanolamine	16:1-16:1	687.9	$L_\beta \rightarrow L_\alpha$	-33.5	40 mM Tris-acetate/ ethyleneglycol, 1:1 v/v, 0.1 M NaCl, pH 7.0	[84]
				$L_\alpha \rightarrow H_{II}$	43.2	20 mM PIPES, 1 mM EDTA, 0.15 M NaCl, 0.02 mg/mL NaN_3, pH 7.4	[82]
DOPE-trans	1,2-dielaidoyl-sn-glycero-3-phosphoethanolamine	18:1-18:1	744.0	$L_\beta \rightarrow L_\alpha$	36.1	10 mM HEPES, pH 7.4	[83]
				$L_\alpha \rightarrow H_{II}$	61.8	10 mM HEPES, pH 7.4	[83]
POPG	1-palmitoyl-2-oleoyl-sn-glycero-3-phospho-rac-(1-glycerol) ammonium salt	18:1-18:1	771.0	$L_\beta \rightarrow L_\alpha$	1.0	50 mM PIPES, 1 mM EDTA, 0.1 M NaCl, 0.1% NaN_3, pH 7.0	[85]
				$L_\alpha \rightarrow H_{II}$	-	-	-

3.3.2. Large Unilamellar Vesicles (LUV)

Large unilamellar vesicles were formed directly from multilamellar vesicles. Aqueous suspensions of POPE/POPG liposomes were prepared as described above with a final phospholipid concentration of 6.5 mM. To obtain homogenous LUVs the dispersion was passed 19 times through a polycarbonate membrane with 100 nm pores using a liposome mini-extruder (Avanti Polar Lipids, Alabaster, USA).

3.4 Bacteria

Bacteria were purchased from Deutsche Sammlung von Mikroorganismen und Zellkulturen GmbH (DSMZ), Braunschweig, Germany:

- *Escherichia coli* K12 (ATCC 23716)
- *Bacillus subtilis* (ATCC 6051)
- *Staphylococcus carnosus* (ATCC 51365)

3.4.1. Bacterial media

Luria–Bertani medium for *E. coli*

- 10 g of NaCl
- 10 g of BD Bacto™ Tryptone
- 5 g of BD Bacto™ Yeast Extract
- add 1 L of double distilled H_2O
- pH 7.4

Nutrient broth for *B. subtilis*

- 5 g of BD Bacto™ Peptone
- 3 g of Meat Extract
- add 1 L of double distilled H_2O

- pH 7.0

Corynebacterium medium for *S. carnosus*

- 10 g of BD Difco™ Casein Digest
- 5 g of BD Bacto™ Yeast Extract
- 5 g of glucose
- 5 g of NaCl
- add 1 L of double distilled H_2O
- pH 7.3

Agar plates were prepared by adding 15 g of BD BBL™ Agar to 1 L of proper medium directly before sterilization.

The liquid media were autoclaved immediately after the preparation for 25 minutes at 121°C.

3.4.2. Cultivation of bacteria

E. coli, S. carnosus and *B. subtilis* were stored on the agar plates at 4°C. Before an experiment one single colony was transferred from each plate to the proper liquid medium (4 mL). The bacteria were grown overnight at 37°C. The next day 15 mL of proper medium was inoculated with 50 μL of the overnight culture. The bacteria were cultivated at 37°C with shaking at 160 rpm. The growth of strains was followed by measuring the optical density at 600 nm (Spectrophotometer Helios, Thermo Scientific, Dreieich, Germany). Bacteria in the logarithmic phase of growth ($OD_{600} \approx 0.1\text{-}0.2 \approx 2.5\times10^7$ CFU/mL), were used for the antibacterial assay. 10 μL of cell suspension were added do 25 mL of fresh medium, giving the concentration of 10^4 CFU/mL.

3.4.3. Antibacterial assay

The antibacterial activity of peptides was determined using the microdilution method. The stock solutions of peptides (1 mM) were diluted with double distilled H_2O to obtain the final concentrations: 10 μM, 5 μM, 2.5 μM, 1.25 μM, 0.62 μM, 0.31 μM, 0.16 μM, 0.08 μM. The bacteria were cultivated until the logarithmic phase of growth. The aliquots of diluted cell suspension (10 μL containing 100 CFU/mL) were added to microtiter plate wells containing 90 μL of peptide solution. The plates were incubated for 18 hours at 37°C and the optical density was measured at 620 nm with a microplate reader (Tecan, Crailsheim, Germany). The minimal inhibitory concentration (MIC) was defined as the lowest concentration of peptide resulting in the suppression of at least 90% of the bacterial growth.

3.5 Hemolytic test

The fresh blood (maximum storage time was two days) was centrifuged for three minutes at 2000 rpm and the supernatant was discarded. The pellet was washed with PBS three times. Erythrocytes were resuspended and diluted in MES buffer until 20 μL of this suspension added to 980 μL of double distilled H_2O gave the absorbance of 1.4 at the wavelength of 412 nm, which was equal to 5×10^8 cells per mL. The peptides were diluted in MES buffer to obtain the desired concentrations. Subsequently 20 μL of erythrocytes suspension was added to 80 μL of peptide solution. As controls, erythrocytes were mixed with MES buffer to determine a spontaneous lysis and double distilled water to determine a maximal lysis. After 30 minutes of incubation at 37°C samples were transferred to the ice bath and MES buffer (900 μL) was added. The specimens were centrifuged (10 minutes, 4°C, 2000 rpm) and the absorbance of released hemoglobin was measured at 412 nm (Spectrophotometer Genesys, Thermo Scientific, Dreieich, Germany). The percentage of lysis was calculated on the basis of Eq. 1:

$$\%Lysis = \frac{(A_{sample} - A_{MES})}{(A_{water} - A_{MES})} \times 100 \quad (1)$$

where A_{sample}, A_{MES} and A_{water} is the absorbance measured for a sample, MES buffer and water, respectively.

3.6 Techniques

3.6.1. Small Angle X-rays Scattering (SAXS)

Small Angle X-rays Scattering is a technique in which X-rays are used as a probe to investigate the structural details of materials varying from metals, oils, surfactants, polymers to biological samples like lipids and proteins. The method is based on a scattering of X-rays which provides a pattern recorded on the detector. This pattern can be subsequently correlated with a molecular structure. The experiments described in this work are based on an elastic scattering. In such scattering the propagation of scattered photon is changed whereas its energy is conserved. In an inelastic scattering incident and scattered photons have different energies. The phenomenon of inelastic scattering will not be considered here.

X-rays are electromagnetic waves with the wavelength (λ) between 0.01 and 1 nm. They can be produced in a laboratory using an X-rays tube or in a synchrotron – a large scale radiation facility providing high X-rays flux. Since the wavelength values are in the same range of magnitude as the size of atoms and interatomic distances in molecules, the X-rays are a perfect probe to study the structure of matter. SAXS technique yields the information on such parameters as the shape and size of macromolecules and characteristic distances of partially ordered materials. Moreover, it delivers a description of intermolecular interactions in biological systems, including assembling and large-scale conformational changes.

The samples for SAXS measurements can be solid or liquid. The biological macromolecules are usually dispersed in aqueous solution. The sample is exposed to a monochromatic X-rays beam. Some of the photons are scattered by the particles, whereas

most of them go through the sample without interacting with it. Scattered photons are registered by a detector. Typically it is a two-dimensional CCD camera localized behind the sample with the screen perpendicular to the primary beam. To avoid the damage of the detector, a beam stop is installed to absorb a very intensive primary beam. Since the biological samples are usually diluted and scatter weakly, they must be measured with a highly intensive X-rays beam provided at a synchrotron. Moreover the beam must be collimated, due to the fact that the measurements are performed at small angles, which is very close to the primary beam. The setup of a SAXS beamline is shown in Fig. 3.1.

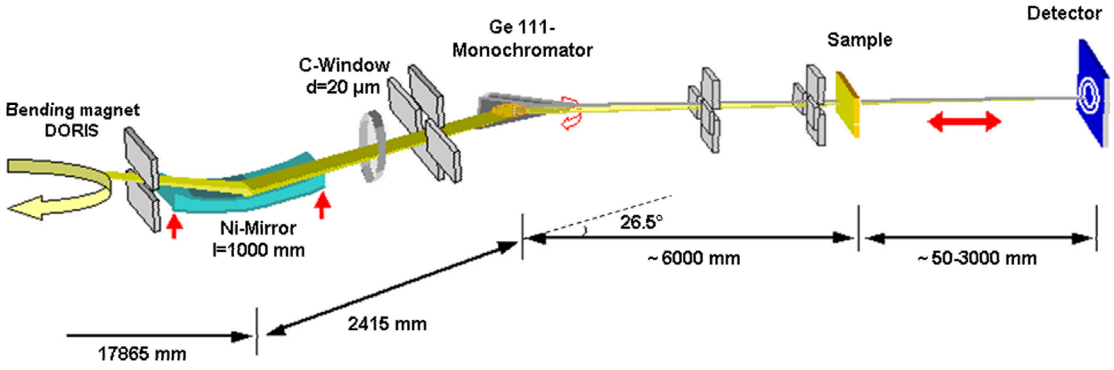

Figure 3.1. The setup of SAXS beamline A2 at DESY in Hamburg.

3.6.1.1. Scattering from two-dimensional (2D) crystals

The principle of scattering from a 2D lattice is based on Bragg's law (Fig. 3.2). The waves of X-rays, scattered by atoms organized in lattice planes, can interfere with each other constructively or destructively. The constructive interference occurs when the overlapping scattered waves add together to produce stronger diffraction peak. The interference is constructive only when a phase shift is a multiple of 2π. This condition is expressed as Bragg's law:

$$n\lambda = 2d\sin\theta \tag{2}$$

where n is an integer determining an order of reflection, λ is a wavelength, d is a distance between crystallographic planes and θ is a scattering angle, defined as an angle between the incident beam and the scattering planes.

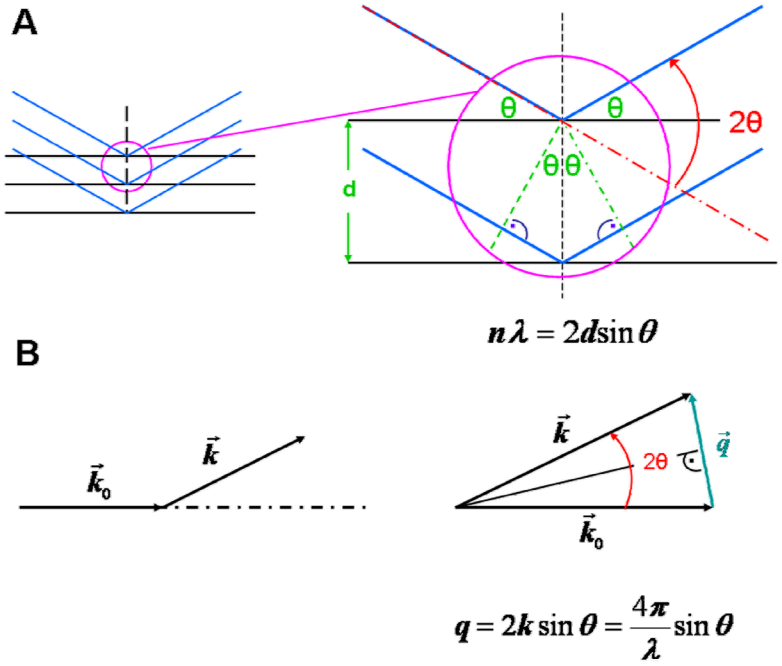

Figure 3.2. (A) Depiction of Bragg's law. X-rays hit the planes of atoms separated by distance d. Both the incoming and scattered beams make an angle θ with respect to the planes of atoms. In case of multilayer lipid vesicles, d corresponds to a thickness of hydrated lipid bilayer. (B) Schematic representation of the scattering vector $\vec{q}$.

When the X-rays strike an atom, they change the direction and/or the velocity, which means that there is a change in momentum. The momentum change can be described by a momentum transfer vector, or a scattering vector, $\vec{q}$. The scattering vector is defined as the vector difference between incoming ($\vec{k}_0$) and scattered ($\vec{k}$) wave vectors:

$$\vec{q} = \vec{k}_0 - \vec{k} \,. \tag{3}$$

From trigonometric dependence shown in Fig. 3.2 B the value of q can be derived:

$$q = 2k \sin\theta \,. \tag{4}$$

Since $k = \frac{2\pi}{\lambda}$, q can be expressed also as:

$$q = \frac{4\pi}{\lambda} \sin\theta \,. \tag{5}$$

Combining Eq. 2 (assuming that n = 1) and Eq. 5, the simple dependence between q and lattice spacing can be obtained:

$$q = \frac{2\pi}{d} \,. \tag{6}$$

Very often the scattering vector is expressed as $\vec{s}$, where

$$s = \frac{q}{2\pi} \,. \tag{7}$$

3.6.1.2. Identification of the structure

SAXS technique can be used to solve the supramolecular structures of partially ordered systems like these adopted by lipid molecules in aqueous environment. The analysis of X-rays spectra is performed by the identification of spacing ratios of recorded Bragg reflections [51]. These ratios can be subsequently assigned to defined three dimensional structures, i.e. lamellar, inverse hexagonal and cubic (Table 3.2).

Table 3.2: Reflections characterizing lamellar, inverse hexagonal and cubic phases represented as the spacing ratios of the lamellar repeat distance (d_l), basic hexagonal periodicity (d_{10}) and fundamental cubic periodicity (d_Q).

Phase		Spacing ratios of reflections
Lamellar	L	1, 1/2, 1/3, 1/4, 1/5, 1/6, etc.
Inverse hexagonal	H_{II}	1, 1/√3, 1/√4, 1/√7, 1/√9, 1/√12, etc.
Cubic	Q^{212}	1, 1/√2, 1/√3, 1/√5, 1/√6, 1/√8, 1/√9, 1/√10, etc.
Cubic	Q^{223}	1, 1/√2, 1/√4, 1/√5, 1/√6, 1/√8, 1/√10, 1/√12, etc.
Cubic	Q^{224}	1, 1/√2, 1/√3, 1/√4, 1/√6, 1/√8, 1/√9, 1/√10, 1/√11, 1/√12, etc.
Cubic	Q^{229}	1, 1/√2, 1/√4, 1/√6, 1/√8, 1/√10, 1/√12, etc.
Cubic	Q^{230}	1, 1/√6, 1/√8, 1/√14, 1/√16, 1/√20, 1/√22, 1/√24, etc.

3.6.1.3. Experimental procedure

SAXS experiments were performed at Soft Condensed Matter Beamline A2 at DESY in Hamburg. For the measurements multilamellar vesicles (MLV) were used (the method of preparation is described in the section 3.3.1). The final concentration of lipids in sodium phosphate buffer was 25 mg/mL. The peptides were added at lipid:peptide molar ratio 100:1 or 300:1. 40 μL of lipid suspension or lipid:peptide mixture were transferred to a glass capillary with a diameter of 1 mm and the capillary was sealed. The measurements were performed in a temperature controlled sample holder, with a rate of 1°C/min. The used range of temperature was chosen individually for each lipid and applied as follows: POPE 20°C - 85°C, DiPoPE 30°C - 70°C and DOPE-trans 30°C - 75°C.

The calibration of the instrument was done measuring rat tail tendon or silver behenate ($CH_3(CH_2)_2OCOO$-Ag). Knowing the order of reflections, the channel number and the repeat distances (d) (nm), the channels were converted into s-values ($s = 1/d$) (nm^{-1}) (Fig. 3.3. and 3.4, Tables 3.3. and 3.4).

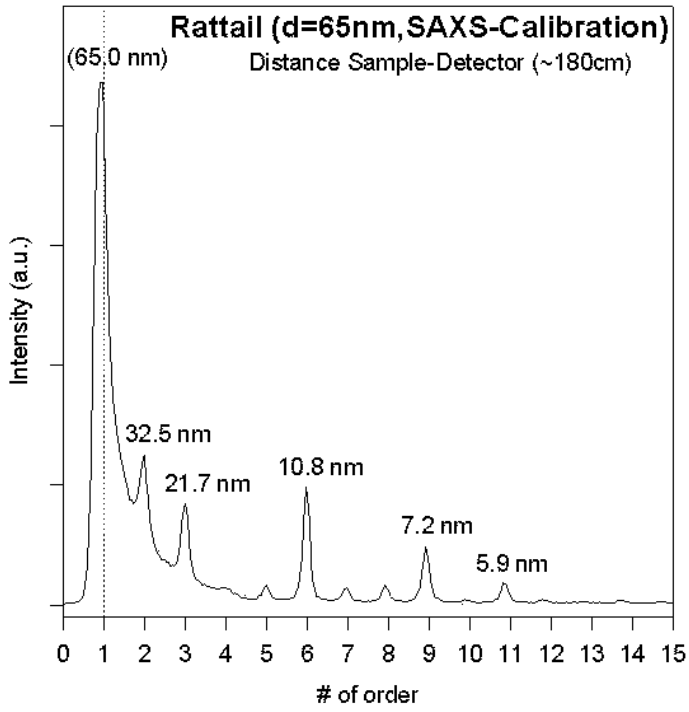

Figure 3.3. SAXS pattern of rat tail tendon (RTT). Source: http://hasylab.desy.de/facilities/doris_iii/beamlines/a2/calibration.

Table 3.3: 2θ, s values and d spacings of the reflections of RTT; (s) strong reflections; (w) weak reflections. Source: http://hasylab.desy.de/facilities/doris_iii/beamlines/a2/calibration.

Order of the reflection	**2θ (for $\lambda = 0.15$ nm)**	**$s = 1/d$ (nm^{-1})**	**d (nm)**
1	0.1322	0.0154	65.0 (s)
2	0.2644	0.0308	32.5 (s)
3	0.3960	0.0462	21.7 (s)
4	0.5272	0.0616	16.3 (w)
5	0.6612	0.0770	13.0 (w)
6	0.7958	0.0924	10.8 (s)
7	0.9242	0.1078	9.3 (w)
8	1.0482	0.1232	8.2 (w)
9	1.1936	0.1386	7.2 (s)
10	1.3222	0.1540	6.5 (w)
11	1.4568	0.1694	5.9 (s)

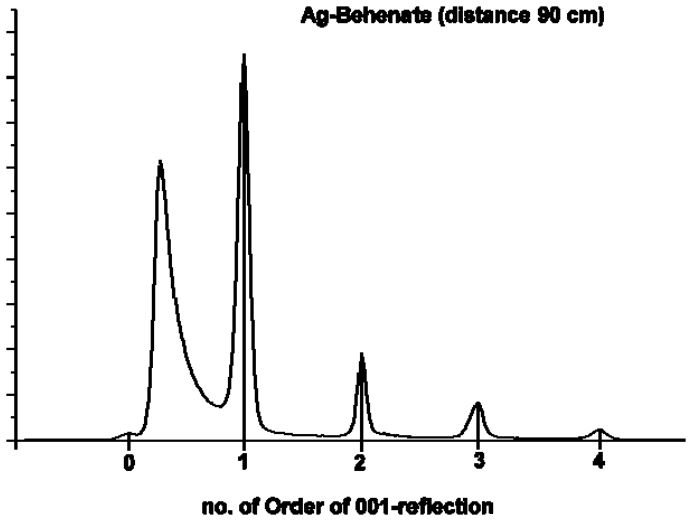

Figure 3.4. SAXS pattern of silver behenate. Source: http://hasylab.desy.de/facilities/doris_iii/beamlines/a2/calibration.

Table 3.4: 2θ, s values and d spacings of the reflections of silver behenate. Source: http://hasylab.desy.de/facilities/doris_iii/beamlines/a2/calibration.

Index of the reflection	**2θ (for λ = 0.15 nm)**	**$s = 1/d$ (nm^{-1})**	**d (nm)**
001	1.4723	0.1713	5.838
002	2.9456	0.3426	2.919
003	4.3847	0.5097	1.962
004	5.8970	0.6849	1.460
005	7.3786	0.8562	1.168
006	8.8682	1.0278	0.973

The raw data were collected as 2D pictures recorded by the detector. With the known sample-detector distance (obtained from the calibration), size of pixels and X-rays wavelength, the data were integrated with program Fit2D, developed at European Synchrotron Research Facility (ESRF) in Grenoble. This program allows for the conversion of 2D pictures into text files containing the information about the recorded intensity and q

values. Further analysis was performed with Origin software. After the background subtraction, the scattering patterns were plotted as *s* values against temperature against intensity. The information on the repeat distance (*d*) was derived from the peak position. The calculated spacing ratios were used to identify the structure formed by the lipids.

3.6.2. Differential Scanning Calorimetry (DSC)

Differential Scanning Calorimetry is a thermoanalytical technique used to study the thermodynamic parameters of molecular systems. In case of biological samples the method is applied mostly to liposomes, nucleic acids and proteins. These structures are stabilized by the cooperation of various weak forces (e.g. hydrophobic and electrostatic interactions, hydrogen bonds) and they undergo the phase transitions resulting from molecular changes. DSC yields the information about the temperature of transition, enthalpy, entropy and heat capacity of the sample [87].

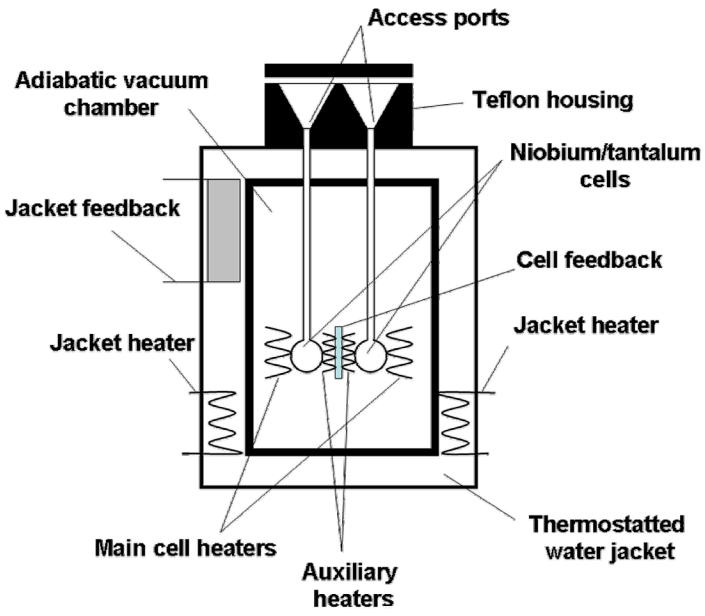

Figure 3.5. Schematic drawing of a calorimeter [87].

Differential scanning calorimeters measure the heat uptake upon the increase of temperature. A typical calorimeter contains two cells: one for the sample and one for the reference, which usually is an aqueous buffer used to suspend the sample (Fig. 3.5). Both cells are heated by two heaters at a constant rate and a temperature difference between the cells is kept at the constant value zero. When the sample undergoes a transition, it absorbs the heat in the case of endothermic process (e.g. melting of acyl chains in lipids) or releases the heat in the case of exothermic process. To maintain the both cells at the same temperature, the heat difference is immediately compensated by the heater. The power difference of the two heaters is recorded as a function of temperature.

In order to obtain thermodynamic information, the power must be converted to apparent molar excess heat capacity with the formula:

$$\frac{dQ_p}{dt}\frac{1}{\sigma M} = c_p \tag{8}$$

where Q_p is the heat absorbed at constant pressure, t is time, σ is the scan rate (dT/dt), T is temperature, M is the number of moles of sample in the sample cell; time is converted to temperature using the formula $t \cdot \sigma$. After the normalization for the sample concentration and subtraction of the baseline from the sample scan, the excess heat capacity (Δc_p) as the function of temperature is obtained. Δc_p is defined as the heat capacity difference between a pre-transitional and post-transitional state of the sample, e.g. in case of melting of lipid acyl chains (β→α transition) it corresponds to a heat capacity difference between the lipids in a gel (L_β) and liquid crystalline (L_α) phase. The melting temperature (T_m) can be derived at the maximum of the Δc_p curve. The enthalpy of transition is derived from the excess heat capacity (Δc_p) curve by integration:

$$\Delta H = \int_{T_0}^{T_1} \Delta c_p dT \,. \tag{9}$$

The entropy of the transition is given by the equation:

$$\Delta S = \int_{T_0}^{T_1} \frac{\Delta c_p}{T} dT \,. \tag{10}$$

If the transition peak is sharp, then $c_p / T \approx c_p / T_m$ and Eq. 10 can be simplified to

$$\Delta S = \frac{\Delta H}{T_m} \,. \tag{11}$$

3.6.2.1. Experimental procedure

For DSC measurements the suspension of large unilamellar vesicles (LUV) composed of POPE/POPG at the molar ratio 7:3 and the final lipid concentration 6.5 mM was used (the preparation procedure is described in the section 3.3.2). The peptides were added at the lipid:peptide molar ratio 100:1. The samples were degassed for 15 min. The experiments were performed with a MicroCal VP scanning calorimeter (GE Healthcare, Freiburg, Germany) with a heating scan rate of 0.5°C/min. Heating curves were measured in the temperature range from 3°C to 75°C. Before each scan the lipid dispersions were equilibrated in the calorimetric cell for 30 min at 3°C. After the first scan the samples were cooled down and rescanned to check the reproducibility of thermograms. The data were analyzed using MicroCal's Origin software.

3.6.3. Attenuated Total Reflection Fourier Transform Infrared (ATR-FTIR) Spectroscopy

Attenuated Total Reflection Fourier Transform Infrared (ATR-FTIR) Spectroscopy is one of the most powerful techniques to investigate biological membranes. It allows studying

the structure of membrane proteins, which cannot be studied by X-rays crystallography or NMR.

The Infrared (IR) Spectroscopy utilizes the radiation from the infrared region of the electromagnetic spectrum. Infrared light is characterized by a longer wavelength (λ) and lower frequency (ν) than the visible and ultraviolet light.

The chemical groups of macromolecules (e.g. C=O or N-H) vibrate. The most common types of vibrations are symmetrical and asymmetrical stretching, scissoring, rocking, wagging and twisting. A chemical bond in such a group occupies a particular vibrational energy level. The vibrational energy level is characterized by a bond length, bond angle and electron density. The chemical group can undergo a vibrational transition from the ground state to the first excited state due to absorption of infrared light with the energy corresponding exactly to ΔE between two vibrational energy levels. The value of ΔE corresponds to the light frequency (ν) by the relationship $\Delta E = h\nu$, where h is Planck's constant. Since the values of ΔE between vibrational energy levels are very small, the radiation with low frequencies, corresponding to the frequencies of infrared light, should be applied. The transition from the ground state to the first excited state is called a fundamental absorption. Although the transitions to the second or third excited state are also possible, they occur less frequently and represent weaker absorbance. The resulting infrared spectrum consists of a plot of absorbance against the frequency or wavenumber ($1/\lambda$). The specific chemical groups are characterized by the absorbance of infrared light near particular frequencies. These frequencies are the fingerprints of these groups and enable the determination of structural aspects of molecules.

Although IR spectrophotometer can be used to study small molecules, its application for biopolymers is limited, mostly due to the fact that it allows scanning comparatively short parts of the infrared spectrum in each measurement. FTIR spectrophotometer can be used as an alternative.

In general, FTIR spectroscopy utilizes a Michelson interferometer and a mathematical tool – Fourier transform (Fig. 3.6) [88]. The experiment consists in the shining a polychromatic beam of infrared light at a sample and measuring how much of that beam is absorbed. The light from broadband light source is split into two paths using a half-silvered mirror (beam splitter). Part of the beam (ideally 50%) is transmitted toward the moving mirror and part (50%) is reflected toward the stationary mirror. The beam splitter is positioned at 45° to the incident beam, which is parallel to the stationary mirror. The moving mirror is arranged

at 90° to the incident beam. The two beams are reflected back by the stationary and moving mirrors and recombine. Ideally 50% of original light passes to the sample compartment. Constructive or destructive interference occurs, if the two beams are in phase or out of phase, respectively. Different IR wavelengths interfere at different mirror positions and the total intensity is measured as a function of the mirror position. Afterwards it is Fourier-transformed to produce eventually a plot of intensity versus the wavenumber. In order to increase sensitivity, a sample is deposited on a material characterized by multiple internal reflections (so-called internal reflection element, IRE). Usually it is a polished plate with beveled edges (ATR plate), so that the incident beam penetrates the plate through a surface perpendicular to its propagation (Fig. 3.7) [89].

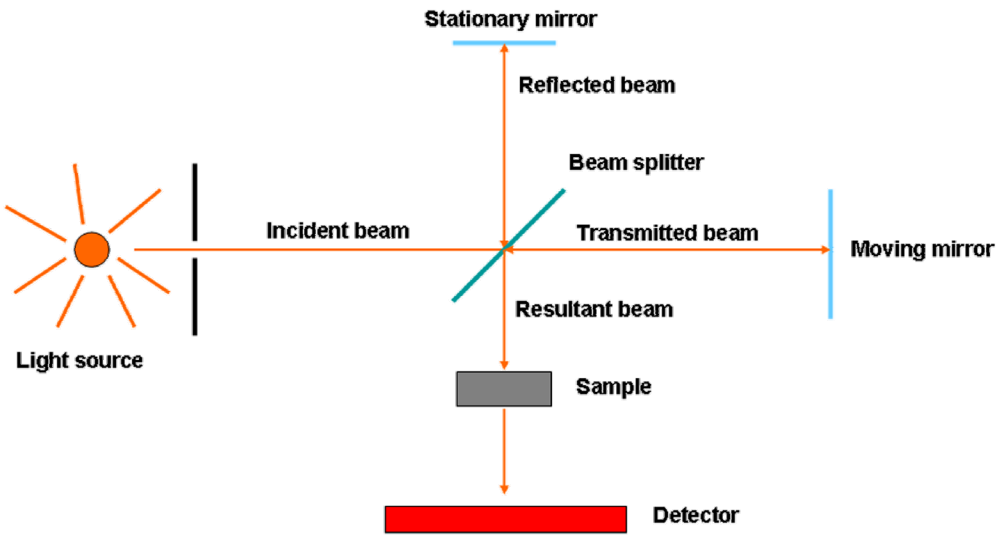

Figure 3.6. The Michelson interferometer used in FTIR spectroscopy [88].

FTIR spectroscopy is a very useful tool in studying the structure and dynamics of peptides and proteins. Infrared spectra are characterized by sharp features specific for particular molecular vibrations. A peptide group in a protein gives up to nine characteristic bands: amide A, B, I, II, III, IV, V, VI and VII. The amide A band (about 3500 cm^{-1}) and

amide B (about 3100 cm^{-1}) originate from the N-H stretching vibration. Amide I (between 1600 and 1700 cm^{-1}) is the most intensive absorption band in proteins. It is connected with the stretching vibrations of C=O (70-85%) and C-N groups (10-20%) and therefore it is directly related to the backbone conformation. Amide II (1510-1580 cm^{-1}) is associated with in-plane N-H bending (40-60%), the C-N (18-40%) and the C-C (about 10%) stretching vibrations. It is conformationally sensitive. Amide III and IV are very complex bands resulting from several coordinate displacements. The out-of-plane motions are assigned to amide V, VI and VII.

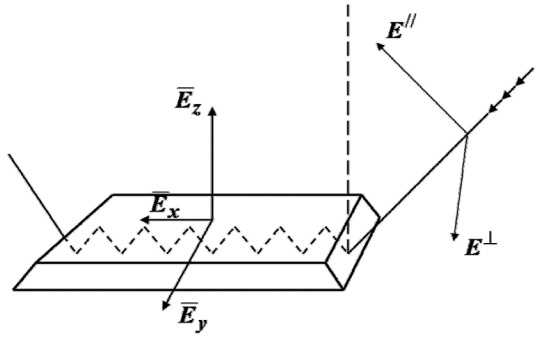

Figure 3.7. Internal reflection element (IRE) and the light pathway. The cartesian components of the electric field are indicated along the *x*, *y* and *z* axes. Two possible planes of polarization are shown as $E^{//}$ and $E^{\perp}$. The incident beam makes an angle θ with respect to the normal to IRE surface [89].

The secondary structure of proteins can be solved on the basis of features of FTIR spectra. For the α-helical structures the frequencies are found in the range 1662-1645 cm^{-1} with the mean frequency at 1652 cm^{-1} for the amide I and 1548 cm^{-1} for the amid II absorptions. For the β-sheet structures the main band is found in the range 1637-1613 cm^{-1} and the smaller band in the range 1689-1682 cm^{-1}. For an antiparallel β-sheet the average frequency of the main component is 1629 cm^{-1} and the average value for the second frequency is 1696 cm^{-1}. For a parallel β-sheet the main band is located at 1640 cm^{-1}. The absorption in the range 1682-1662 cm^{-1} is assigned to turns. Unordered structure (random coil) absorbs in the range 1645-1637 cm^{-1}.

The information on the orientation of a peptide or specific parts of protein in the membrane can be obtained from amide I bands, using polarized ATR-FTIR spectroscopy. The method is based on the fact that the absorption of linearly polarized light is maximal if the dipole transition moment is parallel to the electric field component of the incident light. In contrast, the light is not absorbed at all if the electric field component is perpendicular to the dipole transition moment. The orientation of an α-helix can be obtained from the orientation of C=O group of a peptide bond. Since the hydrogen bonds are formed between C=O and N-H groups in an α-helix, these two groups are oriented roughly along the helical axis. The dipole transition moment in C=O group is oriented along the double bond. If the α-helix is oriented perpendicular to the bilayer plane, the maximal absorption will be recorded with the light parallel polarized with respect to the normal to the germanium plate. If the α-helix is oriented parallel to the bilayer plane, the maximal absorption will be recorded with the light perpendicular polarized with respect to the germanium plate normal. Polarization is expressed as the dichroic ratio:

$$R = \frac{A^{//}}{A^{\perp}}, \tag{12}$$

where $A^{//}$ and $A^{\perp}$ are the absorbances (measured as band areas) with the parallel and perpendicular orientation of the polarizer. Subsequently, the dichroic ratio is converted into an orientational order parameter *S*, which is related to the tilt of the helix axis with respect to the membrane normal [89].

3.6.3.1. Experimental procedure

ATR-FTIR experiment was performed in the Laboratory for the Structure and Function of Biological Membranes at Université Libre de Bruxelles. Multilamellar vesicles (MLVs) with the phospholipid composition POPE/POPG (7/3) were used, with the final lipid concentration of 10 mg/mL (the preparation procedure is described in the section 3.1.1). ATR-FTIR spectra were recorded at room temperature using a Bruker IFS-55 infrared

spectrophotometer equipped with a liquid nitrogen-cooled detector. The internal reflection element was a germanium ATR plate (50 × 20 × 2 mm) with 25 internal reflections. The spectrophotometer was continuously purged with dry air. 20 μL of lipid:peptide mixtures (with molar ratio 70:1) were deposited on the crystal and the solvent was removed by slow evaporation under a gentle stream of nitrogen. This procedure resulted in the formation of oriented multilayers. Spectra were recorded with parallel and perpendicular polarized incident light with respect to a normal to the germanium plate in order to determine the peptides secondary structure and their orientation in the membrane. Polarization was expressed as the dichroic ratio (Eq. 12). For each spectrum 128 scans were recorded.

4 Results

4.1 Construction of new NKCS derivatives

The antimicrobial peptide NKCS was used as a template to design several novel sequences. The modifications were made to understand which structural (α-helicity) and physicochemical (charge, amphipathicity) parameters should be conserved to guarantee a high antibacterial activity. As mentioned in the first chapter of this work, NKCS was derived from the core part of membranolytic polypeptide NK-lysin (residues 39 – 65). The NMR structure of NK-lysin revealed that this particular fragment of polypeptide is folded into two α-helices connected by an unstructured and flexible region (Fig. 1.5). The modifications of NKCS were focused on these three structural sections of the peptide.

The first changes of NKCS sequence were presented in 2006 by Linser [80]. In his work he studied 12 NKCS-derived peptides. He modified the N- and C-terminal fragments as well as the unstructured region by the amino acids substitution or insertion. Moreover, he designed the peptides corresponding to the N-terminal α-helix, N-terminal α-helix with the unstructured region and C-terminal α-helix. He also manipulated the net charge of the peptides by inserting the additional lysine residues.

The further changes of NKCS sequence were made by Andrä et al. [79]. In the abovementioned work the authors presented 18 new peptides. They studied the activity and structural features of N- and C-terminal fragments together with the unstructured region as well as the unstructured region alone. They maintained the positively charged lysine residues

on the ends of the peptide, deleting the amino acids from the unstructured part or from N- and C-terminal parts.

The group of peptides presented in this section comprises eight derivatives of NKCS. Among them, there are two 27-amino-acid sequences, differing from the parental peptide only with single amino acid substitutions (Table 4.1). NKCS-[DK] contains positively charged lysine instead of negatively charged aspartate at the position 21. The idea of this change was to increase the positive charge in the C-terminal fragment. NKCS-[DA] contains alanine instead of aspartate 21. Alanine neutralizes the negative charge and fits an α-helical structure of the peptide much better than any other amino acid.

Table 4.1: The new sequences derived from NKCS. The positively charged amino acids are highlighted in red and negatively charged aspartate in blue. The net charge of peptides was calculated by subtracting the aspartate residue from positively charged lysines, arginines and N-terminus. C-terminus was amidated and did not carry a negative charge.

Peptide	Sequence	Mass (Da)	Charge
NKCS	K I L R G V S K K I M R T F L R R I S K D I L T G K K	3186	+10
NKCS-[DK]	K I L R G V S K K I M R T F L R R I S K K I L T G K K	3199	+12
NKCS-[DA]	K I L R G V S K K I M R T F L R R I S K A I L T G K K	3142	+11
NKCS-[K17]	K K I L R G V S K K I M R T F L R R	2230	+9
NKCS-[VM-KR]	K I L R G M S R K I M R T F L R R	2162	+8
NKCS-[17VF]	K I L R G F S K K I M R T F L R R	2150	+8
NKCS-[15-27]	L R R I S K D I L T G K K	1527	+5
NKCS-[15-27]-S	L R G I S K K I D R T L K	1527	+5
NKCS-[14]-2	K I L R G V S K K I M R T F K I L R G V S K K I M R T F	3335	+11
	1 2 3 4 5 6 7 8 9 10 11 12 13 14 15 16 17 18 19 20 21 22 23 24 25 26 27 28		

Three derivatives represent the N-terminal fragment of NKCS. The peptide NKCS-[K17] comprises the α-helix and the flexible region, which in the parental peptide connects two helices. An additional lysine is inserted at the beginning, to obtain two positive charges at the both ends of the sequence. NKCS-[VM-KR] is characterized by two changes next to the serine 7. Valine is substituted by methionine and lysine by arginine. These modifications were made to analyze how the activity of NKCS may depend on the changes in

the close vicinity of the crucial serine 7. NKCS-[17VF] is 17-amino-acid peptide in which valine 6 is substituted by phenylalanine. The choice of the replacing residue was not random. Phenylalanine is a hydrophobic amino acid which can play an important role in the interactions with the highly hydrophobic core of the bilayer. This provided an idea to enhance the peptide-membrane association by introducing an additional phenylalanine to the sequence of NKCS.

Two peptides represent the C-terminal fragment. NKCS-[15-27] comprises the unmodified fragment of parental NKCS from residue 15 to 27. NKCS-[15-27]-S is composed of the same amino acids as NKCS-[15-27], but arranged in a way resulting in equal distribution of positive charges.

The last peptide, named NKCS-[14]-2, consists of a doubled N-terminal α-helix. The first 14 amino acids of the parental peptide were found to interact strongly with the bacterial membrane [80] and doubling this particular sequence was expected to increase the antimicrobial activity.

4.2 Amphipathicity

The amphipathicity of NKCS and its derivatives was resolved using the helical wheel projections (Fig. 4.1, 4.2 and 4.3). A helical wheel does not show the structure of peptides, but it portrays the allocation of polar and hydrophobic amino acids upon the membrane interaction, assuming that the peptide adopts an ideal α-helix. The wheel was drawn using Membrane Protein Explorer (MPEx), developed in the laboratory of Stephen White at the University of California (http://blanco.biomol.uci.edu/mpex/). MPEx can be used to estimate the thermodynamic properties of the peptide partition into membrane interfaces and the peptide insertion into the bilayer core [90-92].

Using MPEx, the free energy of peptides transfer from water to the bilayer (ΔG_{oct}) was calculated (Table 4.2). The calculation was based on the Wimley-White whole-residue water/octanol hydrophobicity scale [93]. This particular scale represents the free energies of the amino acid residues transfer from the water to the hydrophobic interior of lipid membrane, mimicked by octanol. The sequences of peptides used for calculations had amidated

C-terminus. Moreover, a hydrophobic moment (μ_H), as a quantitative measure of amphipathicity, was determined. The hydrophobic moment was calculated as the vector sum of the hydrophobicities of individual amino acids, normalized to an ideal α-helix [94].

Table 4.2: The free energies of peptide transfer from water to the bilayer (ΔG_{oct}) and the hydrophobic moment (μ_H) of peptides. The low values of ΔG_{oct} imply the higher tendency of peptides to insert into the hydrophobic core of bilayers. The high values of μ_H indicate the high amphipathicity.

Peptide	**Number of amino acids**	**ΔG_{oct} (kcal/mol)**	**μ_H**
NKCS	27	24.63	12.62
NKCS-[DK]	27	23.79	13.38
NKCS-[DA]	27	21.49	15.52
NKCS-[K17]	18	17.02	11.11
NKCS-[VM-KR]	17	13.02	11.86
NKCS-[17VF]	17	12.97	13.05
NKCS-[15-27]	13	17.08	7.92
NKCS-[15-27]-S	13	17.08	13.59
NKCS-[14]-2	28	19.40	24.93

Figures 4.1, 4.2 and 4.3 present the helical wheel diagrams of peptides. The one letter code for amino acids is used. The blue balls stand for positively charged residues, the red balls for negatively charged aspartate and yellow balls for neutral amino acids. The green balls represent nonpolar residues and the purple one is strongly hydrophobic phenylalanine. The blue arrow is a vector indicating the direction and magnitude of the hydrophobic moment of each peptide. These arrows point the hydrophobic face of peptides, which is able to embed and interact with the nonpolar core of the membrane. The helical wheels are drawn starting from the first amino acid of the N-terminus. The residues of each next coil are represented by smaller balls connected by thinner lines.

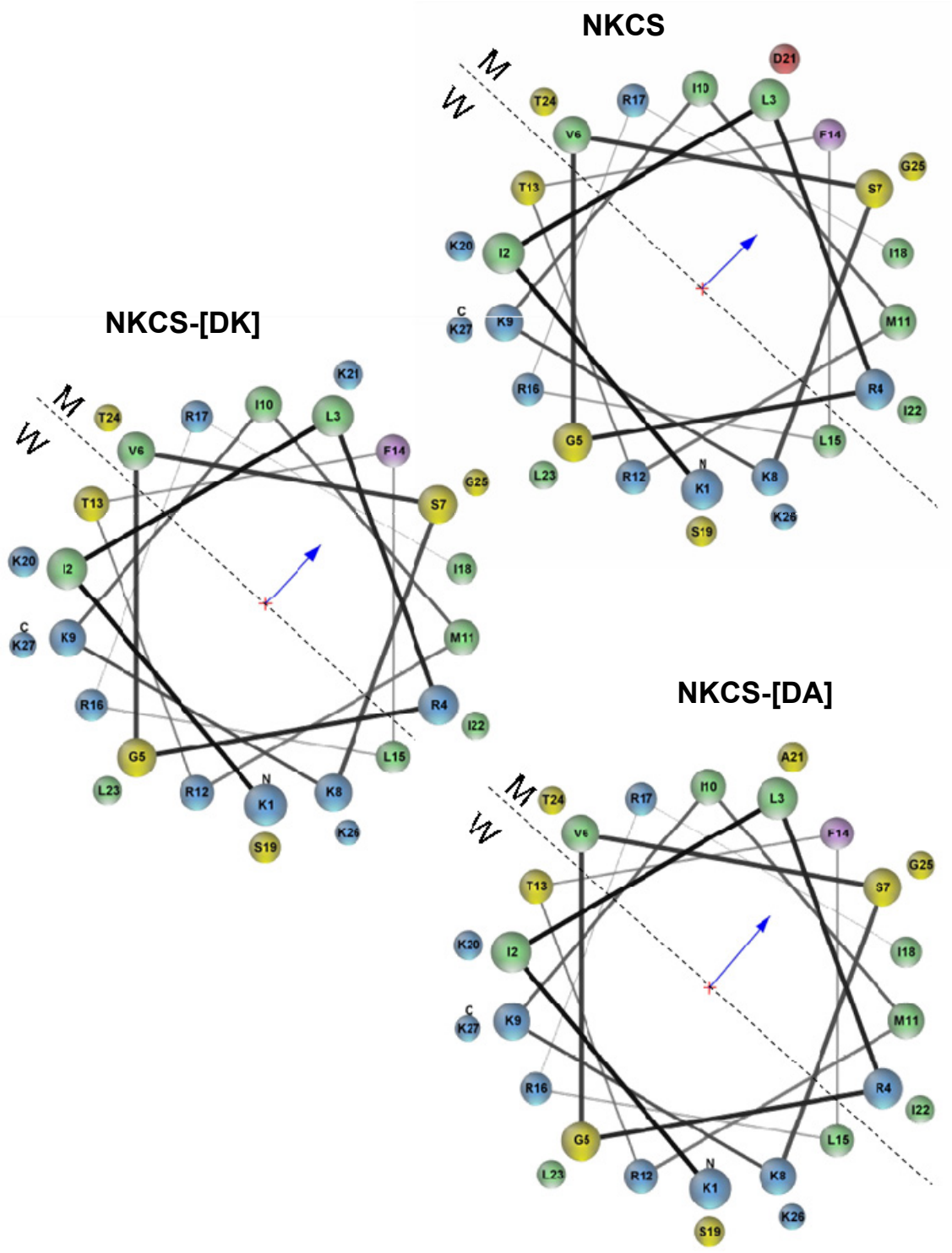

Figure 4.1. Helical wheel diagrams of NKCS, NKCS-[DK] and NKCS-[DA]. The meaning of diagram elements is explained in the text on page 38. The dashed line indicates the interface between water (W) and membrane (M).

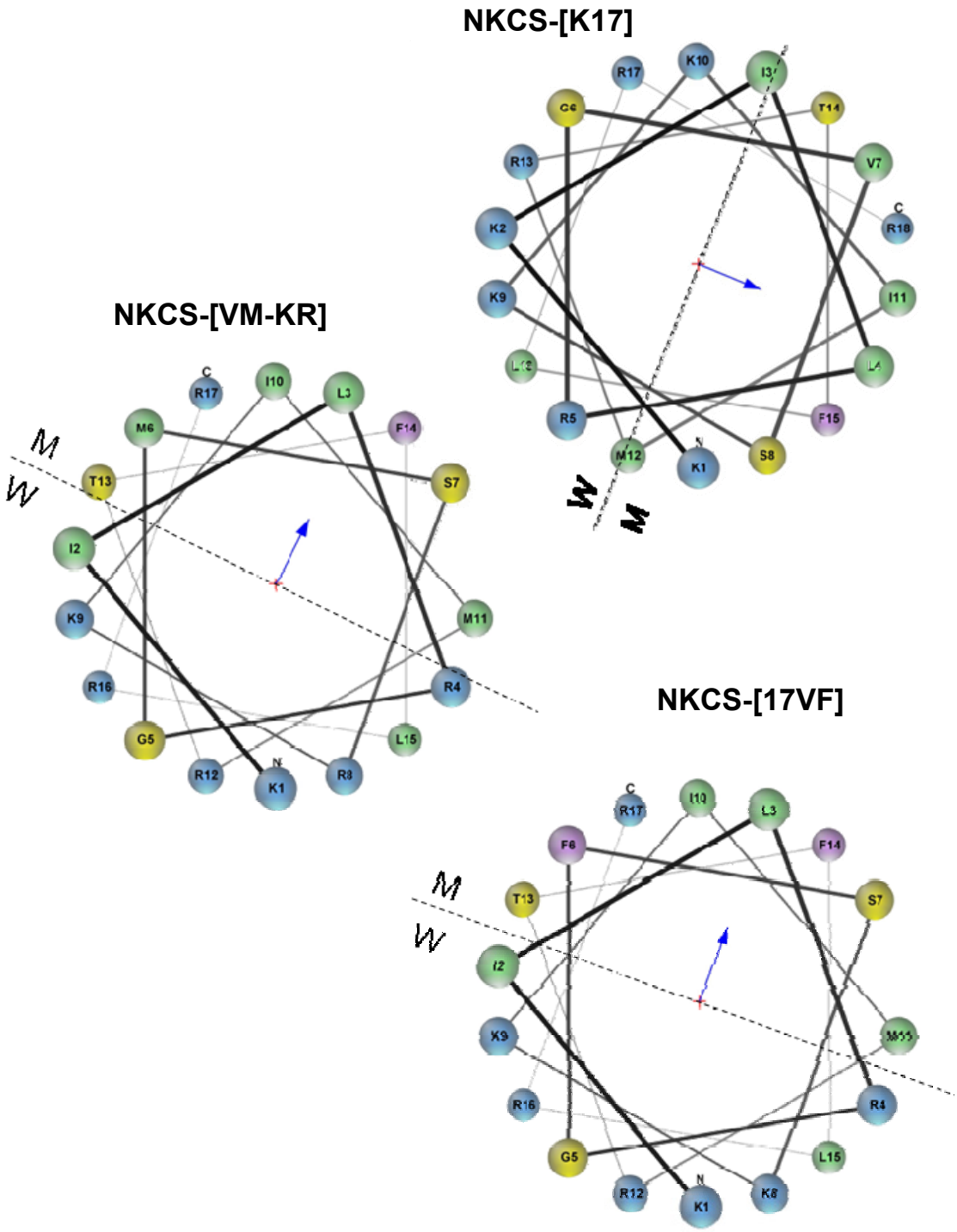

Figure 4.2. Helical wheel diagrams of NKCS-[K17], NKCS-[VM-KR] and NKCS-[17VF]. The meaning of diagram elements is explained in the text on page 38. The dashed line indicates the interface between water (W) and membrane (M).

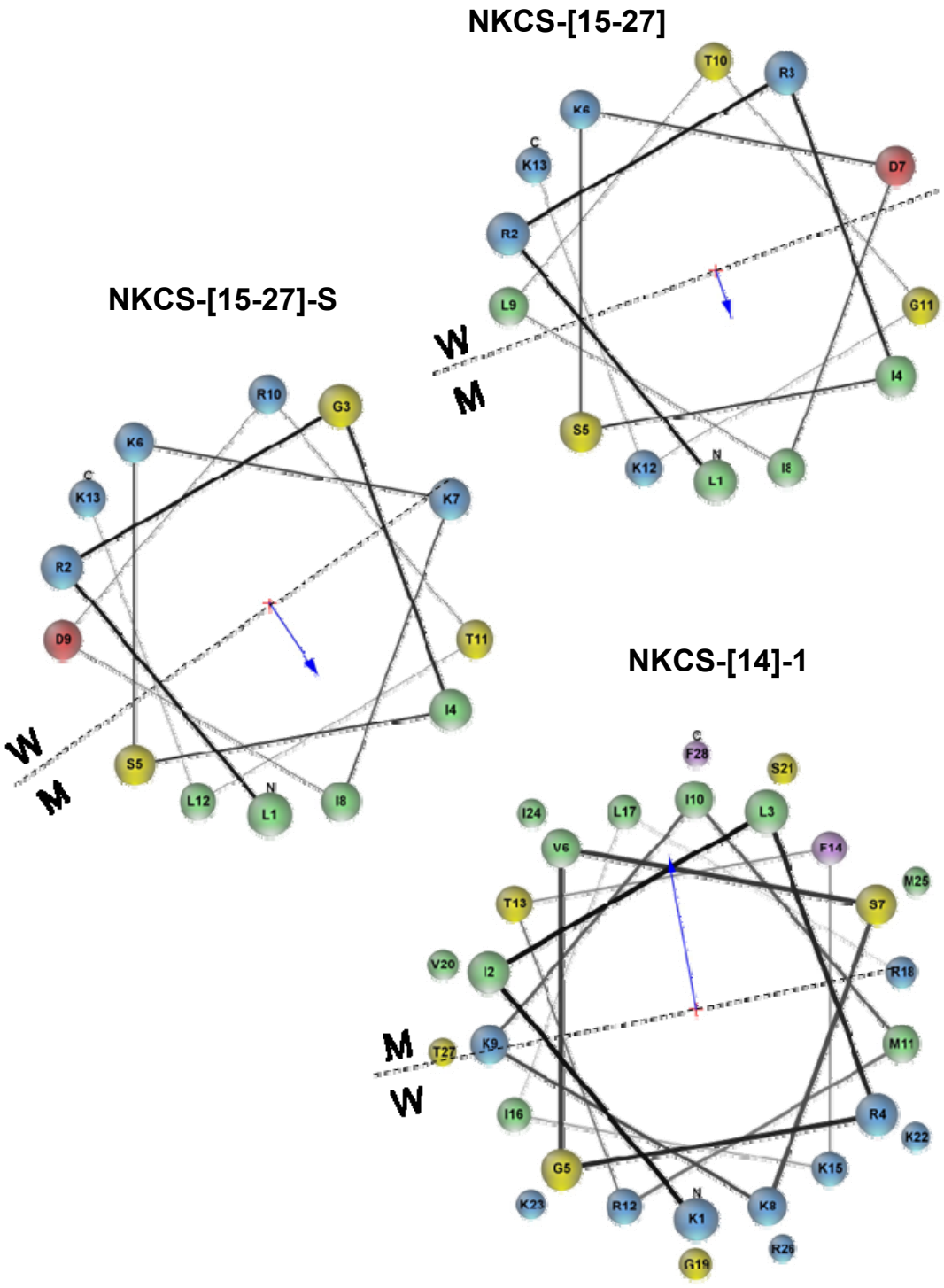

Figure 4.3. Helical wheel diagrams of NKCS-[15-27], NKCS-[15-27]-S and NKCS-[14]-2. The meaning of diagram elements is explained in the text on page 38. The dashed line indicates the interface between water (W) and membrane (M).

The value of ΔG_{oct} estimated for NKCS is high (Table 4.2). It indicates that the insertion of this peptide into the bilayer is unfavorable. The main forces driving the successful partitioning of a peptide from water to bilayer are the hydrophobic interactions, enhancing the expulsion of nonpolar compounds from aqueous environment, and electrostatic attraction between the cationic residues and anionic head groups of lipids [95]. The presence of negatively charged aspartate results in repulsion between this amino acid and the negatively charged surface of membrane. This increases the cost of peptide partitioning and yields a high value of ΔG_{oct} (24.63 kcal/mol). The substitution of aspartate by positively charged lysine in NKCS-[DK] facilitates the electrostatic interaction between positively charged peptide and negatively charged lipids. This results in a lower ΔG_{oct} (23.79 kcal/mol) and a higher hydrophobic moment. The exchange of aspartate for alanine in NKCS-[DA] reduces ΔG_{oct} even further, to 21.49 kcal/mol. Additionally it raises the value of hydrophobic moment what clearly indicates a better amphipathicity of the peptide.

The short peptides representing the N-terminal α-helix of NKCS have in general a lower transfer free energy than the long derivatives. The value of ΔG_{oct} for NKCS-[K17], calculated as 17.02 kcal/mol, suggests that this peptide has a higher affinity to the membrane than the parental peptide, but the overall amphipathicity is lower. In NKCS-[VM-KR] the major contribution to the low free energy of transfer comes from the additional methionine at the position 6. It reduces ΔG_{oct} to 13.02 kcal/mol. Among all studied peptides, NKCS-[17VF] has the lowest free energy of transfer from water to the bilayer (12.97 kcal/mol). It also shows a very good amphipathicity. Phenylalanine increases the hydrophobicity of the peptide, enhancing the possibility of good interactions with the nonpolar core of a membrane.

The free energy calculated for the peptide NKCS-[15-27] is high (17.08 kcal/mol). Moreover, the very low value of the hydrophobic moment suggests the lack of amphipathicity. On the basis of these results it is easy to predict that this peptide has a low activity against bacteria. If the peptide cannot organize itself into an amphipathic structure, the electrostatic interactions with the anionic surface of membrane are weak. Additionally, due to the lack of the well pronounced hydrophobic face of NKCS-[15-27], the partitioning into the bilayer cannot be successful. Better results were computed for NKCS-[15-27]-S. Although the value of ΔG_{oct} is the same as for its unmodified version, the hydrophobic

moment indicates much better amphipathicity. The segregation of amino acids suggests a better antibacterial activity.

The last peptide, NKCS-[14]-2, is the longest one. It displays, however, ΔG_{oct} lower than the other long sequences: NKCS, NKCS-[DK] or NKCS-[DA]. The surprisingly high value of the hydrophobic moment, calculated as 24.93, indicates an extremely good segregation of polar and hydrophobic residues. This suggests that upon the membrane interactions the peptide is localized at the water-bilayer interface with the polar face directed toward aqueous solution and the hydrophobic face buried in the bilayer.

The helical wheel diagrams along with the calculation of ΔG_{oct} and a hydrophobic moment should be treated only as an approximation. For the calculations of abovementioned values and the determination of amino acids distribution, the peptides were assumed to adopt an α-helical structure. The FTIR analysis, which will be shown in a further part of this work, will prove however, that for instance for NKCS-[15-27] this assumption was not correct.

4.3 Antibacterial activity

The peptides were tested against Gram-negative bacterium *Escherichia coli* and two Gram-positive species: *Bacillus subtilis* and *Staphylococcus carnosus*.

The results revealed that the long peptide NKCS-[DK] inhibited the growth of *E. coli* at 0.568 μM (3.39×10^{11} peptide molecules/cell), which was the concentration corresponding to the minimal inhibitory concentration (MIC) of NKCS (Fig. 4.4 A). The MIC of two other long derivatives, NKCS-[DA] and NKCS-[14]-2, found at 1.14 μM (6.77×10^{11} peptide molecules/cell), also indicated a very high antibacterial activity. Interesting results were obtained for shorter peptides (Fig. 4.4 B). The sequences representing the N-terminal helix of NKCS (namely NKCS-[K17], NKCS-[VM-KR] and NKCS-[17VF]) were very active. The C-terminal fragments, however, appeared much less potent. The unmodified derivative NKCS-[15-27] suppressed the growth of only 35% of the culture at the concentration of 9.09 μM (54.2×10^{11} peptide molecules/cell), whereas its analog NKCS-[15-27]-S, with the

equal distribution of positive charges, caused the inhibition of 72% of bacteria at the same concentration.

All studied peptides displayed a very good activity against *B. subtilis* (Fig. 4.5 A and B). The MIC of long derivatives varied from 0.568 μM (3.39×10^{11} peptide molecules/cell) to 1.14 μM (6.77×10^{11} peptide molecules/cell). The short peptides representing the N-terminal fragment inhibited the bacterial growth at 0.568 μM. NKCS-[15-27] and NKCS-[15-27]-S, which were found much less active against *E. coli*, this time showed MIC at 2.27 μM (13.5×10^{11} peptide molecules/cell).

The activity of NKCS and its derivatives against the second Gram-positive strain (*S. carnosus*) significantly differed from the toxicity pattern obtained for *B. subtilis* and surprisingly reminded the behavior observed in the case of Gram-negative *E. coli*. Here again the long peptides were very active, the MIC differed from 0.568 μM (3.39×10^{11} peptide molecules/cell) for NKCS and NKCS-[DK] to 1.14 μM (6.77×10^{11} peptide molecules/cell) for NKCS-[DA] and NKCS-[14]-2 (Fig. 4.6 A). The peptides NKCS-[K17], NKCS-[VM-KR] and NKCS-[17VF] suppressed the bacterial growth at 1.14 μM, but the derivatives of the C-terminal fragment were less potent (Fig. 4.6 B). The MIC of the modified NKCS-[15-27]-S was found at 9.09 μM (54.2×10^{11} peptide molecules/cell), but its analog NKCS-[15-27] did not suppress the growth of bacteria in the studied range of concentrations.

Table 4.3: Antibacterial activity of peptides given in MIC in μg/mL.

Peptide	***E. coli***	***B. subtilis***	***S. carnosus***
NKCS	1.8	3.6	1.8
NKCS-[DK]	1.8	1.8	1.8
NKCS-[DA]	3.5	1.8	3.5
NKCS-[14]-2	3.8	3.8	3.8
NKCS-[K17]	5.0	1.3	2.5
NKCS-[VM-KR]	4.9	1.2	2.4
NKCS-[17VF]	4.8	4.8	2.4
NKCS-[15-27]	> 13.8	3.4	> 13.8
NKCS-[15-27]-S	> 13.7	3.4	13.7

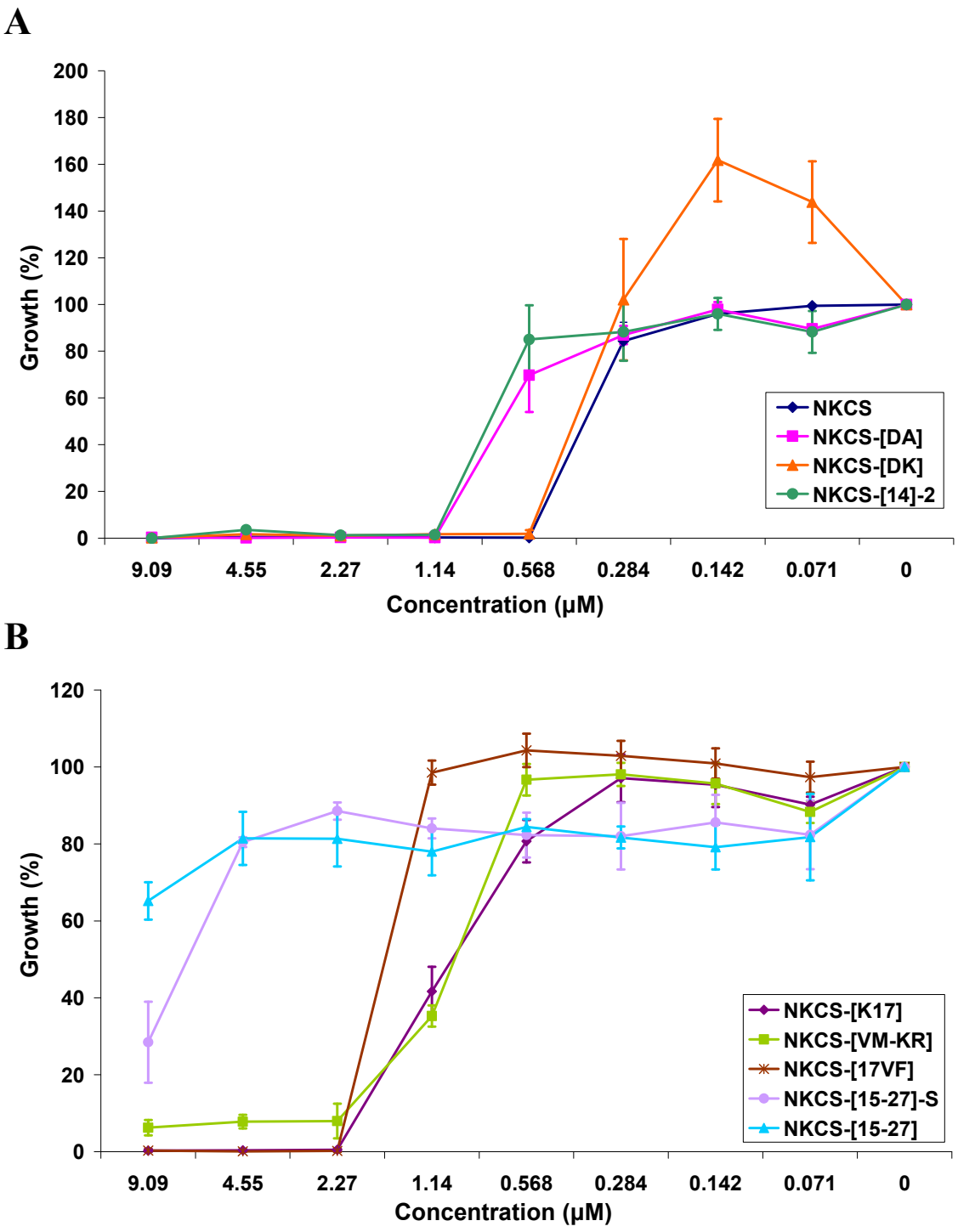

Figure 4.4. Antimicrobial activity of peptides against *E. coli*.

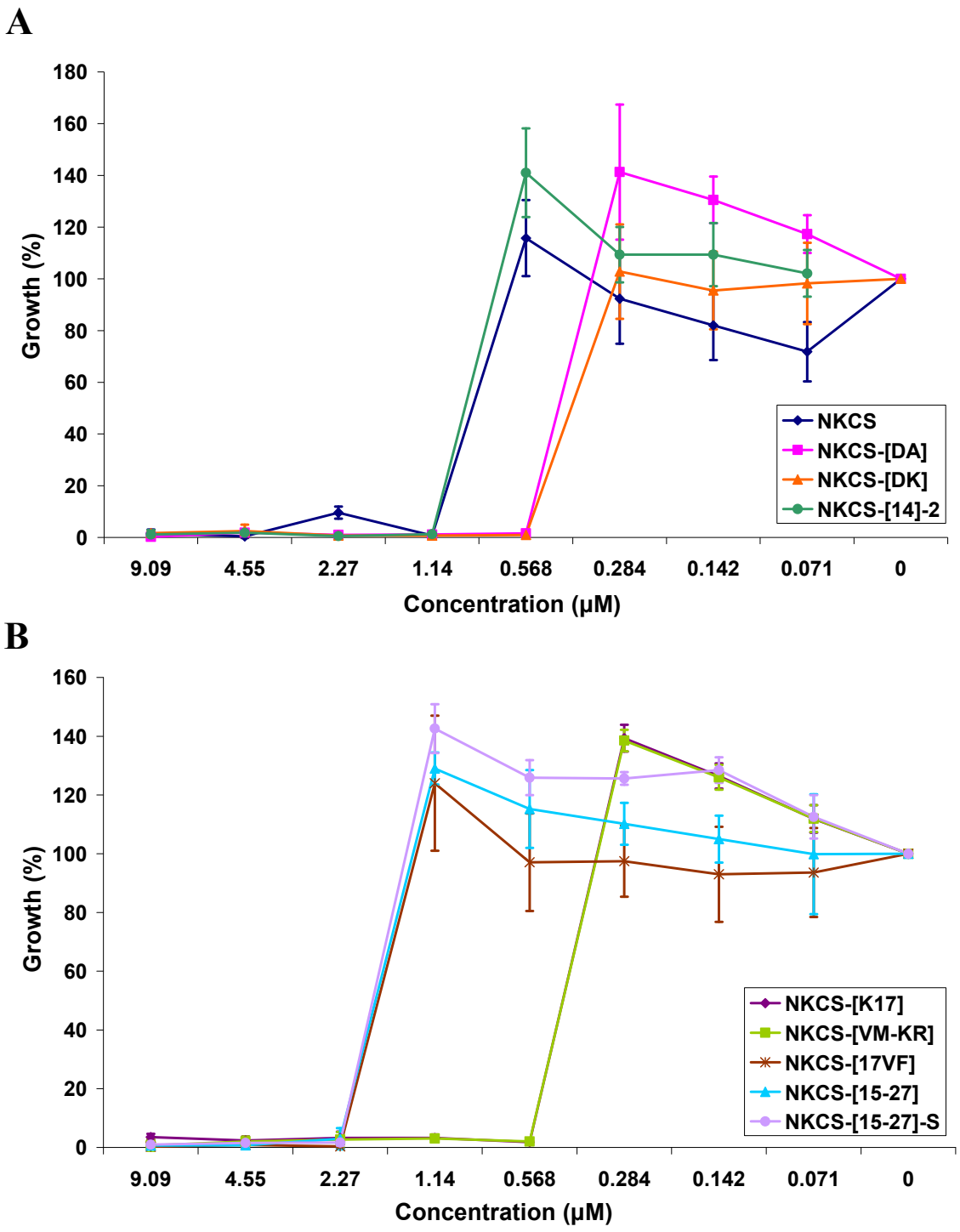

Figure 4.5. Antimicrobial activity of peptides against *B. subtilis*.

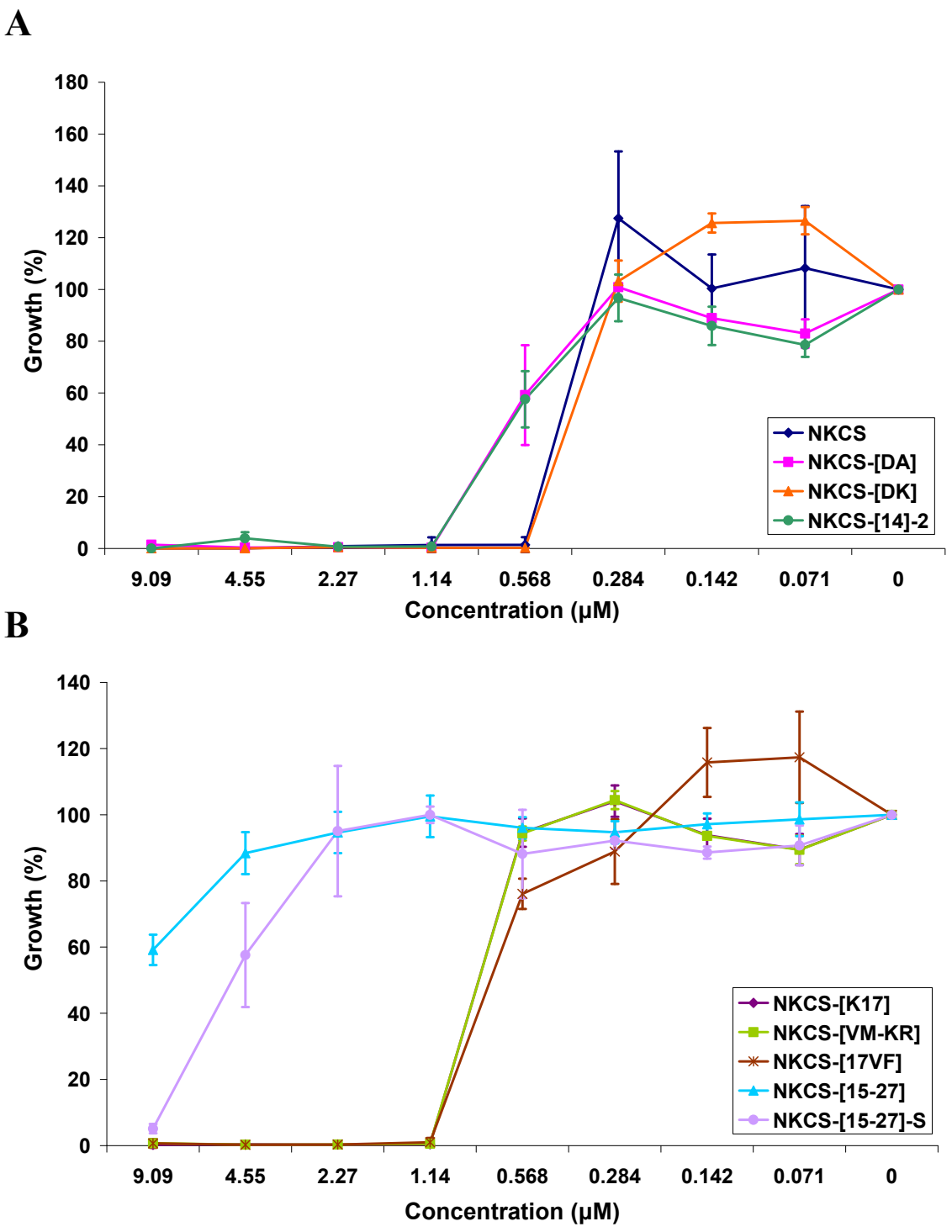

Figure 4.6. Antimicrobial activity of peptides against *S. carnosus*.

Antimicrobial peptides are considered as active if their MIC is lower than 8 μg/mL [96]. Most of the NKCS-derivatives fulfill this requirement (Table 4.3). The two exceptions are NKCS-[15-27] and NKCS-[15-27]-S. These two peptides are active only against Gram-positive *B. subtilis*.

4.4 Hemolytic activity

The toxicity of peptides toward healthy human cells was investigated by measuring their membranolytic potency against erythrocytes. The results obtained for NKCS derivatives were compared to the lytic activity of melittin. Melittin is a peptide isolated from the venom of the European honey bee *Apis melliffera* and it is well known for its nonselective membranolytic activity [97]. All NKCS-peptides showed a low toxicity, even at a very high concentration of 100 μM (Fig. 4.7). In contrast, melittin at this concentration caused a total lysis of red blood cells.

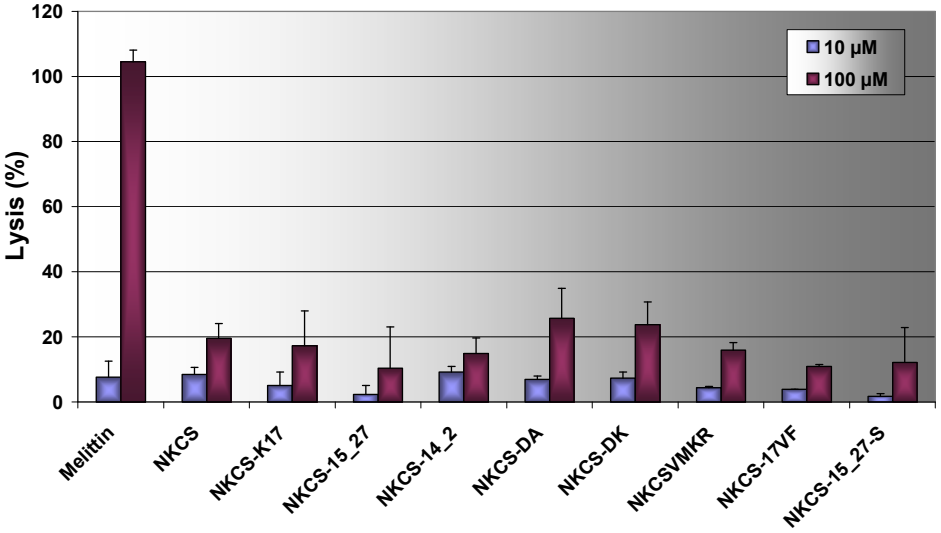

Figure 4.7. Hemolytic activity of NKCS and its derivatives compared with melittin.

4.5 SAXS – interactions with PE membranes

In the following part of this work the emphasis is put on the interactions between antimicrobial peptide NKCS and the cytoplasmic membrane of *E. coli*. To gain an insight into the molecular mechanism of interactions, the biophysical methods such as small angle X-rays scattering (SAXS), differential scanning calorimetry (DSC) and Fourier transform infrared (FTIR) spectroscopy were applied. Since NKCS is a membrane active peptide targeting the lipids, the cytoplasmic membrane was reduced to a phospholipid matrix. The artificial systems composed of the single lipids or the mixture of two lipids were used. NKCS was studied along with its two derivatives: the active against *E. coli* NKCS-[K17] representing the N-terminal fragment with the flexible region and the inactive NKCS-[15-27] representing the C-terminal fragment. The choice of these peptides was not random. Although both of them were derived from NKCS, where together enhanced the activity of the peptide, they showed different behavior acting separately. The choice was based on the hypothesis that the direct comparison of these two peptides in terms of their structural features and their effect on the lipid phase behavior can shed light on the mechanism involved in the interaction of NKCS with the cytoplasmic membrane of *E. coli*.

The cytoplasmic membrane of *E. coli* contains 69% of phosphatidylethanolamine (PE) and 19% of phosphatidylglycerol (PG) (Table 1.1). PE is a zwitterionic molecule and it was expected that it behaves in a way similar to the one presented by another neutral lipid: phosphatidylcholine (PC). PC is a dominating lipid in the outer leaflet of human erythrocytes (Table 1.1). The earlier studies confirmed that the neutral surface of red blood cells prevents the binding of antimicrobial peptides [39]. The lack of exposed charges decides about the selectivity of NKCS and makes this peptide harmless for erythrocytes. The similar results were initially assumed for NKCS-PE interactions.

4.5.1. POPE

4.5.1.1. Influence of peptides on the phase behavior

The first SAXS experiment was performed with POPE liposomes. This lipid was chosen as the most representative for the membrane of *E. coli*. Except PE headgroup, also the acyl chains (16:0-18:1) correspond to the composition of the hydrophobic core found in the cytoplasmic membrane of bacteria grown at 30°C (Table 1.2).

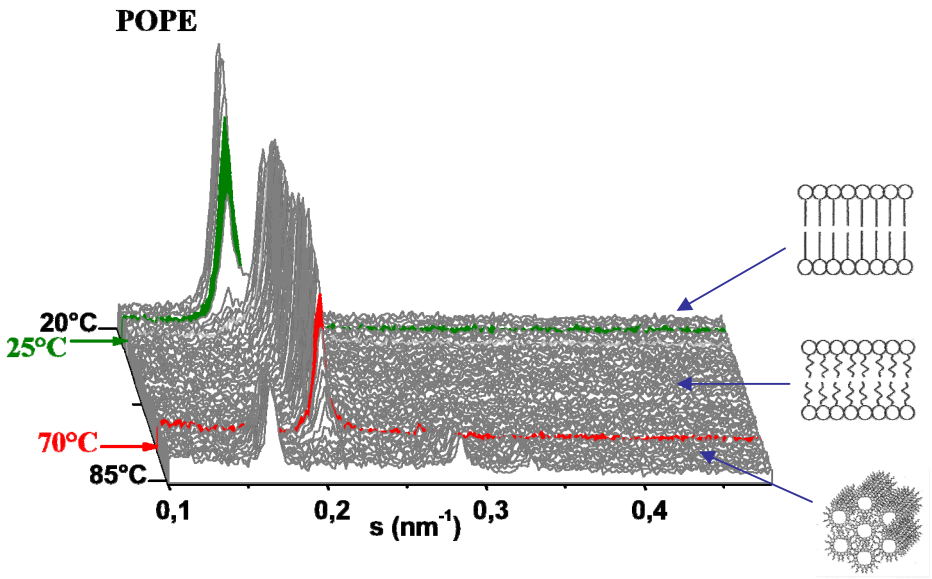

Figure 4.8. The phase behavior of POPE. The liquid crystalline phase transition is marked in green and the inverse hexagonal phase transition is marked in red.

The measurement started at 20°C. The sample was heated at the rate of 1°C/min. Every 1°C the sample was exposed to the X-rays beam for 20 s and the data were collected. At the beginning of the measurement (20°C) POPE existed in a gel phase known also as a solid ordered phase (Fig. 4.8). The repeat distance, defined as a sum of lipid bilayer thickness and water layer between two lipid bilayers, was determined as 62.8 ± 1.1 Å. At 25°C the acyl

chain melting was observed. The repeat distance in POPE multilayers existing in a liquid crystalline state was calculated as 53.5 ± 0.8 Å at 37°C. At 70°C the second phase transition was recorded. The new structure was identified as an inverse hexagonal phase. In this phase the lipids form long cylinders with the acyl chains directed to the outside.

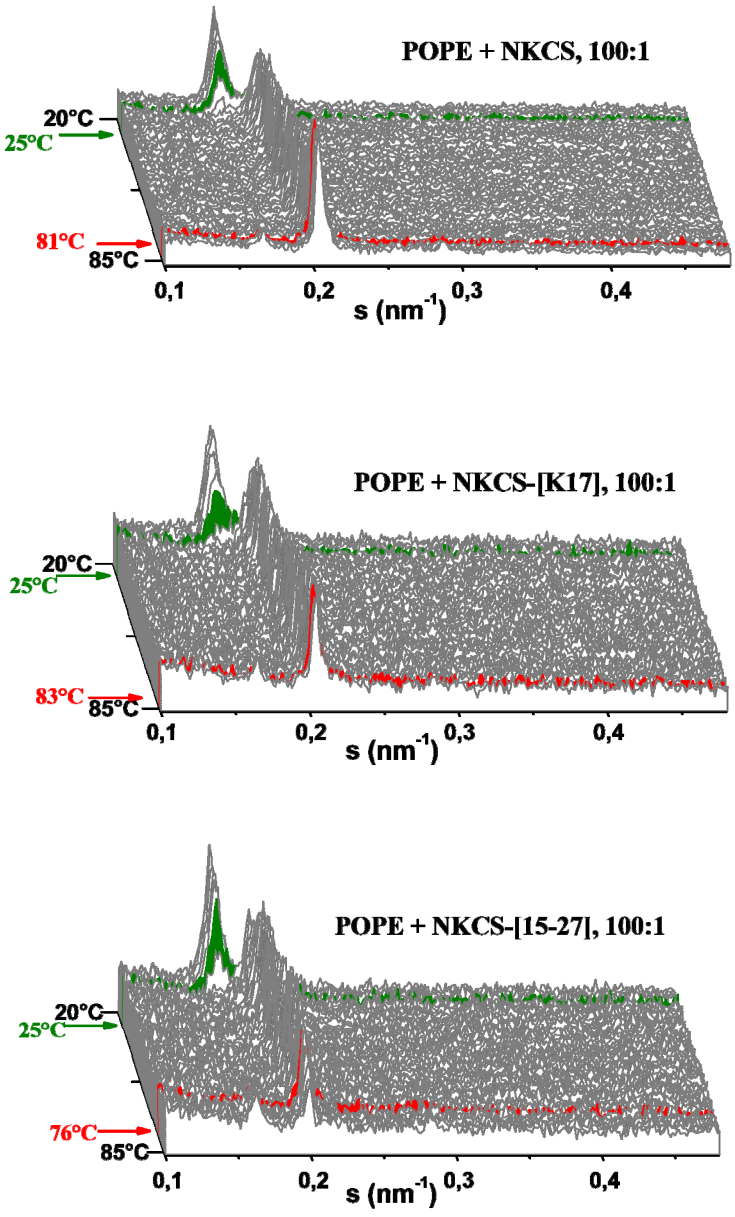

Figure 4.9. Diffraction patterns of POPE mixed with peptides at the lipid:peptide molar ratio 100:1.

The addition of peptides at the lipid:peptide molar ratio 100:1 (348 μM of peptide concentration) did not change the temperature of the acyl chain melting, however there was a significant influence of peptides on the hexagonal phase transition (Fig. 4.9). The active NKCS and NKCS-[K17] shifted the transition to higher temperature, by 11°C and 13°C, respectively. The least active NKCS-[15-27] also interacted with the POPE liposomes, however in this case, as it was expected, the change was much smaller (6°C). All three peptides stabilized the lamellar phase: the reflection found at *s* value of 0.2 nm^{-1} existed also at the temperature of 85°C, at which the measurement was terminated.

4.5.1.2. Influence of peptides on the repeat distance

The SAXS experiment provided also the information about the influence of peptides on the membrane thickness. The results revealed that the thickness of the lipid bilayer was always changing in the course of the heating in the same manner independently from the presence or absence of peptides (Fig. 4.10). NKCS and its derivatives caused neither thickening nor thinning of the lipid bilayer.

The results of SAXS experiment described in this chapter are little different than the results published by Gofman et al. [81]. In that earlier work we reported the hexagonal phase transition of pure POPE at 67°C. Moreover the repeat distance in the liquid crystalline phase was calculated as 55 ± 9 Å at 37°C. The experiment portrayed here showed the phase transition at 70°C and the repeat distance was determined as 53.5 ± 0.8 Å at 37°C. These discrepancies result from different POPE used for both experiments. For the first measurements POPE purchased from Sigma Aldrich was applied. For the latest experiments POPE was bought from Avanti Polar Lipids. Unexpectedly, the same lipid from different manufacturers had slightly different properties. The addition of NKCS in the earlier and the latest experiment had the same effect on the POPE liposomes.

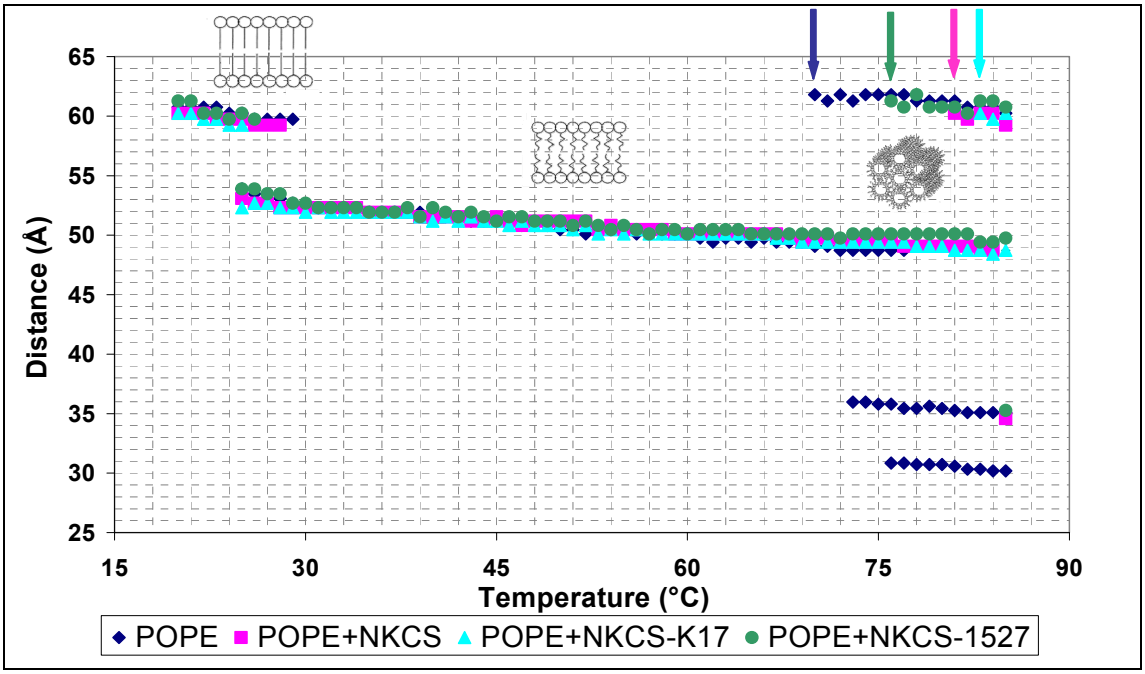

Figure 4.10. The change of repeat distance (corresponding to the thickness of hydrated bilayer) during the heating of pure POPE and after the addition of peptides at the lipid:peptide molar ratio 100:1. The arrows indicate the inverse hexagonal phase transitions.

4.5.2. DiPoPE

The influence of the acyl chain composition on the interactions between antimicrobial peptides and lipid membranes was investigated. The liposomes composed of DiPoPE (16:1-16:1) and DOPE-trans (18:1-18:1) were prepared. These systems were fully artificial because there is no cell membrane with only unsaturated lipids existing in the nature. In both cases the measurements were performed with the heating rate of 1°C/min. The samples were exposed to the X-rays beam for 20 s per each degree.

DiPoPE is a phospholipid characterized by a low temperature of acyl chain melting – this transition occurs already at -33.5°C [84]. The second transition – from liquid crystalline to inverse hexagonal phase – was observed at 44°C (Fig. 4.11 A).

After the addition of peptides, the temperature of the hexagonal phase transition was shifted to the higher values. The biggest change was observed for NKCS-[K17]. Already at

the lipid:peptide molar ratio 300:1 (121 μM of peptide concentration) the temperature was shifted from 44°C to 51°C (Fig. 4.11 B). At the higher concentration of peptide (363 μM, lipid:peptide molar ratio 100:1) the temperature was altered by 13°C (Table 4.4). NKCS-[K17] stabilized the lamellar structure, which coexisted with the inverse hexagonal phase up to temperature of 70°C, at which the measurement was terminated.

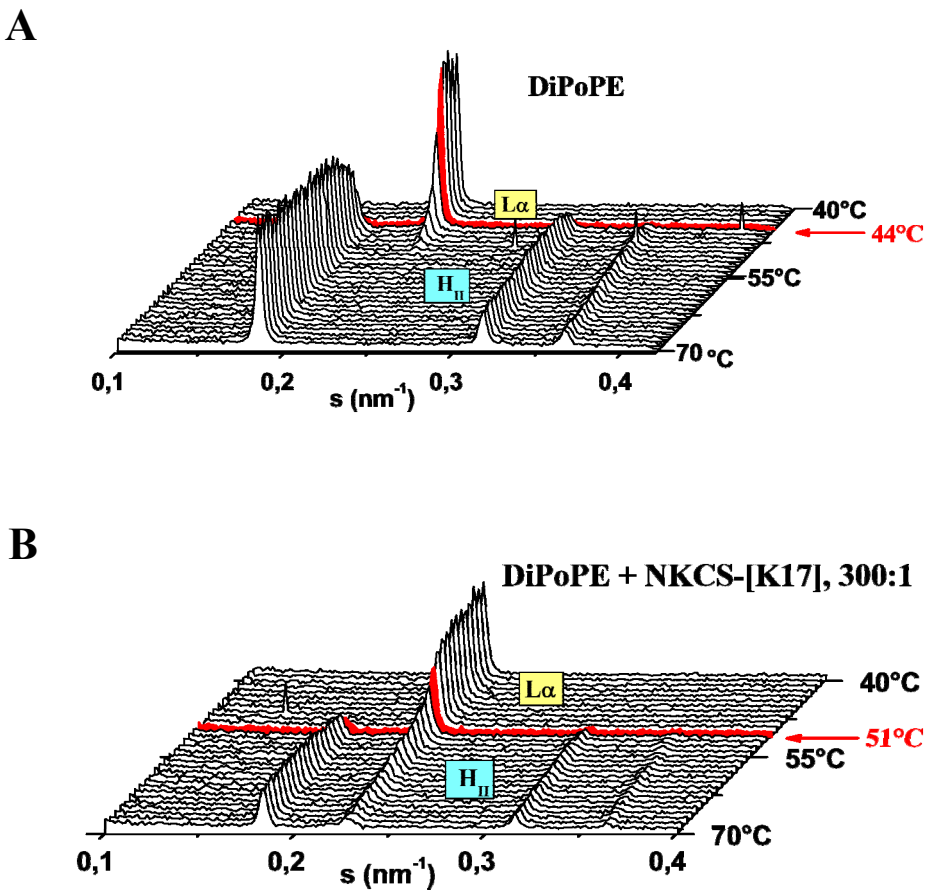

Figure 4.11. Scattering patterns of pure DiPoPE (A) and DiPoPE mixed with NKCS-[K17] at lipid:peptide molar ratio 300:1 (B). The transitions from a liquid crystalline (L_α) to an inverse hexagonal (H_{II}) phase are marked with arrows.

The smaller changes were observed for two other peptides. At the lipid:peptide molar ratio 300:1, NKCS shifted the temperature by 4°C and NKCS-[15-27] by 6°C (Table 4.4).

The higher concentration of NKCS and NKCS-[15-27] did not have any further influence on the phase transition temperature. Interesting fact is that NKCS-[15-27], which was considered as inactive, had bigger effect on the DiPoPE liposomes than NKCS.

The repeat distance for DiPoPE liposomes was determined as 47.6 ± 1.6 Å at 40°C and remained the same within the error also after the addition of peptides.

4.5.3. DOPE-trans

DOPE-trans underwent two phase transitions. At 38°C the acyl chain melting occured and a liquid crystalline phase appeared (Fig. 4.12 A). The second transition was observed at 66°C. The new structure was characterized as an inverse hexagonal phase.

Table 4.4: The change of the inverse hexagonal phase transition temperature of DiPoPE and DOPE-trans vesicles mixed with peptides at the lipid:peptide molar ratio 300:1 and 100:1, expressed as ΔT.

Lipid	Lipid:Peptide molar ratio	Peptide		
		NKCS	NKCS-[K17]	NKCS-[15-27]
DiPOPE	300:1	+4°C	+7°C	+6°C
DiPOPE	100:1	+4°C	+13°C	+6°C
DOPE-trans	300:1	+2°C	+1°C	+0°C
DOPE-trans	100:1	+6°C	+5°C	+0°C

The addition of peptides had very small influence on the structure of DOPE-trans bilayer. The transition from a gel to a liquid crystalline phase was altered by ± 1°C. This change stays in the measurement error margin. The peptide NKCS-[K17], which caused very big change in the case of DiPoPE vesicles, here altered the phase transition temperature only by 1°C at the lipid:peptide molar ratio 300:1 (112 μM of peptide concentration). This 1°C can be a measurement error. The biggest shift, 2°C, was induced by NKCS (Table 4.4). The bigger change was observed for the lipid:peptide molar ratio 100:1 (336 μM of peptide

concentration): NKCS-[K17] shifted the phase transition temperature by 5°C and NKCS by 6°C. NKCS-[15-27] had no influence on the inverse hexagonal phase transition. The results suggested that the interactions between NKCS peptides and DOPE-trans liposomes were weaker than these observed for POPE and DiPoPE and did not affect significantly the structure of lipid vesicles.

The thickness of hydrated DOPE-trans bilayer was calculated as 65.7 ± 1.3 Å at 30°C (liquid crystalline phase) and 54.9 ± 1.3 Å at 45°C (gel phase). The presence of peptides did not affect the bilayer thickness.

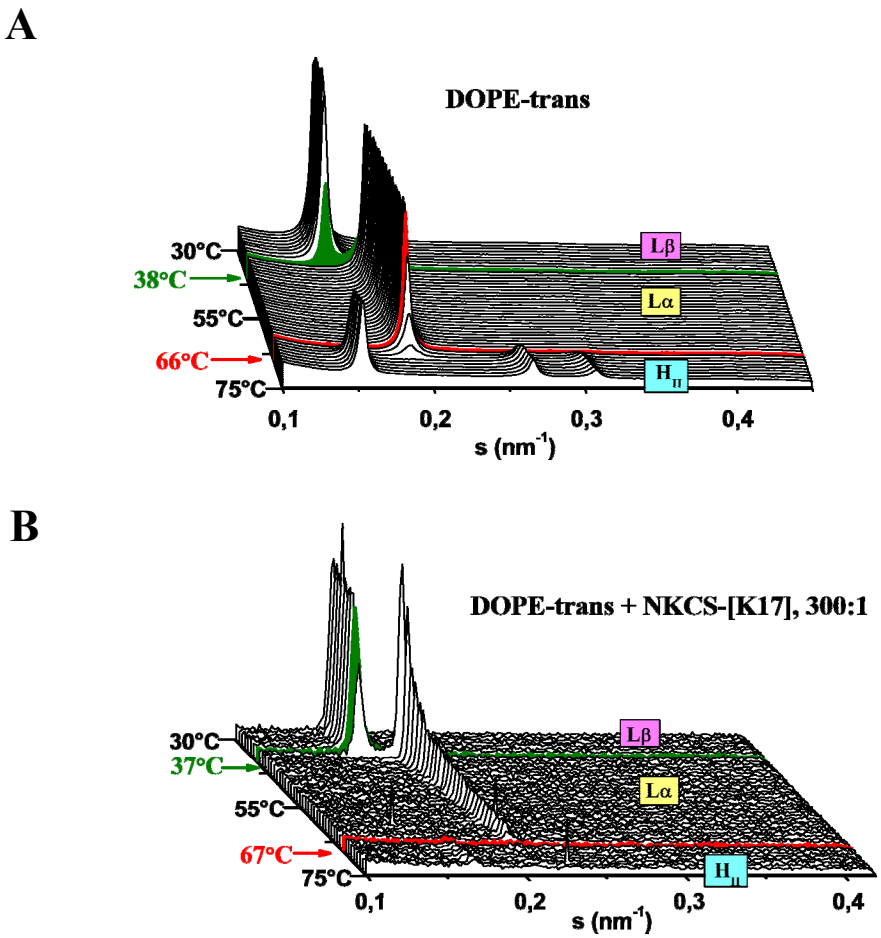

Figure 4.12. Scattering patterns of pure DOPE-trans (A) and DOPE-trans mixed with NKCS-[K17] at the lipid:peptide molar ratio 300:1 (B). The transitions from a gel (L_β) to a liquid crystalline (L_α) phase and from a liquid crystalline (L_α) to an inverse hexagonal (H_{II}) phase are marked with arrows.

4.6 DSC – interactions with PE/PG membrane

The microcalorimetry method was applied to study the interactions of peptides with a more complex lipid system. For this experiment the mixture of phosphatidylethanolamine (PE) and phosphatidylglycerol (PG) at the molar ratio 7:3 was used. Such choice of the components directly reflected the composition of *E. coli* cytoplasmic membrane (Table 1.1). This particular lipid system is not suitable for the SAXS measurements. Since the vesicles containing PG are unilamellar, the reflections are not sharp and it is very difficult to analyze the scattering pattern. On the other hand, the analysis of the pure POPE, DiPoPE or DOPE-trans lipids behavior with DSC is difficult due to their high tendency to aggregate.

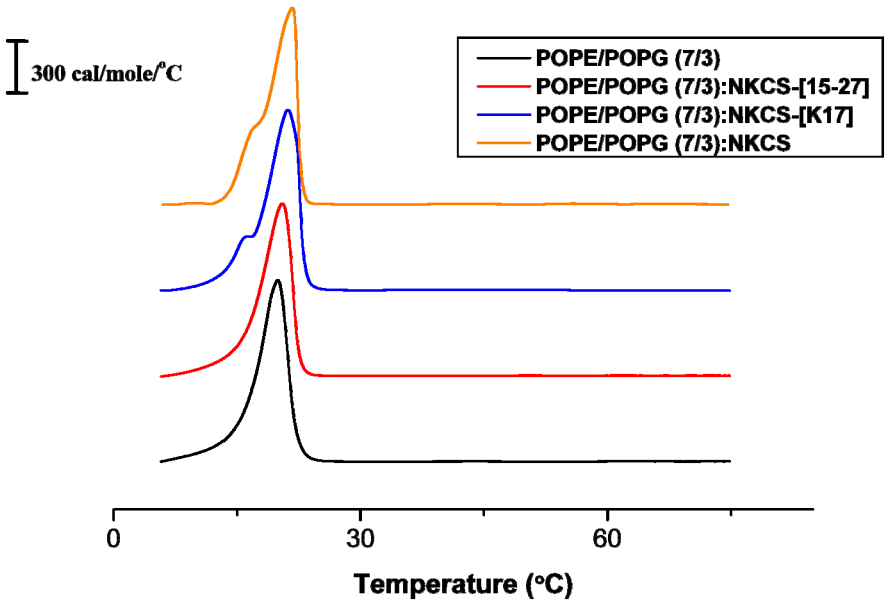

Figure 4.13. Heat capacity function of liposomes composed of POPE (70%) and POPG (30%) mixed with the peptides at the molar ratio 100:1.

The experiment performed with the pure POPE/POPG (7/3) liposomes showed that this system existed in a stable lamellar phase during the measurement in the temperature range from 3°C to 75°C. The single phase transition from gel into liquid crystalline state was recorded at 19.9°C (Fig. 4.13). The observed peak was narrow and symmetrical what indicated a good mixing of phospholipids and cooperative chain melting. Very similar temperature of acyl chain melting was earlier reported for a native *E. coli* membrane [34]. The addition of NKCS-[15-27] to the liposomes did not induce big changes in the system. Despite the high concentration of the peptide (65 μM, what corresponded to the lipid:peptide molar ratio 100:1), there was practically no influence on the lipids phase behavior. The only recorded change was the shift of the phase transition temperature to 20.5°C. This indicated that the binding of NKCS-[15-27] to the phospholipid bilayer was weak, short and insignificant for an overall antibacterial activity.

Different situation was observed for NKCS and NKCS-[K17]. In both cases the phase transition temperature was slightly shifted to the higher values: 21.7°C and 21.2°C, respectively. Moreover, a shoulder of the peak appeared. This indicated the demixing of lipids and the segregation of POPE and POPG into domains, induced by the strong interactions with active NKCS and NKCS-[K17].

Table 4.5: The enthalpy (ΔH) of transition from a gel to liquid crystalline phase, calculated by the integration of the heat capacity curve.

Sample	**Lipid:Peptide molar ratio**	**ΔH (kJ/mol)**
POPE/POPG (7/3)	-	21.2 ± 0.5
NKCS	100:1	21.9 ± 0.5
NKCS-[K17]	100:1	22.0 ± 0.9
NKCS-[15-27]	100:1	19.4 ± 0.9

The enthalpy of liquid crystalline phase transition for POPE/POPG (7/3) liposomes was determined as 21.2 ± 0.5 kJ/mol (Table 4.5). The addition of NKCS and NKCS-[K17] increased this value to 21.9 ± 0.5 kJ/mol and 22.0 ± 0.9 kJ/mol, respectively. This change of enthalpy can be explained by the fact that the peptides induced the formation of domains

within the lipid mixture. These domains underwent the phase transition separately, what was observed in the thermograms as a shoulder indicating two overlapping peaks. The peptide NKCS-[15-27] decreased the enthalpy to 19.4 ± 0.9 kJ/mol.

The DSC technique is a very sensitive tool to study the lipid phase behavior. The results obtained for POPE/POPG (7/3) liposomes before and after the addition of peptides were highly reproducible, what confirmed their reliability.

4.7 ATR-FTIR spectroscopy – the secondary structure and orientation of peptides upon membrane interactions

In the previous experiments the behavior of lipids under the influence of NKCS-derived peptides was shown. In the present chapter the structure and the orientation of peptides upon the membrane association will be presented.

The secondary structure of peptides was studied using ATR-FTIR spectroscopy. This method is a very useful tool commonly applied to determine the structure of these proteins and peptides, which cannot be investigated with other techniques [89, 98-101]. FTIR spectroscopy has many advantages. In contrast to NMR, it requires only a small amount of a peptide. It can successfully replace X-rays crystallography to study the structure of membrane active peptides or membrane proteins. Obtaining high quality crystals of membrane proteins is very difficult. Moreover, crystallography requires replacing a lipid bilayer by detergents. Circular dichroism (CD) spectroscopy also is not suitable to study the peptides structure upon membrane interactions. This method is prone to errors in the presence of lipid vesicles, which scatter the light. An additional advantage of polarized ATR-FTIR is the possibility to gain the information about an orientation of a peptide in a lipid bilayer.

In the ATR-FTIR experiment the mixture of POPE and POPG at the molar ratio 7:3 was chosen to reflect the composition of *E. coli* membrane (Table 1.1). In addition to NKCS, the structure of NKCS-[K17] and NKCS-[15-27] was studied. The motivation for the structure determination of these three peptides was the possibility of direct comparison of their secondary structures and the judgment if the structure may influence the activity.

The results of ATR-FTIR spectroscopy revealed the meaningful differences between the peptides. The spectrum recorded for NKCS showed the peak at 1678 cm^{-1}, what corresponds to a turn, and at 1654 cm^{-1}, what is typical for an α-helical fold (Fig. 4.14). The same structural elements were found for NKCS-[K17], representing the N-terminal fragment of the parental peptide. In the case of NKCS-[15-27] the peak at 1678 cm^{-1} was found, but the spectrum lacked well defined peak at 1654 cm^{-1}. Instead, a peak centered at 1640 cm^{-1} was present, indicating a randomly coiled structure.

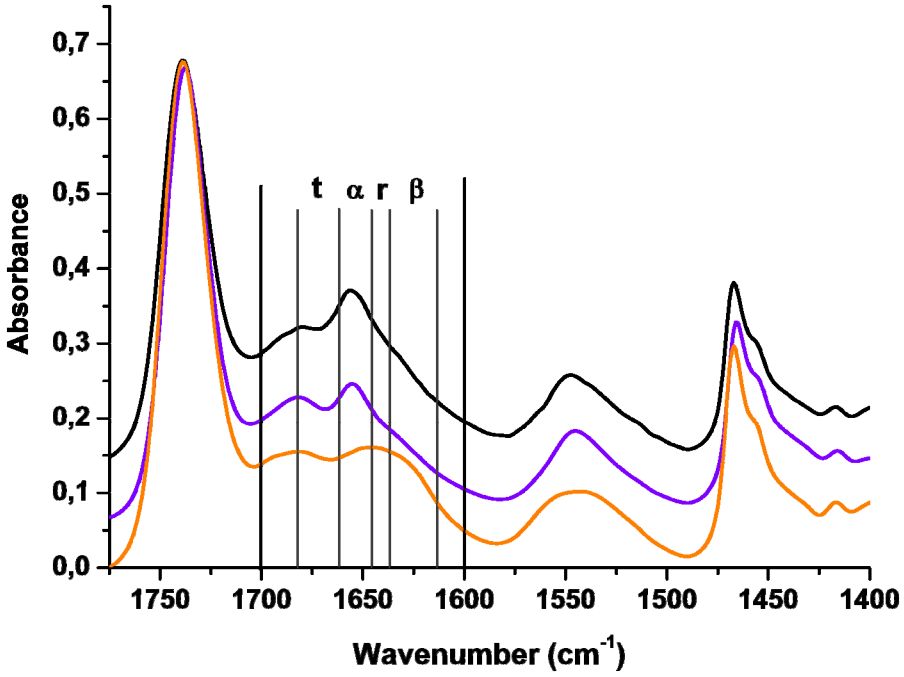

Figure 4.14. The spectra showing the secondary structure of NKCS (black), NKCS-[K17] (violet) and NKCS-[15-27] (orange) upon the interaction with POPE/POPG (7/3) bilayers. The amide I region (1600-1700 cm^{-1}) is marked and divided into subregions corresponding to the structural elements: t, turn; α, α-helix; r, random coil; β, β-strand.

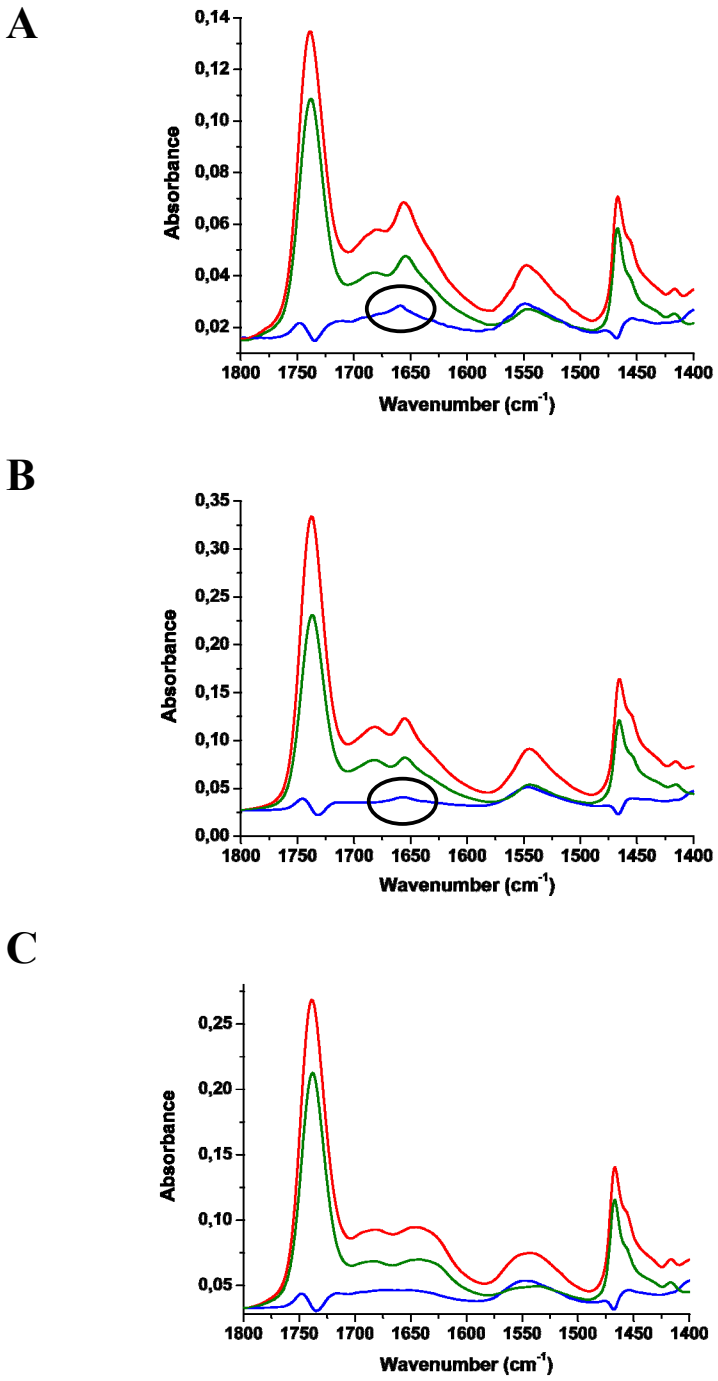

Figure 4.15. The spectra recorded for NKCS (A), NKCS-[K17] (B) and NKCS-[15-27] (C). The dichroic spectrum (blue) is obtained by subtracting the spectrum recorded with perpendicular polarization (green) from the spectrum recorded with parallel polarization (red). The positive deviation in the dichroic spectrum of NKCS and NKCS-[K17] is marked with a circle.

To analyze the orientation of peptides in the bilayer, the spectra were recorded with parallel and perpendicular polarized light with respect to a normal to the germanium plate (Fig. 4.15 A, B and C). The dichroic spectrum was obtained by subtracting the spectrum recorded with the perpendicular polarized light from the one recorded with the parallel polarized light. For the long peptide NKCS the positive deviation around 1655 cm^{-1} was observed, indicating perpendicular orientation of the helix to the bilayer. The dichroic ratio calculated for the α-helix revealed the maximum tilt of approximately 30° from the normal to the germanium plate. The positive deviation was also observed in the case of NKCS-[K17]. The maximum tilt from a germanium plate normal calculated for this peptide was 40°. In contrast, for NKCS-[15-27] there was no specific orientation observed in the amide I region (1700-1600 cm^{-1}) suggesting either an orientation of the peptide at the magic angle or more likely no specific orientation. On the basis of calculated dichroic ratios, a maximum tilt between the lipid acyl chains and a normal to the germanium surface was determined as 5°.

ATR-FTIR spectroscopy is a fast method yielding the information about the structure and orientation of peptides or protein fragments upon the membrane interaction. Establishing a proper peptide:lipid molar ratio was the biggest difficulty encountered during the sample preparation. The ratio used for the experiment described in this chapter was 1:70. It was necessary to apply a concentration high enough to have a sufficient amount of a peptide on the germanium plate. On the other hand, too high concentration of a peptide caused the sample aggregation. Such aggregates cannot be deposited on the germanium surface because they would not form an oriented bilayer. Preparation of POPE/POPG (7/3) : NKCS-[15-27] sample was very challenging. The quality of the spectra obtained for this sample was much worse than the quality of NKCS and NKCS-[K17] spectra. The higher concentration of NKCS-[15-27] resulted however in the formation of aggregates. This aggregation was additionally enhanced by the presence of impurities left after the peptide purification.

4.8 NKCS and NK-2 – similarities and differences

NKCS, as already mentioned in the section 1.3, has been derived from the antimicrobial peptide NK-2. Both sequences comprise 27 amino acids and they differ only at

one position, where cysteine 7 in NK-2 has been replaced by serine in NKCS (Table 4.6). Surprisingly, this apparently insignificant substitution had serious consequences.

Table 4.6: Sequences of NK-2 and NKCS. The peptides differ only at position 7 (marked in red).

Peptide	Sequence
NK-2	K I L R G V C K K I M R T F L R R I S K D I L T G K K
NKCS	K I L R G V S K K I M R T F L R R I S K D I L T G K K
	1 2 3 4 5 6 7 8 9 10 11 12 13 14 15 16 17 18 19 20 21 22 23 24 25 26 27

Both peptides had a very low toxicity toward human cells [74, 77-79, 81] and a very good activity against both Gram-positive and Gram-negative bacteria [74, 78, 79, 81]. The SAXS experiment with POPC revealed that neither NK-2 nor NKCS had any influence on the lipid phase behavior [39, 86]. The results suggested the lack of relevant interactions between the studied peptides and phosphatidylcholine (PC), which is the main phospholipid component of human erythrocytes membrane.

The *in vitro* activity of NKCS against *E. coli* was very comparable to the one of NK-2. However, the outcome of SAXS and DSC measurements of the interactions between these peptides and POPE was highly unexpected. NK-2 decreased the temperature of the inverse hexagonal phase transition from 66.4°C to 61.1°C at the lipid:peptide molar ratio 100:1. At the higher peptide concentration (lipid:peptide molar ratio 30:1) this effect was even more pronounced, and the temperature of the phase transition dropped to 52.3°C [39, 86]. Exactly opposite situation was observed for NKCS. At the lipid:peptide molar ratio 100:1 the peptide shifted the hexagonal phase transition temperature by 11°C to the higher values (the results of this experiment are described in detail in the section 4.5.1.1).

This incredible difference in the way NK-2 and NKCS affect the lipid phase behavior suggests completely different mode of interactions. NK-2 induces a negative curvature within the membrane, what is reflected by a decrease in the phase transition temperature. This peptide destabilizes the bilayer and catalyzes the formation of non-lamellar structures. In contrast, NKCS generates the positive curvature, which inhibits the formation of an inverse hexagonal phase. The interactions with NKCS lead to the changes in biophysical properties of membrane and eventually cause its disruption.

In the second case, in which a significant difference in the behavior of NK-2 and NKCS was noticed, was the activity of peptides against *E. coli* in the excess of divalent cations. The physiological concentration of Ca^{2+} and Mg^{2+} in serum is 3 mM (1 mM of Mg^{2+} and 2 mM of Ca^{2+}) [102]. The experiment was performed in the presence of 10 mM $MgCl_2$ and the results are shown in Fig. 4.16.

Both peptides, when diluted in double distilled water, presented a very good activity against *E. coli* (Fig. 4.16 A). In the presence of Mg^{2+}, the activity of NK-2 significantly decreased (Fig. 4.16 B). At the highest tested concentration of 10 μM, the peptide caused the inhibition of 82% of the culture. NKCS, in the same situation, appeared inactive.

The lack of activity of antimicrobial peptides in an excess of divalent cations can be explained. A cell of *E. coli* is covered by an inner (cytoplasmic) and outer membrane with a thin layer of peptidoglycan between them. The external leaflet of the outer membrane contains lipopolysaccharide (LPS), which is its major component. LPS is a polyanionic molecule. The divalent cations (Ca^{2+} or Mg^{2+}) bind the negative charges of LPS, forming the bridges between the molecules and stabilizing the membrane [103, 104]. The cationic antimicrobial peptides have much higher affinity to the negative charges of LPS than the divalent cations. They replace Ca^{2+} and Mg^{2+}, destabilize the outer bilayer and enter the periplasmic space. However, in the situation where the divalent cations are present in excess, they create a "shield" on the cell surface. In result, the antimicrobial peptides have no access to the sides binding Ca^{2+} or Mg^{2+} on LPS and the peptides appear harmless for bacteria.

Although the behavior of NKCS can be explained with the theory described above, the remaining activity of NK-2 against *E. coli* is striking. It is possible that NK-2 forms dimers, not necessarily via the disulfide bonds between cysteines. The formation of oligomers might be also possible. An accumulation of the positive charges in such an aggregate would explain the remaining affinity to the divalent cation binding sites on LPS, and consequently the antibacterial activity despite the presence of $MgCl_2$. The dimers/oligomers may have a different effect on the lipid phase behavior, what was observed in SAXS experiments. The assumption that NK-2, in contrast to NKCS, does not act as a monomer, can elucidate why only a single amino acid substitution leads to such big differences in the activity against bacterial cells or in the interactions with the artificial lipid systems. This hypothesis requires a further investigation.

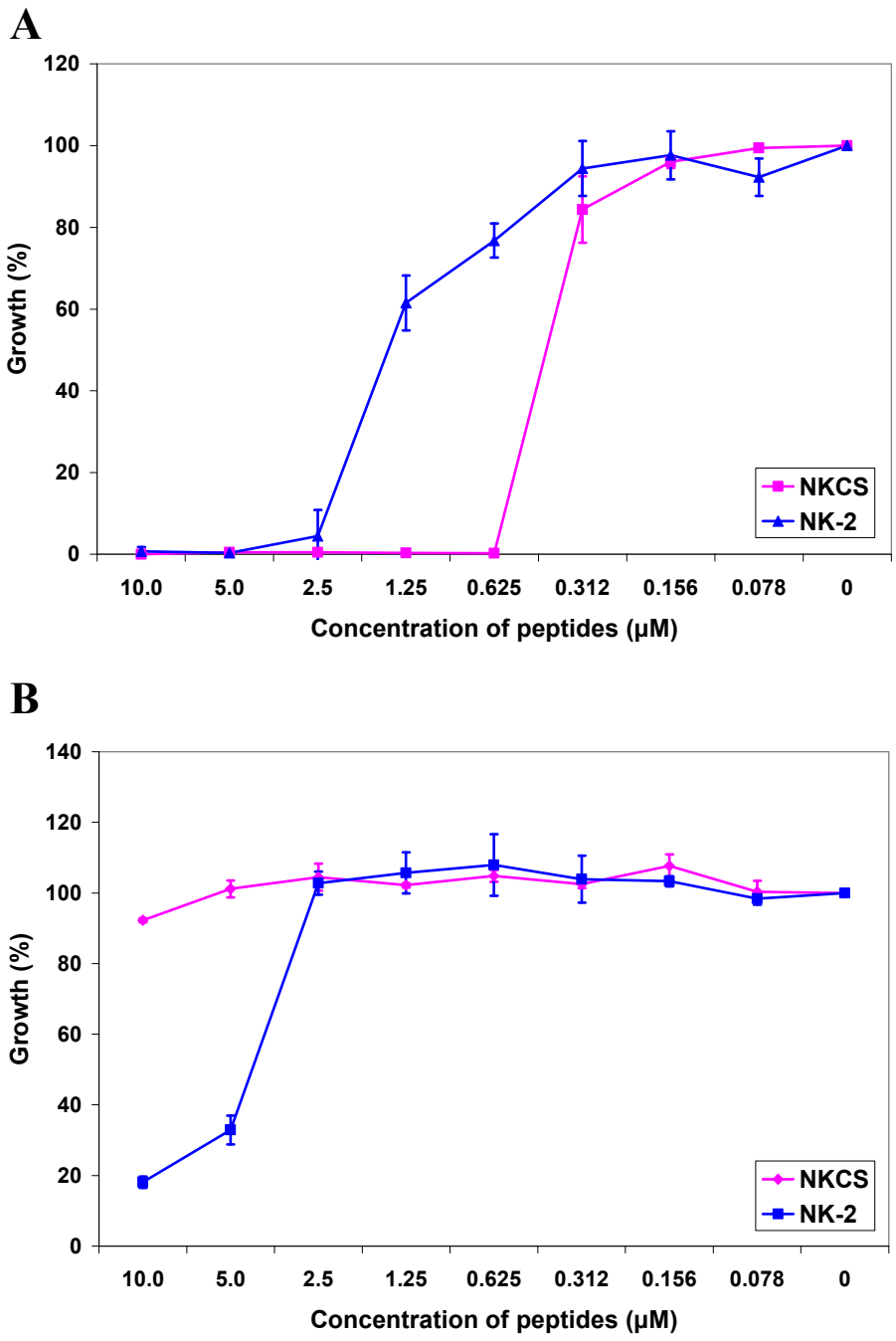

Figure 4.16. Activity of NKCS and NK-2 against *E. coli*. (A) The peptides were diluted in double distilled water. (B) The peptides were diluted in double distilled water in the presence of 10 mM $MgCl_2$.

The comparison between NK-2 and NKCS has been published in a peer reviewed book chapter: A. Rzeszutek, R. Willumeit, **Antimicrobial peptides and their interactions with model membranes**, in: A. Iglic (Ed.), Advances in Planar Lipid Bilayers and Liposomes, vol. 12, Academic Press, 2010, pp. 147-165.

5 Discussion

5.1 Biological activity and amphipathicity

The peptide NKCS is very active against both Gram-negative and Gram-positive bacteria, with negligible toxicity toward human erythrocytes. The substitution of single amino acids, resulting in two new peptides NKCS-[DK] and NKCS-[DA], did not have a significant influence on the antibacterial activity. The further modifications, based on the division of a parental sequence into two fragments corresponding to the N-terminal and C-terminal parts, had an interesting outcome. The results of antibacterial tests revealed, that only the N-terminal fragment is crucial for the interactions with the cytoplasmic membrane of microorganisms. The MIC of all peptides representing this part of NKCS together with the long NKCS-analogs is equal or lower than 5 μg/mL (Table 4.3). According to Hancock et al. [96], the antimicrobial peptides can be considered as active in the *in vitro* tests if they show the MIC in the range 1-8 μg/mL. In contrast, the C-terminal part (namely NKCS-[15-27]) inhibits the growth of *B. subtilis*, but it is harmless for *E. coli* and *S. carnosus*. The modification resulting in an equal distribution of positive charge (peptide NKCS-[15-27]-S]) was a step in a good direction, leading to the improvement of activity.

The comparison between the activity of peptides against Gram-positive and Gram-negative species revealed interesting results. A clear difference in the activity against Gram-negative *E. coli* and Gram-positive *B. subtilis* was observed. It can be easily explained by a difference in the cell surface morphology of these two strains. Surprisingly, the activity against the second Gram-positive strain, *S. carnosus*, does not resemble the activity observed for *B. subtilis*, but rather shows the pattern comparable to the one recorded for *E. coli*. It is possible that the phospholipid compositions of the cytoplasmic membrane of *S. carnosus* and

E. coli are very similar, however, it is only the speculation, because no information on the membrane composition of the former strain can be found.

The antimicrobial peptides are characterized by a high amphipathicity. The arrangement of cationic and hydrophobic amino acids on two different sides of a peptide is essential for the successful interactions with the cytoplasmic membrane of pathogens. The accumulation of cationic residues enables the electrostatic attraction to the negatively charged bacterial surface. On the other hand, the hydrophobic face facilitates the interactions with the nonpolar core of a lipid bilayer.

Table 5.1: The values of hydrophobic moment (μ_H) and minimal inhibitory concentrations (MIC) expressed in μM. The peptides are segregated from the highest value of μ_H, indicating the highest amphipathicity, to the lowest one.

Peptide	μ_H	**MIC (μM)**		
		E. coli	***B. subtilis***	***S. carnosus***
NKCS-[14]-2	24.93	1.14	1.14	1.14
NKCS-[DA]	15.52	1.14	0.568	1.14
NKCS-[15-27]-S	13.59	> 9.09	2.27	9.09
NKCS-[DK]	13.38	0.568	0.568	0.568
NKCS-[17VF]	13.05	2.27	2.27	1.14
NKCS	12.62	0.586	1.14	0.568
NKCS-[VM-KR]	11.86	2.27	0.568	1.14
NKCS-[K17]	11.11	2.27	0.568	1.14
NKCS-[15-27]	7.92	> 9.09	2.27	> 9.09

The amphipathicity of peptides was determined as a hydrophobic moment (μ_H). The values of hydrophobic moment together with the MIC are presented in Table 5.1. NKCS, its analogs with the single amino acid substitutions (NKCS-[DA] and NKCS-[DK]) and the shorter derivatives representing the N-terminal fragment, have the hydrophobic moment in the range from 11.11 to 15.52. These peptides are characterized also by a very good antimicrobial activity. The least active peptide NKCS-[15-27] shows the lowest hydrophobic moment

(7.92). However, the peptide NKCS-[15-27]-S, composed of the same amino acids as NKCS-[15-27], but organized in a way yielding an equal redistribution of positive charge along the sequence, has much better amphipathicity (hydrophobic moment: 13.59). The enhancement of the amphipathicity, obtained by the segregation of amino acids, results in an improved activity against *E. coli* and *S. carnosus* (Fig. 4.4 B and Fig. 4.6 B). Surprisingly, the peptide NKCS-[14]-2, characterized by a very high value of the hydrophobic moment (24.93), does not show an outstanding antibacterial activity.

These results show that the exact correlation between the hydrophobic moment and MIC is not possible (Table 5.1). Such interdependence is very difficult to obtain for antimicrobial peptides in general [105]. This results from the fact that the hydrophobic moment is calculated with the assumption that a peptide adopts an ideal α-helix upon the membrane association. The experiments show however, that a helical content of peptides is very often much smaller than 100%. For example, the peptide NK-2, which is a precursor of NKCS (described in chapters 1.3 and 4.8 of this work), contains only 46% of helical structure [106]. Moreover, in many cases, the distribution of polar and hydrophobic residues along the peptide is not regular. Therefore, the regions with higher or lower hydrophobic moment of a peptide can be found [105].

5.2 Interactions with single-lipid membranes

The analysis of peptides activity against *E. coli* and *S. carnosus* revealed that particular fragments of NKCS show different toxicity. The most striking difference was observed between the N- and C-terminal parts, comprising the residues 1-17 and 15-27, respectively. To understand the mechanism involved in the bacteriostatic activity, three peptides were chosen for a detailed investigation: the active NKCS-[K17] related to the N-terminal part, the inactive NKCS-[15-27] representing the C-terminal fragment and NKCS as a reference. Since the phospholipid composition of *E. coli* cytoplasmic membrane is well known (Table 1.1), the bacterium was chosen as a model microorganism to investigate the mechanisms involved in peptide-membrane interactions. The artificial lipid systems, mimicking the bacterial cytoplasmic membrane, were applied for the biophysical studies.

Phosphatidylethanolamine (PE) is the major lipid present in the membrane of *E. coli* (Table 1.1). The molecule of PE is zwitterionic and it does not carry a net charge at neutral pH. Another zwitterionic phospholipid is phosphatidylcholine (PC), which does not exist in the bacterial cell, but dominates in the outer leaflet of erythrocytes cytoplasmic membrane. The neutral surface of red blood cells decides about the lack of interactions with the cationic antimicrobial peptides. Initially the similar results were expected for the interactions of NKCS with PE. However, the SAXS experiment delivered the evidence that the interactions of antimicrobial peptides with PE are possible. Despite an apparent similarity between PE and PC, there is an important difference in their structure. The head group of PC is built of a voluminous trimethylamine group, which shields the negative charge of the phosphate like an umbrella. Such bulky head group determines a cylindrical shape of molecule (Fig. 1.4). The electrostatic interaction is the force attracting the peptides to the bacterial surface. Since the only negative charge of phosphate is hidden, the binding of NKCS to the PC bilayer does not occur. Consequently, the peptide is harmless for the human erythrocytes [39]. In contrast to PC, the head group of PE is much smaller. It contains only three hydrogen atoms bound to the nitrogen. The small head group and the space consuming acyl chains decide about a molecular shape of PE, which can be characterized as a truncated cone (Fig. 1.4). The possibility of binding NKCS to a PE membrane indicates that the negative charge of phosphate might be partially exposed on the surface. This hypothesis is confirmed by the Zeta-potential measurements, reported by Willumeit et al. [86]. The results presented in the mentioned work reveal that the surface of PE liposomes has the potential of -32.4 ± 3.4 mV, whereas the potential of phosphatidylcholine is determined as -2.3 ± 2.0 mV.

All three peptides: NKCS, NKCS-[K17] and NKCS-[15-27] behaved in a similar way. They did not induce the formation of cubic phases, however, they were able to modulate the temperature of the inverse hexagonal phase transition. The change was always toward higher temperature values, what implied a stabilization of a membrane bilayer structure. The increase of the phase transition temperature leads also to the formation of positive curvature. This observation is very interesting in the case of PE. Phosphatidylethanolamine lipids are known as non-bilayer-prone molecules. It means that the membrane composed of them tends to adopt a spontaneous negative curvature, which eventually brings to the formation of an inverse hexagonal phase. The addition of the investigated peptides inhibited the process of membrane "curling" and induced the rigidification of bilayer. In consequence, much higher temperature

had to be applied to force the system to undergo the bilayer – non-bilayer transition. The membrane stiffening and changes in the spontaneous curvature have the repercussions on the bacterial physiology. The addition of NKCS modifies the biophysical properties of membrane and prevents the formation of non-lamellar structures. Since these structures intermediate the cell division process, their inhibition does not allow the cells to divide.

The three PE lipids, namely POPE, DiPoPE and DOPE-trans, chosen for the experiment present an extraordinary example of how the acyl chains composition changes the physicochemical properties of a lipid molecule. The acyl chains have a profound effect on the temperature of transition from a gel to a liquid crystalline phase (T_m). According to the results presented in the section 4.5.1.1, the fluid disordered structure of POPE (acyl chain composition: 16:0-18:1) appears at 25°C. The lipid DiPoPE, with two identical unsaturated chains (16:1-16:1), undergoes this transition at -33.5°C [84], whereas the lipid DOPE-trans, characterized by little longer acyl chains (18:1-18:1), at 38°C (section 4.5.3). The addition of peptides has an interesting effect. The results show that the influence of peptides on a bilayer structure strongly depends on the state of lipids at which the peptides are added.

Table 5.2: The influence of NKCS-[K17] on the inverse hexagonal phase transition temperature depends on the acyl chain state at which peptide is mixed with the lipid vesicles. The presented results were obtained for NKCS-[K17] added to the lipids at the molar ratio 1:100. The samples were prepared at the room temperature, at which DOPE-trans is in the gel phase, DiPoPE in the liquid crystalline phase and POPE on the edge of the phase transition.

	Lipid		
	DOPE-trans	**POPE**	**DiPoPE**
T_m of pure lipids (°C)	38.0	25.0	-33.5
ΔT_H after the addition of NKCS-K17 (°C)	+5	+13	+13

When NKCS-[K17] was mixed with DiPoPE vesicles (lipid:peptide molar ratio 100:1) at the room temperature (~24°C), at which the lipid existed in the liquid crystalline phase, the peptide had a significant influence on the hexagonal phase transition temperature, which was shifted by 13°C (Table 5.2). The similar effect was observed for POPE. The peptide added on the edge of T_m also induced the change of 13°C. Much lower influence was however observed

in the case of DOPE-trans. At the room temperature, at which the peptide was mixed with the lipid vesicles, DOPE-trans was still in the solid ordered phase. This state prevented the strong peptide-membrane interactions, what was reflected by a little influence of NKCS-[K17] on the hexagonal phase transition.

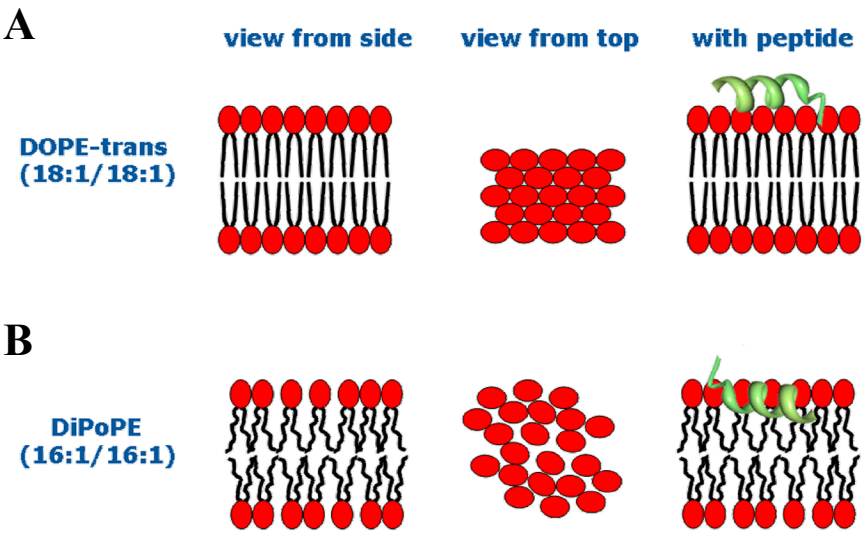

Figure 5.1. The simplified model presenting the interaction of antimicrobial peptides with a membrane in a gel phase (A) and liquid crystalline phase (B).

The explanation of described results can be found in the nature of a bilayer existing in a gel and a liquid crystalline state. In a gel phase the interactions between the acyl chains are very strong and in result the hydrophobic core of a bilayer is highly ordered (Fig. 5.1 A). Moreover, the head groups are tightly packed. The interactions between a peptide and membrane in such a solid state are superficial and limited only to the interactions with the head groups. Since PE is less negatively charged than PG, the electrostatic binding is also weak. In contrast, membrane in a liquid crystalline phase is characterized by high fluidity and disorder of acyl chains (Fig. 5.1 B). The head groups are randomly organized. In such a liquid disordered state the area per molecule is approximately 25% bigger than the area per molecule in a gel phase [34]. Consequently, there is more free space between the head groups. Since the

peptides adopt an amphipathic structure upon the association with a membrane, two different types of interactions are possible with a fluid lipid bilayer. The polar side of positively charged peptide binds to the negative charges of phosphate groups. Since there is a free space between the head groups, the peptide binding leads to their further disorganization. In result, the intercalation into the bilayer and the hydrophobic interactions with the acyl chains are possible. The peptide embedded into a fluid membrane induces stronger changes in the bilayer structure than the peptide superficially interacting with a membrane existing in a gel phase.

Table 5.3: Minimal inhibitory concentration (MIC) of peptides determined for *E. coli* and their influence on the inverse hexagonal phase transition of three different PE lipids at the lipid:peptide molar ratio 100:1, expressed as ΔT. The temperature of phase transition was determined with ± 2°C of measurement error.

Peptide	**MIC (μM)**	**POPE**	**DiPoPE**	**DOPE-trans**
NKCS	0.568	+11°C	+4°C	+6°C
NKCS-[K17]	2.27	+13°C	+13°C	+5°C
NKCS-[15-27]	> 9.09	+6°C	+6°C	+0°C

It is possible to draw a correlation between antimicrobial activity of peptides and their influence on the inverse hexagonal (H_{II}) phase transition. Such interdependence can be observed especially in the case of POPE and DOPE-trans. POPE, due to its head group and acyl chains, is the most representative for the composition of the *E. coli* cytoplasmic membrane (Tables 1.1 and 1.2). The active peptides NKCS and NKCS-[K17] shift the H_{II} temperature to the higher values by 11°C and 13°C, respectively. NKCS-[K17], although characterized by a slightly higher MIC, affects the POPE bilayer stronger than NKCS. The peptide interacts with the lipids more effectively, causes the rigidification and stabilization of the bilayer, what is visible in the higher temperature of phase transition. The less active NKCS-[15-27] also interacts with the liposomes, but it is not able to significantly change the physicochemical properties of lipids and its influence on the phase transition is much smaller. The discrepancy between antibacterial activity of NKCS and NKCS-[K17] and their influence on the lipid phase behavior can be explained by the fact that a bacterial cell is more complex than a single-lipid liposome. Consequently, the mechanism of killing is a more complicated

process, which cannot be fully reflected by such a simple system as the one used for the SAXS measurements. Moreover, the difference of 2°C is negligible, because it stays in the margin of measurement error.

The second system which is affected by the peptides in the way similar to POPE, is DOPE-trans. Here however the changes are much smaller. This directly results from a different physicochemical nature of DOPE-trans liposomes and is elucidated in detail earlier in this section.

The results obtained for the third lipid used for the SAXS experiment, DiPoPE, correlate well with a very high activity of NKCS-[K17]. The temperature of H_{II} phase transition was shifted by 13°C. Surprisingly, the interactions between DiPoPE and NKCS were weaker than the interactions with NKCS-[15-27]. The results imply that the interactions of NKCS and NKCS-[K17] with various PE bilayers involve different mechanisms, although the antibacterial activities are comparable. Such behavior is possible due to a different length of both peptides. Moreover, as predicted by Monte Carlo simulations, NKCS does not resemble a rigid α-helical rod, but rather two α-helices separated by an unstructured flexible region. This unstructured region may enforce a different behavior of NKCS upon membrane binding.

SAXS is a very useful tool commonly applied to analyze the lipid phase behavior under the influence of peptides. Unfortunately, not all lipids are suitable for this kind of measurements. The main condition that must be fulfilled is the ability of lipids to form multilamellar vesicles. Only such liposomes, composed of several layers, give the clear Bragg's reflections.

PE lipids have a strong tendency to form multilamellae. The weak point of the systems composed of pure POPE, DiPoPE or DOPE-trans is that they easily aggregate. The big aggregates cannot be transferred to the capillaries. Moreover, the process of aggregation removes the water from the liposomes, what has a very strong influence on the physicochemical properties of lipid bilayers. The preparation of samples, in particular ensuring the same conditions and good hydration, was difficult and crucial for the reproducibility of measurements.

The second problem encountered during the SAXS measurements was connected with the temperature control. The sample holder at A2 beamline is a metal block with two apertures, through which the X-rays beam hits a sample in a capillary. Although the

temperature of the metal can be well controlled, there is the exchange of heat between the metal block and air in an aperture. Consequently, the temperature of a sample in the capillary might be slightly different from the temperature of the sample holder itself. In result, the recorded values of temperatures at which the phase transitions are observed can carry an error of ±2°C.

5.3 Interactions with a binary lipid system

The mixture of POPE and POPG at the molar ratio 7:3 was chosen to reflect the composition of *E. coli* cytoplasmic membrane (Table 1.1). According to the DSC results, this system forms stable bilayers at least up to 75°C (Fig 4.13). Due to the presence of the negatively charged POPG, the liposomes are unilamellar. This excludes the possibility to employ the SAXS technique, but enables the application of POPE/POPG (7/3) mixture for the DSC studies (section 4.6).

The results of microcalorimetry revealed a remarkable difference between the behavior of active peptides (NKCS and NKCS-[K17]) and the peptide NKCS-[15-27], which was inactive against *E. coli* in the range of studied concentrations. The inactive peptide did not influence the bilayer structure and the thermogram looked almost the same as for pure POPE/POPG (7/3) vesicles (Fig. 4.13). The only change was a small shift in the acyl chain melting temperature from 19.9°C to 20.5°C. Although the peptide NKCS-[15-27] is positively charged (its net charge is +5), it is not able to adopt an amphipathic structure. The amphipathicity guarantees a high local density of positive charge and enhances the electrostatic interaction with the negatively charged phospholipids. In contrast to NKCS-[15-27], the addition of NKCS and NKCS-[K17] induced the changes in the lipid system, which were recorded as a shoulder of the main peak. The shoulder indicated two overlapping peaks. This observation can be explained. Highly active cationic NKCS and NKCS-[K17], able to adopt an amphipathic structure, interacted strongly with the negatively charged POPG, inducing the migration of this anionic lipid to the sites of association. The domains of POPG interacting with the peptide were formed. The shoulder visible on thermograms indicated a new fraction, with the temperature of acyl chain melting (T_m) lower

than T_m of the POPE/POPG (7/3) mixture. It means that the peptides interacting with the areas of fluid PG intercalated into the bilayer. This intercalation caused the stiffening of domains enriched in PG. In result, the temperature of acyl chain melting of POPG (found at 1°C for the pure lipid, Table 3.1) significantly increased upon the interaction with the active peptides. These results provide evidence that the positive charge alone does not ensure successful interactions and the organization of positively charged amino acids in an amphipathic structure is crucial.

The observation that cationic antimicrobial peptides are able to demix lipids in the artificial membranes mimicking the bacterial cytoplasmic membrane was reported earlier by Arouri et al. [107]. The authors of this work studied the interactions of hexapeptide Ac-RW and its cyclic analog C-RW with the binary lipid systems: DPPG/DPPE (1/1) and DPPG/DPPE (3/1). In both cases the peptides caused the lipid demixing and two well separated peaks appeared: one of them corresponded to DPPG-rich domain with bound peptides and the second peak corresponded to the domain enriched in DPPE mixed with the remaining DPPG and peptides.

5.4 The secondary structure and membrane orientation of peptides

The antimicrobial peptides are characterized by flexibility in adaptation of a secondary structure. In an aqueous solution they are usually randomly coiled whereas they fold in an α-helix or a β-strand upon the membrane interactions. The conformation of NKCS in water and in the presence of SDS mimicking a hydrophobic environment was studied previously [81] by circular dichroism (CD) spectroscopy. According to the results presented in the mentioned work, the peptide NKCS is randomly coiled in double distilled water, but in the presence of 10 mM SDS (critical micelle concentration (CMC) of SDS is 8 mM) it folds in an α-helical structure. In the same work the *in silico* analysis of the secondary structure of NKCS was described. According to the Monte Carlo simulations, upon the membrane association

NKCS does not resemble a rigid α-helical rod, but it is rather composed of two helices connected by a more flexible region comprising threonine 13 and phenylalanine 14.

ATR-FTIR spectroscopy was used to determine the secondary structure of the peptides upon the interactions with POPE/POPG (7/3) membrane. The spectrum recorded for NKCS revealed two peaks: one corresponding to an α-helix and the second one corresponding to a turn. This turn can be assigned to a flexible hinge (threonine 13 and phenylalanine 14) connecting the N- and C-terminal fragments of the peptide. The identical structural elements were found in the spectrum obtained for NKCS-[K17]. The results showed that the C-terminus of NKCS, represented by the peptide NKCS-[15-27], did not adopt a well defined secondary structure. Instead, it presented the mixture of random coils and turns.

On the basis of the outcome of ATR-FTIR spectroscopy and DSC experiments it is possible to draw an important conclusion regarding NKCS and its interaction with the membrane of *E. coli*. It has been proved that both NKCS and NKCS-[K17] (representing the N-terminal fragment of NKCS) adopt an α-helical structure upon the membrane association. Such behavior is typical for many active antimicrobial peptides. Changing the environment from hydrophilic (water) to hydrophobic (membrane interior) requires partitioning into the water-membrane interface. This partitioning is connected with a high energy barrier. To overcome this barrier a peptide must adopt an ordered secondary structure [108]. Only then the interaction with the lipids of the cytoplasmic membrane is possible and only the peptides fulfilling this condition can be effective antimicrobial agents. In contrast to the whole NKCS sequence and the peptide corresponding to its N-terminus (NKCS-[K17]), the 13-amino-acid fragment representing the C-terminus (NKCS-[15-27]) appears inactive against *E. coli* in the range of tested concentrations. The lack of activity is connected with the fact that this particular fragment alone is not able to adopt a defined secondary structure upon the membrane interaction. This inability has the consequences observed in DSC experiment. NKCS-[15-27], unable to fold into a well defined amphipathic α-helix with a high density of positive charges, cannot interact with POPE/POPG bilayer effectively enough to cause changes in the lipid phase behavior. Since there is no interaction, or the interaction is short-term and very weak, the peptide is harmless for bacteria.

The ATR-FTIR spectroscopy provided also the information about the orientation of the peptides in the lipid bilayer. The maximum tilt of NKCS from a normal to the membrane surface was approximately 30°, indicating that the peptide or its part was oriented almost

perpendicularly to the lipid bilayer. The maximum tilt calculated for NKCS-[K17] (the N-terminal fragment) was 40°. In contrast, NKCS-[15-27] did not show any preferential orientation.

Based on these results, it is possible to build a model presenting how NKCS is oriented upon the membrane association (Fig. 5.2). Since the peptide is almost perpendicular to the membrane surface, it can be assumed that it adopts a transmembrane orientation (Fig. 5.2 A). In such situation the peptide would most likely resemble an α-helical rod and the flexible kink connecting the N- and C-terminal fragments would not be detected in the spectrum. Since the results of ATR-FTIR revealed in the structure of NKCS a turn, which can be assigned to the abovementioned kink, the transmembrane orientation of the peptide seems to be unlikely.

The second model is shown in Fig. 5.2 B. Here only the N-terminal part of NKCS is embedded in the membrane at the angle of 30° to a bilayer normal. The C-terminal part is localized on the surface, parallel to the bilayer. Although ATR-FTIR spectroscopy is a very useful technique, the orientation determination can be difficult. For example, the part of peptide or protein perpendicularly oriented with respect to the membrane absorbs the infrared light stronger that the part oriented parallel and thus the part localized parallel might not be seen in the spectrum. Such a situation was very likely to occur also in the case of NKCS. Only the orientation presented in Fig. 5.2 B can explain the presence of the turn in the FTIR spectrum. The possibility that the C-terminal fragment is embedded into the bilayer and the N-terminal helix lays on the surface must be excluded. The dichroic spectrum obtained for NKCS-[K17] (the N-terminal fragment) revealed that this peptide is also inserted into the bilayer with the maximal tilt of 40° from a bilayer normal. In addition, the C-terminal fragment (studied as the peptide NKCS-[15-27]) has a very low affinity to the lipid bilayer (shown in the antibacterial assay and subsequently proved by SAXS and DSC results). Since the exposure of polar residues to the hydrophobic core of the bilayer is energetically unfavorable, NKCS must form clusters (Fig. 5.2 C). In such clusters the polar amino acids of one peptide monomer can interact with the polar amino acids of the other monomer, whereas the hydrophobic residues can interact with the lipid acyl chains.

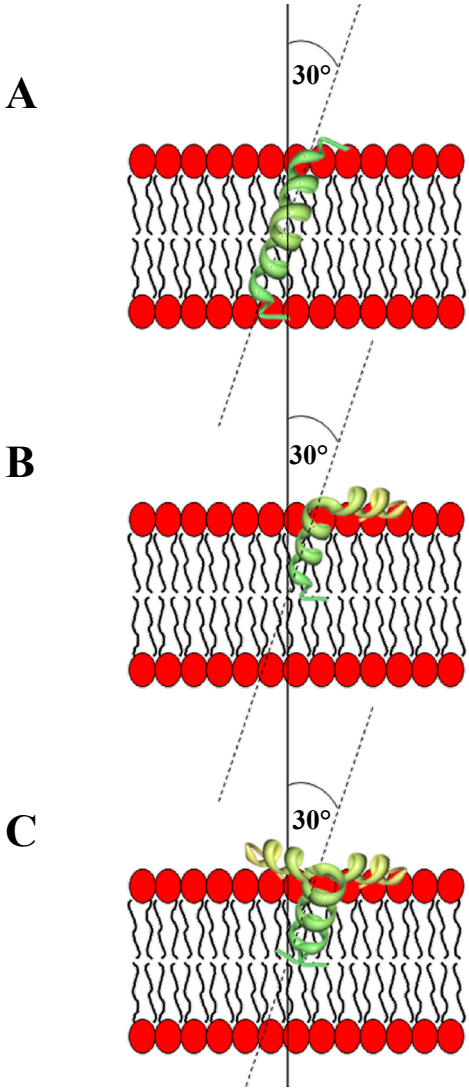

Figure 5.2. Orientation of NKCS upon the interaction with a model lipid bilayer. (A) Fully transmembrane orientation. (B) Orientation at which only the N-terminal part of the peptide is inserted into the membrane and the C-terminal part lays on the bilayer surface. (C) Orientation similar to the one presented in (B), but with NKCS forming the clusters.

The performed ATR-FTIR experiment gives a very good idea about how the peptide NKCS looks like upon the membrane interactions. It must be underlined however that the obtained results are not definite and should be confirmed by a more precise technique, such as NMR, which would allow for the orientation determination with a high resolution [109]. Moreover, it cannot be excluded that the orientation of NKCS, similar to melittin, depends on

the peptide concentration [97]. The concentration effect on the peptide orientation was not studied in this work. An additional aspect, which cannot be solved with the ATR-FTIR, is whether the peptide is embedded into the membrane within the induced domains (the presence of which was shown by DSC) or rather on their borders.

5.5 Possibility of pore formation

In the SAXS experiment, in addition to the lipid phase behavior, also the influence of the peptides on the membrane thickness was investigated. The membrane thinning has been considered as a prerequisite and an intermediate step in the mechanism of pore formation [110, 111]. Recent research revealed however that the pore formation might occur without the membrane thinning [112]. According to this theory, a possible deformation of the bilayer might be imposed by a hydrophobic matching. Hence, the membrane thinning can be observed when the peptide is shorter than the hydrophobic core of the bilayer. In such situation, in order to prevent the exposure of hydrophobic lipid segments to water and to compensate for the unfavorable hydrophobic interactions, the membrane will deform. This deformation will be observed as a decrease in thickness (Fig. 5.3 A). On the other hand, if the hydrophobic peptide length exactly matches the hydrophobic lipid core, there is no change in the membrane thickness, however the pore formation cannot be excluded (Fig. 5.3 B). If the peptide is much longer than the core of the bilayer, an increase in thickness might be observed (Fig. 5.3 C, D).

In the performed experiment the repeat distance in the pure POPE multilayers and the repeat distance in POPE multilayers after the addition of peptides were changing in the same manner in the course of heating (Fig. 4.10). The membrane thickness was not affected by the peptides. Based on the theory that membrane thinning is a prerequisite of pore formation, it is possible to conclude that the interactions between NKCS and POPE bilayer do not lead to the creation of pores.

One can argue however, that according to the hydrophobic matching theory, a membrane thickness may not be altered, but the pore formation would be still possible (Fig. 5.3 B). In such situation the hydrophobic length of NKCS would have to match the

hydrophobic core of POPE bilayer. If we assume that NKCS forms an ideal α-helix in which the distance between two amino acids along the axis is 1.5 Å, the peptide should be 40.5 Å long [27].

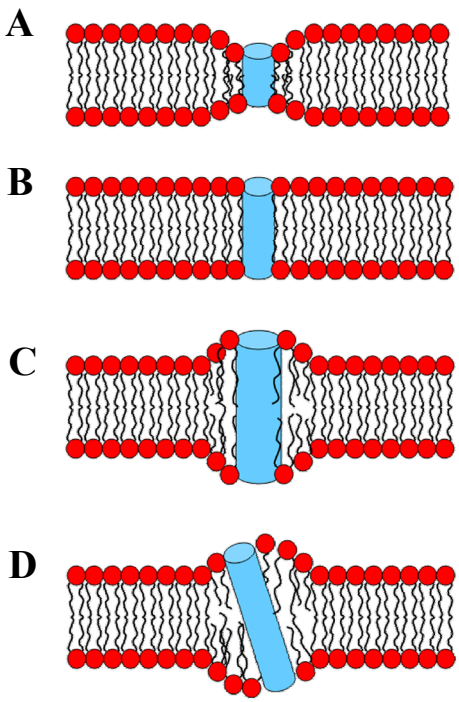

Figure 5.3. Representation of the hydrophobic matching theory. A pore formed by peptides is depicted as a blue cylinder. When the hydrophobic peptide length is shorter than the hydrophobic core of the bilayer, a decrease in the bilayer thickness occurs (A). No membrane deformation is observed when the hydrophobic peptide length matches the core of the bilayer (B). An increase in bilayer thickness results from the insertion of long peptides vertically (C) or at an angle (D).

The length of the hydrophobic core of POPE bilayer can be calculated from the electron density profile. Rappolt et al. [113] performed a detailed structural analysis of POPE in a lamellar liquid crystalline and inverse hexagonal phase. In their work they report the repeat distance (*d*) in POPE liposomes equal to 52.9 Å at 35°C. This value is comparable with the value obtained in the experiment described in the section 4.5.1, where the repeat distance is equal to 53.6 ± 1.1 Å at 35°C. Based on the electron density maps, the authors of the mentioned work performed the decomposition of the lamellar *d*-spacing into structural

components, such as the thickness of bilayer (d_B = 47.5 Å) and the thickness of water layer between the bilayers (d_W = 5.4 Å). Assuming that the size of PE head group is 8 Å [113], it is possible to determine the length of the hydrophobic core as 31.5 Å (Fig. 5.4).

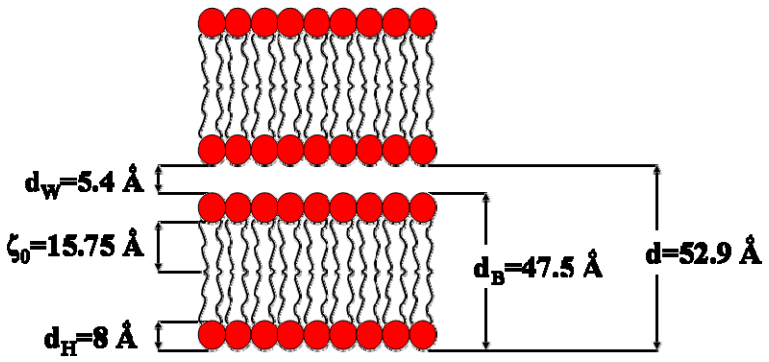

Figure 5.4. Distances in the POPE bilayer at 35°C, calculated on the basis of Ref. [113]; d, repeat distance; d_B, thickness of the bilayer; d_W, thickness of water layer between two bilayers; d_H, size of the headgroup; ζ_0, average length of the hydrocarbon chains.

Comparing the hydrophobic core length of POPE with the length of NKCS, the prospect of the pore formation without the membrane thickness deformation cannot be excluded. Since the peptide is inserted at the angle of 30° to a membrane normal, the minimum length of NKCS should be 36.4 Å to match only the hydrophobic core of the POPE bilayer, and maximum of 54.8 Å to match the thickness of the hydrophobic core together with the head groups (Fig. 5.5). On the other hand, the results of FTIR indicate that the peptide NKCS does not adopt fully transmembrane orientation, but rather remains in a helix-kink-helix fold, with the N-terminal part inserted into the membrane and the C-terminal fragment localized on the surface of the bilayer (Fig. 5.2 B). Assuming that the N-terminal helix (12 amino acids) and one amino acid of the kink are inserted into the bilayer, it gives in total 13-amino-acid fragment with the length of only 19.5 Å. Based on these results it is possible to exclude the possibility of the pore formation by NKCS.

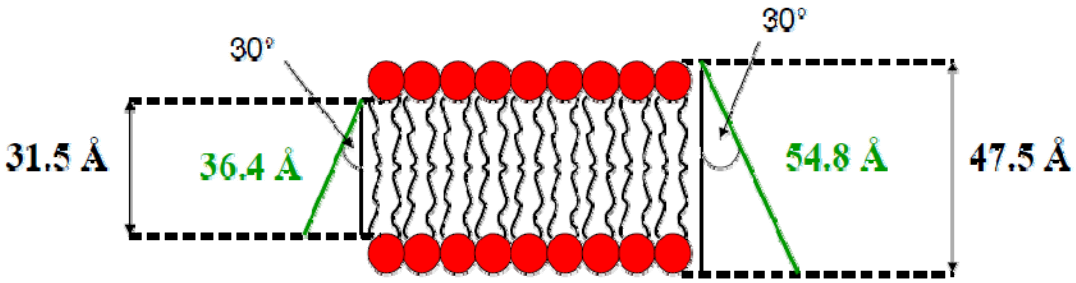

Figure 5.5. The schematic picture used to calculate the minimal (36.4 Å) and maximal (54.8 Å) length of the peptide necessary for the transmembrane orientation in the process of pore formation without altering the membrane thickness.

5.6 NKCS – mode of action

On the basis of the results presented in this work it is possible to build a model mechanism involved in the inhibition of *E. coli* growth, caused by the antimicrobial peptide NKCS.

In an aqueous solution, far from the cell surface, NKCS is randomly coiled, but upon the membrane association it adopts an α-helical structure. The peptide is positively charged (the net charge of the molecule is +10) and the main force driving the attachment to the membrane is the electrostatic interaction with the anionic phosphatidylglycerol (PG). Cationic NKCS has a high affinity to the negatively charged phospholipids and it induces the migration of PG to the sites of peptide binding. In result, the domains enriched in PG-NKCS are formed. The SAXS measurements show that the interactions between the peptide and zwitterionic phosphatidylethanolamine (PE) are possible, most likely due to the nature of PE: the negative charge of the phosphate group is partially exposed on the surface, what makes PE bilayer slightly anionic. The same experiment shows that NKCS does not induce membrane thinning, what in most cases is considered as a prerequisite of pore formation. Although the hydrophobic length of NKCS is sufficient for the formation of pores without altering the membrane thickness, the FTIR spectroscopy indicates that the peptide is only partially

embedded into the bilayer rather than adopting a fully transmembrane orientation. When the N-terminal helix is inserted almost perpendicularly to the membrane plane, the C-terminal fragment stays on the bilayer surface where it can interact with the lipid head groups. These results suggest that the interactions between NKCS and the cytoplasmic membrane of *E. coli* resemble the so-called "carpet" model, but only to a certain degree.

In a "carpet" mechanism peptides accumulate on the surface of a bilayer (Fig. 1.1 C). Four steps are involved in this model [114]. At first the positively charged peptides are attracted to the negative membrane surface. Subsequently, the peptides are bound to the membrane in such a way that the positively charged residues can interact with the negatively charged phospholipid head groups. In the following step the peptides rotate, adopting an amphipathic structure, what enables the interaction between the hydrophobic peptide residues and the hydrophobic core of the membrane. Finally, the lysis of the membrane occurs, leading eventually to its micellarization. The membrane is disintegrated when the threshold local peptide concentration is reached. Moreover, in this mechanism, the peptides are not inserted into the membrane, but they rather stay on the membrane surface, interacting with the phospholipid head groups.

The results presented in this work indicate a new model of interactions between antimicrobial peptides and the bacterial membrane. NKCS does not fully adopt in-plane orientation on the bilayer surface, as it would be in a "carpet" mode of interactions. Instead, its N-terminal fragment is inserted almost perpendicularly into the bilayer. Such orientation has not been reported so far in the literature. Moreover, the activity of the peptide is not reduced only to the membrane disruption. NKCS is capable of changing the biophysical properties of its target membrane. The peptide, interacting with PE, stabilizes the bilayer and inhibits the formation of non-lamellar phases. The non-lamellar structures, such as an inverse hexagonal phase, are important for living cells, because they are intermediates of the cell fusion and division [46]. Since they cannot be formed within the membrane of *E. coli*, the bacteria cannot divide and grow. Although the inhibition of the division process seems to be a primary mechanism suppressing the growth of *E. coli*, it is also possible that the high concentration of NKCS eventually causes the disruption and micellarization of the membrane.

6 Summary and Outlook

In the presented work the activity of the antimicrobial peptide NKCS was studied and a new model of interactions with a lipid membrane has been introduced.

NKCS is very active against Gram-positive and Gram-negative bacteria. Moreover, it shows insignificant toxicity toward human erythrocytes. High antimicrobial activity is guaranteed by two structural prerequisites. Firstly, the distribution of charged and hydrophobic residues, leading to a high amphipathicity and a high local density of positive charges, is important for the membrane binding. Secondly, the peptide must be able to adopt an ordered secondary structure to interact with the lipid bilayer.

In the model presented in this work, the main force driving the attachment of NKCS to the cytoplasmic membrane of *E. coli* is electrostatic interaction between cationic residues of the peptide and anionic phospholipids. NKCS has a very high affinity to the negatively charged phosphatidylglycerol (PG) and induces the segregation of lipids in the mixture of anionic PG and zwitterionic phosphatidylethanolamine (PE). This results in the formation of PG domains interacting with the peptide. Next to the very strong electrostatic interaction with the negatively charged PG, NKCS is able to interact effectively also with PE.

The interactions with the lipid bilayer are not limited only to the accumulation of the peptide on the surface, with in-plane orientation (as it can be observed in the “carpet” model, described in the literature). Instead, a part of the peptide representing the N-terminal fragment (residues 1-12) is inserted almost perpendicularly into the membrane. The C-terminal part (residues 15-27) lays on the bilayer surface interacting with the phospholipids head groups. Moreover, the role of the peptide is not reduced to the disintegration of the membrane when the threshold concentration is reached. NKCS modifies the biophysical properties of the cytoplasmic membrane. It changes the bilayer curvature and blocks an inverse hexagonal

phase transition. This results in the inhibition of the cell division process, observed *in vitro* as a bacteriostatic effect. The high concentrations of peptide increase the lateral pressure promoting further destabilization. This most likely brings to the final destruction of the cytoplasmic membrane and its micellarization.

The primary objective of an investigation of the natural or synthetic antimicrobial peptides is to use them as an alternative drug against the antibiotic-resistant bacterial strains. However, the systemic application requires the precise studies of all possible toxicity mechanisms which can be triggered by AMP in the human cells. Moreover, the stability of the peptides, for example in the presence of proteases must be provided. To reduce the number of obstacles, the antimicrobial peptides are aimed rather for the topical applications. Another possibility is to immobilize such peptides on the implants in order to obtain anti-infectious surfaces. The studied peptide NKCS can be used for this particular application.

7 References

[1] M.-C. Roghmann, L. McGrail, Novel ways of preventing antibiotic-resistant infections: What might the future hold?, American journal of infection control 34 (2006) 469-475.

[2] S.B. Levy, Antibiotic resistance - the problem intensifies, Advanced Drug Delivery Reviews 57 (2005) 1446-1450.

[3] M. Leeb, Antibiotics: A shot in the arm, Nature 431 (2004) 892-893.

[4] C. Nathan, Antibiotics at the crossroads, Nature 431 (2004) 899-902.

[5] H.G. Boman, Peptide Antibiotics and their Role in Innate Immunity, Annual Review of Immunology 13 (1995) 61-92.

[6] R.E.W. Hancock, R. Lehrer, Cationic peptides: a new source of antibiotics, Trends in Biotechnology 16 (1998) 82-88.

[7] M. Zaiou, Multifunctional antimicrobial peptides: therapeutic targets in several human diseases, Journal of Molecular Medicine 85 (2007) 317-329.

[8] R.E.W. Hancock, G. Diamond, The role of cationic antimicrobial peptides in innate host defences, Trends in Microbiology 8 (2000) 402-410.

[9] A. Tossi, L. Sandri, A. Giangaspero, Amphipathic, alpha-helical antimicrobial peptides, Peptide Science 55 (2000) 4-30.

[10] M. Zasloff, Antimicrobial peptides of multicellular organisms, Nature 415 (2002) 389-395.

[11] P. Bulet, R. Stöcklin, L. Menin, Anti-microbial peptides: from invertebrates to vertebrates, Immunological Reviews 198 (2004) 169-184.

[12] T. Ganz, Defensins and Host Defense, Science 286 (1999) 420-421.

[13] K.L. Brown, R.E.W. Hancock, Cationic host defense (antimicrobial) peptides, Current Opinion in Immunology 18 (2006) 24-30.

[14] T. Baba, O. Schneewind, Instruments of microbial warfare: Bacteriocin synthesis, toxicity and immunity, Trends in Microbiology 6 (1998) 66-71.

[15] H. Jenssen, P. Hamill, R.E.W. Hancock, Peptide Antimicrobial Agents, Clinical Microbiology Reviews 19 (2006) 491-511.

[16] A. Giuliani, G. Pirri, S. Nicoletto, Antimicrobial peptides: an overview of a promising class of therapeutics, Central European Journal of Biology 2 (2007) 1-33.

[17] R.M. Epand, H.J. Vogel, Diversity of antimicrobial peptides and their mechanisms of action, Biochimica et Biophysica Acta (BBA) - Biomembranes 1462 (1999) 11-28.

[18] K.A. Brogden, Antimicrobial peptides: pore formers or metabolic inhibitors in bacteria?, Nature Reviews. Microbiology. 3 (2005) 238-250.

[19] M.R. Yeaman, N.Y. Yount, Mechanisms of Antimicrobial Peptide Action and Resistance, Pharmacological Reviews 55 (2003) 27-55.

[20] R.E.W. Hancock, Peptide antibiotics, The Lancet 349 (1997) 418-422.

[21] J.D.F. Hale, R.E.W. Hancock, Alternative mechanisms of action of cationic antimicrobial peptides on bacteria, Expert Review of Anti-infective Therapy 5 (2007) 951-959.

[22] L. Zhang, T.J. Falla, Potential therapeutic application of host defense peptides, Methods in Molecular Biology 618 (2010) 303-327.

[23] R. Bucki, K. Leszczyńska, A. Namiot, W. Sokołowski, Cathelicidin LL-37: A Multitask Antimicrobial Peptide, Archivum Immunologiae et Therapiae Experimentalis 58 (2010) 15-25.

[24] Y.E. Lau, A. Rozek, M.G. Scott, D.L. Goosney, D.J. Davidson, R.E.W. Hancock, Interaction and Cellular Localization of the Human Host Defense Peptide LL-37 with Lung Epithelial Cells, Infection and Immunity 73 (2005) 583-591.

[25] S. Sandgren, A. Wittrup, F. Cheng, M. Jonsson, E. Eklund, S. Busch, M. Belting, The Human Antimicrobial Peptide LL-37 Transfers Extracellular DNA Plasmid to the Nuclear Compartment of Mammalian Cells via Lipid Rafts and Proteoglycan-dependent Endocytosis, Journal of Biological Chemistry 279 (2004) 17951-17956.

[26] R.E.W. Hancock, H.-G. Sahl, Antimicrobial and host-defense peptides as new anti-infective therapeutic strategies, Nature Biotechnology 24 (2006) 1551-1557.

[27] J.M. Berg, J.L. Tymoczko, L. Stryer, Biochemistry, 5th ed., W. H. Freeman and Co, New York, 2002.

[28] S.J. Singer, G. Nicolson, The Fluid Mosaic Model of the Structure of Cell Membranes, Science 175 (1972) 720-731.

[29] A.G. Lee, How lipids affect the activities of integral membrane proteins, Biochimica et Biophysica Acta (BBA) - Biomembranes 1666 (2004) 62-87.

[30] J.A. Killian, T.K.M. Nyholm, Peptides in lipid bilayers: the power of simple models, Current Opinion in Structural Biology 16 (2006) 473-479.

[31] J.A. Virtanen, K.H. Cheng, P. Somerharju, Phospholipid composition of the mammalian red cell membrane can be rationalized by a superlattice model, Proceedings of the National Academy of Sciences of the United States of America 95 (1998) 4964-4969.

[32] G.F. Ames, Lipids of Salmonella typhimurium and Escherichia coli: Structure and Metabolism, Journal of Bacteriology 95 (1968) 833-843.

[33] S. Clejan, T.A. Krulwich, K.R. Mondrus, D. Seto-Young, Membrane lipid composition of obligately and facultatively alkalophilic strains of Bacillus spp, Journal of Bacteriology 168 (1986) 334-340.

[34] T. Heimburg, Thermal Biophysics of Membranes, Wiley-Vch, Weinheim, 2007.

[35] R.M. Epand, Membrane Lipid Polymorphism, Methods in Membrane Lipids, vol. 400, 2007, pp. 15-26.

[36] A.G. Marr, J.L. Ingraham, Effect of temperature on the composition of fatty acids in *Escherichia coli*, Journal of Bacteriology 84 (1962) 1260-1267.

[37] E. Sutherland, B.S. Dixon, H.L. Leffert, H. Skally, L. Zaccaro, F.R. Simon, Biochemical localization of hepatic surface-membrane Na+,K+-ATPase activity depends on membrane lipid fluidity, Proceedings of the National Academy of Sciences of the United States of America 85 (1988) 8673-8677.

[38] C. Le Grimellec, G. Friedlander, E.H.E. Yandouzi, P. Zlatkine, M.-C. Giocondi, Membrane fluidity and transport properties in epithelia, Kidney International 42 (1992) 825-836.

[39] A. Rzeszutek, R. Willumeit, Antimicrobial peptides and their interactions with model membranes, in: A. Iglic (Ed.), Advances in Planar Lipid Bilayers and Liposomes, vol. 12, Academic Press, 2010, pp. 147-165.

[40] R.A. Cooper, Influence of increased membrane cholesterol on membrane fluidity and cell function in human red blood cells, Journal of Supramolecular Structure 8 (1978) 413-430.

[41] O. Mouritsen, M. Zuckermann, What's so special about cholesterol?, Lipids 39 (2004) 1101-1113.

[42] C. Bernsdorff, R. Winter, Differential Properties of the Sterols Cholesterol, Ergosterol, beta-Sitosterol, trans-7-Dehydrocholesterol, Stigmasterol and Lanosterol on DPPC Bilayer Order, The Journal of Physical Chemistry B 107 (2003) 10658-10664.

[43] C.E. Dahl, J.S. Dahl, K. Bloch, Effect of alkyl-substituted precursors of cholesterol on artificial and natural membranes and on the viability of *Mycoplasma capricolum*, Biochemistry 19 (1980) 1462-1467.

[44] J.S. Dahl, C.E. Dahl, K. Bloch, Role of membrane sterols in *Mycoplasma capricolum*., Reviews of Infectious Diseases. 4 (1982) S93-96.

[45] D. Huster, H.A. Scheidt, K. Arnold, A. Herrmann, P. Müller, Desmosterol May Replace Cholesterol in Lipid Membranes, Biophysical Journal 88 (2005) 1838-1844.

[46] E. van den Brink-van der Laan, J. Antoinette Killian, B. de Kruijff, Nonbilayer lipids affect peripheral and integral membrane proteins via changes in the lateral pressure profile, Biochimica et Biophysica Acta (BBA) - Biomembranes 1666 (2004) 275-288.

[47] G. Tresset, The multiple faces of self-assembled lipidic systems, PMC Biophysics 2 (2009) 3.

[48] M.W. Tate, E.F. Eikenberry, D.C. Turner, E. Shyamsunder, S.M. Gruner, Nonbilayer phases of membrane lipids, Chemistry and Physics of Lipids 57 (1991) 147-164.

[49] M. Luckey, Membrane Structural Biology: With Biochemical and Biophysical Foundations, Cambridge University Press, New York, 2008.

[50] G. Lindblom, L. Rilfors, Cubic phases and isotropic structures formed by membrane lipids - possible biological relevance, Biochimica et Biophysica Acta (BBA) - Reviews on Biomembranes 988 (1989) 221-256.

[51] K. Brandenburg, W. Richter, M.H.J. Koch, H.W. Meyer, U. Seydel, Characterization of the nonlamellar cubic and HII structures of lipid A from Salmonella enterica serovar Minnesota by X-ray diffraction and freeze-fracture electron microscopy, Chemistry and Physics of Lipids 91 (1998) 53-69.

[52] P.R. Cullis, B. De Kruijff, Lipid polymorphism and the functional roles of lipids in biological membranes, Biochimica et Biophysica Acta (BBA) - Reviews on Biomembranes 559 (1979) 399-420.

[53] W. Dowhan, M. Bogdanov, E. Mileykovskaya, E.V. Dennis, E.V. Jean, Functional roles of lipids in membranes, in: D.E. Vance, J.E. Vance (Eds.), Biochemistry of Lipids, Lipoproteins and Membranes (Fifth Edition), Elsevier, San Diego, 2008, pp. 1-37.

[54] T. Mares, M. Daniel, S. Perutkova, A. Perne, G. Dolinar, A. Iglic, M. Rappolt, V. Kralj-Iglic, Role of Phospholipid Asymmetry in the Stability of Inverted Hexagonal Mesoscopic Phases, The Journal of Physical Chemistry B 112 (2008) 16575-16584.

[55] S. Perutková, M. Daniel, G. Dolinar, M. Rappolt, V. Kralj-Iglic, A. Iglic, Chapter 9 Stability of the Inverted Hexagonal Phase, in: A. Leitmannova Liu (Ed.), Advances in Planar Lipid Bilayers and Liposomes, vol. 9, Academic Press, 2009, pp. 237-278.

[56] P.C. Noordam, C.J.A. van Echteld, B. de Kruijff, A.J. Verkleij, J. de Gier, Barrier characteristics of membrane model systems containing unsaturated phosphatidylethanolamines, Chemistry and Physics of Lipids 27 (1980) 221-232.

[57] M. Bogdanov, J. Sun, H.R. Kaback, W. Dowhan, A Phospholipid Acts as a Chaperone in Assembly of a Membrane Transport Protein, Journal of Biological Chemistry 271 (1996) 11615-11618.

[58] B.d. Kruijff, Lipid polymorphism and biomembrane function, Current Opinion in Chemical Biology 1 (1997) 564-569.

[59] D.P. Siegel, R.M. Epand, The mechanism of lamellar-to-inverted hexagonal phase transitions in phosphatidylethanolamine: implications for membrane fusion mechanisms, Biophysical Journal 73 (1997) 3089-3111.

[60] E.F. Haney, S. Nathoo, H.J. Vogel, E.J. Prenner, Induction of non-lamellar lipid phases by antimicrobial peptides: a potential link to mode of action, Chemistry and Physics of Lipids 163 (2010) 82-93.

[61] J.-P.S. Powers, A. Tan, A. Ramamoorthy, R.E.W. Hancock, Solution Structure and Interaction of the Antimicrobial Polyphemusins with Lipid Membranes, Biochemistry 44 (2005) 15504-15513.

[62] A. Angelova, R. Ionov, M.H.J. Koch, G. Rapp, Interaction of the Peptide Antibiotic Alamethicin with Bilayer- and Non-bilayer-Forming Lipids: Influence of Increasing

Alamethicin Concentration on the Lipids Supramolecular Structures, Archives of Biochemistry and Biophysics 378 (2000) 93-106.

[63] R. El Jastimi, M. Lafleur, Nisin promotes the formation of non-lamellar inverted phases in unsaturated phosphatidylethanolamines, Biochimica et Biophysica Acta (BBA) - Biomembranes 1418 (1999) 97-105.

[64] C.J.A. Van Echteld, R. Van Stigt, B. De Kruijff, J. Leunissen-Bijvelt, A.J. Verkleij, J. De Gier, Gramicidin promotes formation of the hexagonal HII phase in aqueous dispersions of phosphatidylethanolamine and phosphatidylcholine, Biochimica et Biophysica Acta (BBA) - Biomembranes 648 (1981) 287-291.

[65] J.A. Szule, R.P. Rand, The Effects of Gramicidin on the Structure of Phospholipid Assemblies, Biophysical Journal 85 (2003) 1702-1712.

[66] K. Matsuzaki, K. Sugishita, N. Ishibe, M. Ueha, S. Nakata, K. Miyajima, R.M. Epand, Relationship of Membrane Curvature to the Formation of Pores by Magainin 2 Biochemistry 37 (1998) 11856-11863.

[67] K.A. Henzler Wildman, D.-K. Lee, A. Ramamoorthy, Mechanism of Lipid Bilayer Disruption by the Human Antimicrobial Peptide, LL-37, Biochemistry 42 (2003) 6545-6558.

[68] K. Lohner, E.J. Prenner, Differential scanning calorimetry and X-ray diffraction studies of the specificity of the interaction of antimicrobial peptides with membrane-mimetic systems, Biochimica et Biophysica Acta (BBA) - Biomembranes 1462 (1999) 141-156.

[69] Y. Shai, Mechanism of the binding, insertion and destabilization of phospholipid bilayer membranes by [alpha]-helical antimicrobial and cell non-selective membrane-lytic peptides, Biochimica et Biophysica Acta (BBA) - Biomembranes 1462 (1999) 55-70.

[70] M. Andersson, H. Gunne, B. Agerberth, A. Boman, T. Bergman, R. Sillard, H. Jornvall, V. Mutt, B. Olsson, H. Wigzell, A. Dagerlind, H.G. Boman, G.H. Gudmundsson, NK-lysin, a novel effector peptide of cytotoxic T-cells and NK-cells - structure and cDNA cloning of the porcine form, induction by interleukin-2, antibacterial and antitumour activity, EMBO Journal 14 (1995) 1615-1625.

[71] R.S. Munford, P.O. Sheppard, P.J. O'Hara, Saposin-like proteins (SAPLIP) carry out diverse functions on a common backbone structure, J. Lipid Res. 36 (1995) 1653-1663.

[72] C.M.A. Linde, S. Grundstrom, E. Nordling, E. Refai, P.J. Brennan, M. Andersson, Conserved Structure and Function in the Granulysin and NK-Lysin Peptide Family, Infection and Immunity 73 (2005) 6332-6339.

[73] E. Liepinsh, M. Andersson, J.-M. Ruysschaert, G. Otting, Saposin fold revealed by the NMR structure of NK-lysin, Nature Structural and Molecular Biology 4 (1997) 793-795.

[74] J. Andra, M. Leippe, Candidacidal activity of shortened synthetic analogs of amoebapores and NK-lysin, Medical Microbiology and Immunology 188 (1999) 117-124.

[75] T. Jacobs, H. Bruhn, I. Gaworski, B. Fleischer, M. Leippe, NK-Lysin and Its Shortened Analog NK-2 Exhibit Potent Activities against Trypanosoma cruzi, Antimicrobial Agents and Chemotherapy 47 (2003) 607-613.

[76] C. Gelhaus, T. Jacobs, J. Andra, M. Leippe, The Antimicrobial Peptide NK-2, the Core Region of Mammalian NK-Lysin, Kills Intraerythrocytic Plasmodium falciparum, Antimicrobial Agents and Chemotherapy 52 (2008) 1713-1720.

[77] H. Schröder-Borm, R. Bakalova, J. Andrä, The NK-lysin derived peptide NK-2 preferentially kills cancer cells with increased surface levels of negatively charged phosphatidylserine, FEBS Letters 579 (2005) 6128-6134.

[78] H. Schröder-Borm, R. Willumeit, K. Brandenburg, J. Andrä, Molecular basis for membrane selectivity of NK-2, a potent peptide antibiotic derived from NK-lysin, Biochimica et Biophysica Acta (BBA) - Biomembranes 1612 (2003) 164-171.

[79] J. Andra, D. Monreal, G.M. de Tejada, C. Olak, G. Brezesinski, S.S. Gomez, T. Goldmann, R. Bartels, K. Brandenburg, I. Moriyon, Rationale for the Design of Shortened Derivatives of the NK-lysin-derived Antimicrobial Peptide NK-2 with Improved Activity against Gram-negative Pathogens, Journal of Biological Chemistry 282 (2007) 14719-14728.

[80] S. Linser, Development of new antimicrobial peptides based on the synthetic peptide NK-2, Universität Hamburg, Hamburg, 2006.

[81] Y. Gofman, S. Linser, A. Rzeszutek, D. Shental-Bechor, S.S. Funari, N. Ben-Tal, R. Willumeit, Interaction of an Antimicrobial Peptide with Membranes: Experiments and Simulations with NKCS, The Journal of Physical Chemistry B 114 (2010) 4230-4237.

[82] R.M. Epand, Hydrogen bonding and the thermotropic transitions of phosphatidylethanolamines, Chemistry and Physics of Lipids 52 (1990) 227-230.

[83] A. Noseda, P.L. Godwin, E.J. Modest, Effects of antineoplastic ether lipids on model and biological membranes, Biochimica et Biophysica Acta (BBA) - Biomembranes 945 (1988) 92-100.

[84] P.W.M. Van Dijck, B. De Kruijff, L.L.M. Van Deenen, J. De Gier, R.A. Demel, The preference of cholesterol for phosphatidylcholine in mixed phosphatidylcholine-phosphatidylethanolamine bilayers, Biochimica et Biophysica Acta (BBA) - Biomembranes 455 (1976) 576-587.

[85] T. Wiedmann, A. Salmon, V. Wong, Phase behavior of mixtures of DPPC and POPG, Biochimica et Biophysica Acta (BBA) - Lipids and Lipid Metabolism 1167 (1993) 114-120.

[86] R. Willumeit, M. Kumpugdee, S.S. Funari, K. Lohner, B.P. Navas, K. Brandenburg, S. Linser, J. Andrä, Structural rearrangement of model membranes by the peptide antibiotic NK-2, Biochimica et Biophysica Acta (BBA) - Biomembranes 1669 (2005) 125-134.

[87] S.A. Leharne, B.Z. Chowdhry, Thermodynamic Background to Differential Scanning Calorimetry, in: J.E. Ladbury, B.Z. Chowdhry (Eds.), Biocalorimetry: Applications of Calorimetry in the Biological Sciences, John Wiley & Sons Ltd., 1998, pp. 157-182.

[88] D. Sheehan, Physical Biochemistry: Principles and Applications, 2 ed., John Wiley & Sons Ltd., Chichester, UK, 2009.

[89] E. Goormaghtigh, V. Raussens, J.-M. Ruysschaert, Attenuated total reflection infrared spectroscopy of proteins and lipids in biological membranes, Biochimica et Biophysica Acta (BBA) - Reviews on Biomembranes 1422 (1999) 105-185.

[90] P.F. Almeida, A. Pokorny, Mechanisms of Antimicrobial, Cytolytic, and Cell-Penetrating Peptides: From Kinetics to Thermodynamics, Biochemistry 48 (2009) 8083-8093.

[91] M. Fernández-Vidal, S. Jayasinghe, A.S. Ladokhin, S.H. White, Folding Amphipathic Helices Into Membranes: Amphiphilicity Trumps Hydrophobicity, Journal of Molecular Biology 370 (2007) 459-470.

[92] L.E. Yandek, A. Pokorny, P.F.F. Almeida, Wasp mastoparans follow the same mechanism as the cell-penetrating peptide transportan 10, Biochemistry 48 (2009) 7342-7351.

[93] S.H. White, W.C. Wimley, Hydrophobic interactions of peptides with membrane interfaces, Biochimica et Biophysica Acta (BBA) - Reviews on Biomembranes 1376 (1998) 339-352.

[94] D. Eisenberg, Three-Dimensional Structure of Membrane and Surface Proteins, Annual Review of Biochemistry 53 (1984) 595-623.

[95] S.H. White, W.C. Wimley, Membrane protein folding and stability: Physical Principles, Annual Review of Biophysics and Biomolecular Structure 28 (1999) 319-365.

[96] R.E.W. Hancock, D.S. Chapple, Peptide Antibiotics, Antimicrobial Agents and Chemotherapy 43 (1999) 1317-1323.

[97] H. Raghuraman, A. Chattopadhyay, Melittin: a Membrane-active Peptide with Diverse Functions, Bioscience Reports 27 (2007) 189-223.

[98] M.C. Houbiers, C.J.A.M. Wolfs, R.B. Spruijt, Y.J.M. Bollen, M.A. Hemminga, E. Goormaghtigh, Conformation and orientation of the gene 9 minor coat protein of bacteriophage M13 in phospholipid bilayers, Biochimica et Biophysica Acta (BBA) - Biomembranes 1511 (2001) 224-235.

[99] V. Raussens, J. Drury, T.M. Forte, N. Choy, E. Goormaghtigh, J.-M. Ruysschaert, V. Narayanaswami, Orientation and mode of lipid-binding interaction of human apolipoprotein E C-terminal domain, The Biochemical Journal 387 (2005) 747-754.

[100] C. Vigano, L. Manciu, F. Buyse, E. Goormaghtigh, J.M. Ruysschaert, Attenuated total reflection IR spectroscopy as a tool to investigate the structure, orientation and tertiary structure changes in peptides and membrane proteins, Peptide Science 55 (2000) 373-380.

[101] M.S. Vinchurkar, K.H.C. Chen, S.S.F. Yu, S.-J. Kuo, H.-C. Chiu, S.-H. Chien, S.I. Chan, Polarized ATR-FTIR Spectroscopy of the Membrane-Embedded Domains of the Particulate Methane Monooxygenase Biochemistry 43 (2004) 13283-13292.

[102] C. Friedrich, M.G. Scott, N. Karunaratne, H. Yan, R.E.W. Hancock, Salt-Resistant Alpha-Helical Cationic Antimicrobial Peptides, Antimicrobial Agents and Chemotherapy 43 (1999) 1542-1548.

[103] R.T. Coughlin, S. Tonsager, E.J. McGroarty, Quantitation of metal cations bound to membranes and extracted lipopolysaccharide of Escherichia coli, Biochemistry 22 (1983) 2002-2007.

[104] H. Nikaido, Molecular Basis of Bacterial Outer Membrane Permeability Revisited, Microbiology and Molecular Biology Reviews 67 (2003) 593-656.

[105] M. Dathe, T. Wieprecht, Structural features of helical antimicrobial peptides: their potential to modulate activity on model membranes and biological cells, Biochimica et Biophysica Acta (BBA) - Biomembranes 1462 (1999) 71-87.

[106] C. Olak, A. Muenter, J. Andrä, G. Brezesinski, Interfacial properties and structural analysis of the antimicrobial peptide NK-2, Journal of Peptide Science 14 (2008) 510-517.

[107] A. Arouri, M. Dathe, A. Blume, Peptide induced demixing in PG/PE lipid mixtures: A mechanism for the specificity of antimicrobial peptides towards bacterial membranes?, Biochimica et Biophysica Acta (BBA) - Biomembranes 1788 (2009) 650-659.

[108] D. Shental-Bechor, T. Haliloglu, N. Ben-Tal, Interactions of Cationic-Hydrophobic Peptides with Lipid Bilayers: A Monte Carlo Simulation Method, Biophysical Journal 93 (2007) 1858-1871.

[109] S. Toraya, K. Nishimura, A. Naito, Dynamic Structure of Vesicle-Bound Melittin in a Variety of Lipid Chain Lengths by Solid-State NMR, Biophysical Journal 87 (2004) 3323-3335.

[110] F.-Y. Chen, M.-T. Lee, H.W. Huang, Evidence for Membrane Thinning Effect as the Mechanism for Peptide-Induced Pore Formation, Biophysical Journal 84 (2003) 3751-3758.

[111] K. Lohner, E. Sevcsik, G. Pabst, Chapter Five Liposome-Based Biomembrane Mimetic Systems: Implications for Lipid-Peptide Interactions, in: A. Leitmannova Liu (Ed.), Advances in Planar Lipid Bilayers and Liposomes, vol. 6, Academic Press, 2008, pp. 103-137.

[112] G. Pabst, S.L. Grage, S. Danner-Pongratz, W. Jing, A.S. Ulrich, A. Watts, K. Lohner, A. Hickel, Membrane Thickening by the Antimicrobial Peptide PGLa, Biophysical Journal 95 (2008) 5779-5788.

[113] M. Rappolt, A. Hickel, F. Bringezu, K. Lohner, Mechanism of the Lamellar/Inverse Hexagonal Phase Transition Examined by High Resolution X-Ray Diffraction, Biophysical Journal 84 (2003) 3111-3122.

[114] Z. Oren, Y. Shai, Mode of action of linear amphipathic α-helical antimicrobial peptides, Peptide Science 47 (1998) 451-463.

8 Abbreviations

AMP	antimicrobial peptide
ATR-FTIR spectroscopy	attenuated total reflection Fourier transform infrared spectroscopy
B. subtilis	*Bacillus subtilis*
CD spectroscopy	circular dichroism spectroscopy
CFU	cell forming unit
CL	cardiolipin
CMC	critical micelle concentration
DiPoPE	1,2-dipalmitoleoyl-sn-glycero-3-phosphoethanolamine
DOPE-trans	1,2-dielaidoyl-sn-glycero-3-phosphoethanolamine
DSC	differential scanning calorimetry
E. coli	*Escherichia coli*
EDTA	ethylenediaminetetraacetic acid
FTIR spectroscopy	Fourier transform infrared spectroscopy
HEPES	4-(2-hydroxyethyl)-1-piperazineethanesulfonic acid
IR spectroscopy	infrared spectroscopy
IRE	internal reflection element
LPS	lipopolysaccharide
LUV	large unilamellar vesicles
MES	morpholinoethanesulfonic buffer
MIC	minimal inhibitory concentration
MLV	multilamellar vesicles
MPEx	Membrane Protein Explorer

MS	mass spectrometry
NaP	sodium phosphate buffer
NK cells	natural killer cells
NMR	nuclear magnetic resonance
OD	optical density
PA	phosphatidic acid
PBS	phosphate buffered saline
PC	phosphatidylcholine
PDB	Protein Data Bank
PE	phosphatidylethanolamine
PG	phosphatidylglycerol
PI	phosphatidylinositol
PIPES	1,4-piperazinediethanesulfonic acid
POPC	1-palmitoyl-2-oleoyl-sn-glycero-3-phosphocholine
POPE	1-palmitoyl-2-oleoyl-sn-glycero-3-phosphoethanolamine
POPG	1-palmitoyl-2-oleoyl-sn-glycero-3-phospho-rac-(1-glycerol) ammonium salt
PS	phosphatidylserine
S. carnosus	*Staphylococcus carnosus*
SAXS	small angle X-rays scattering
SDS	sodium dodecyl sulfate
SM	sphingomyelin

9 Appendix

1. Y. Gofman, S. Linser, A. Rzeszutek, D. Shental-Bechor, S.S. Funari, N. Ben-Tal, R. Willumeit, Interaction of an Antimicrobial Peptide with Membranes: Experiments and Simulations with NKCS, The Journal of Physical Chemistry B, 114 (2010) 4230-4237.

2. A. Rzeszutek, R. Willumeit, Antimicrobial peptides and their interactions with model membranes, in: A. Iglic (Ed.), Advances in Planar Lipid Bilayers and Liposomes, vol. 12, Academic Press, 2010, pp. 147-165.

Interaction of an Antimicrobial Peptide with Membranes: Experiments and Simulations with NKCS

Yana Gofman,[†] Sebastian Linser,[†] Agnieszka Rzeszutek,[†] Dalit Shental-Bechor,[‡] Sergio S. Funari,[§] Nir Ben-Tal,*[,‡] and Regine Willumeit*[,†]

GKSS Research Center, 21502 Geesthacht, Germany, Department of Biochemistry, The George S. Wise Faculty of Life Sciences, Tel-Aviv University, Ramat-Aviv, 69978 Tel-Aviv, Israel, and Hasylab, DESY, 22603 Hamburg, Germany

Received: September 23, 2009; Revised Manuscript Received: January 6, 2010

We used Monte Carlo simulations and biophysical measurements to study the interaction of NKCS, a derivative of the antimicrobial peptide NK-2, with a 1-palmitoyl-2-oleoyl-*sn*-glycero-3-phosphoethanolamine (POPE) membrane. The simulations showed that NKCS adsorbed on the membrane surface and the dominant conformation featured two amphipathic helices connected by a hinge region. We designed two mutants in the hinge to investigate the interplay between helicity and membrane affinity. Simulations with a Leu-to-Pro substitution showed that the helicity and membrane affinity of the mutant (NKCS-[LP]) decreased. Two Ala residues were added to NKCS to produce a sequence that is compatible with a continuous amphipathic helix structure (NKCS-[AA]), and the simulations showed that the mutant adsorbed on the membrane surface with a particularly high affinity. The circular dichroism spectra of the three peptides also showed that NKCS-[LP] is the least helical and NKCS-[AA] is the most. However, the activity of the peptides, determined in terms of their antimicrobial potency and influence on the temperature of the transition of the lipid to hexagonal phase, displayed a complex behavior: NKCS-[LP] was the least potent and had the smallest influence on the transition temperature, and NKCS was the most potent and had the largest effect on the temperature.

Introduction

After half a century of almost complete control over microbial infections, the past decade has brought a worldwide resurgence of infectious diseases due to the evolution of antibiotic-resistant strains at an alarming rate.[1,2] As a potential class of novel antimicrobial agents, animal-derived antimicrobial peptides (AMP) have recently emerged.[3−5] These peptides are fast and lethal toward a broad spectrum of pathogens but are quite harmless to eukaryotic cells. Some AMPs also possess anticancer and antiviral activity, as well as the capacity to manipulate the innate immune response.[3] The first generation of antimicrobial peptides is already at the edge of application.[4,6] However, the dose effective in vitro is very close to the toxic dose in animal models, indicating that a concerted effort to understand the interaction of antibacterial peptides with their target membrane is of utmost importance.

The precise mechanism of action of antimicrobial peptides and the molecular basis for their selective cytotoxicity are not fully understood. Data suggest that, regardless of their origin and the diversity in their primary and secondary structure, the antimicrobial activity of the peptides is a result of direct interactions with the phospholipids of the pathogens' membrane rather than association with a specific receptor. It is generally believed that most antimicrobial peptides lyse their target cell by the destabilization of the cytoplasmic membrane.[3,7−10] The selectivity of the cytolytic mechanism is assumed to stem from inherent differences in the lipid composition of the target cells.[10]

The NK-2 peptide, corresponding to residues 39−65 of the NK-lysin protein, has been investigated extensively due to its high antimicrobial[11−13] and anticancer qualities[14] as well as low hemolytic activity.[11] The peptide was found to reduce the transition temperature of the lipid bilayer in a concentration dependent manner by up to 10 °C.[15] The replacement of cysteine residue within the NK-2 sequence with a serine (C7S), resulted in a peptide with an improved antibacterial activity referred to as NKCS in the current study.[16] Both peptides are randomly coiled in water and adopt a helical structure upon interaction with the lipid bilayer.[11,16]

Several approaches are used to investigate the interaction between antibacterial peptides and lipid membranes. These include biophysical studies using techniques such as differential scanning calorimetry (DSC),[17] Fourier transform infrared (FTIR) spectroscopy,[18] circular dichroism (CD) spectroscopy,[19] scattering techniques (X-ray and neutron scattering),[17,20] NMR,[21] and surface plasmon resonance (SPR),[22] as well as computational studies including molecular dynamics simulations,[23,24] continuum solvent models,[25,26] and Monte Carlo (MC) simulations.[27−34] In this work we characterized the interactions between the cationic peptide NKCS and 1-palmitoyl-2-oleoyl-*sn*-glycero-3-phosphoethanolamine (POPE) membranes. We employed small-angle X-ray scattering (SAXS) and SPR along with measurements of the antibacterial and hemolytic activity in cells. We used CD spectroscopy to estimate the peptide's helicity. In addition, we performed MC simulations of NKCS and its derivatives in a POPE membrane.[35−38]

Phosphoethanolamine (PE) is a prominent example for the capability of a lipid to create nonbilayer forms such as hexagonal phases. Under suitable conditions even cubic structures are formed.[39,40] The local formation of nonbilayer structures is a prerequisite for the fusion and division of cell membranes when,

* Corresponding authors. E-mail: N.B.-T., NirB@tauex.tau.ac.il; R.W., Regine.Willumeit@gkss.de.
[†] GKSS Research Center.
[‡] Tel-Aviv University.
[§] Hasylab.

10.1021/jp909154y © 2010 American Chemical Society
Published on Web 03/04/2010

TABLE 1: Amino Acid Sequences of the Peptides

NKCS	KILRGVSKKIMRT	FLRRISKDILTGKK
NKCS-[LP]	KILRGVSKKIMRT	F**P**RRISKDILTGKK
NKCS-[AA]	KILRGVSKKIMRT**AA**FLRRISKDILTGKK	

[a] The changes are marked in bold fonts.

for very short periods of time, these structures are built in a living system.[41] The fraction of PE in the cytoplasmic membrane varies between, e.g., 69% of the total phospholipid in *Escherichia coli*,[42] 10% in *Bacillus subtilis*,[43] and 0% in *Staphylococcus aureus*.[44] Even though PE is not always the most abundant lipid in bacterial membranes, it interacts strongly with cationic peptides, leading to changes in the phase transition temperature. Specifically, magainin[45] and its analog MSI-78[46] show a significant increase in the lipid hexagonal phase transition temperature, whereas gramicidin,[47] alamethicin,[48] and the wasp venom peptide mastoparan[49] reduce the temperature.

The central hypothesis of this paper is that simple structural features, such as α-helicity and amphipathicity can be used to interpret changes in the membrane affinity of NKCS. We design two mutants, NKCS-[AA] and NKCS-[LP], to examine it, and to correlate the membrane affinity and activity of the peptides. We show that NKCS, NKCS-[AA], and NKCS-[LP] are, in essence, random coils in the aqueous solution. Upon membrane association, NKCS and NKCS-[AA] assume helical conformations, while the helical content of NKCS-[LP] stays low. This is demonstrated both in the CD spectroscopy studies and in the simulations. However, the assumption that the biological activity of a peptide increases with its membrane affinity might not always be true. For example, NKCS-[AA] and NKCS-[LP] manifest similar activities despite significant changes in the values of their calculated membrane-association free energies.

Theoretical Calculations

Monte Carlo simulations of the interaction of a peptide molecule with POPE membranes were performed as described previously.[35−38] The peptide was described using a reduced representation with each amino acid represented as two interaction sites, one corresponding to the α-carbon and the other to the side chain. The initial conformations of the peptides were modeled using the Nest program,[50] based on the structure of NK-lysin from the Protein Data Bank (entry 1NKL, model 1). The lipid membrane was approximated as a hydrophobic profile, corresponding to the hydrocarbon region of the membrane. The model membrane included also surface charges, corresponding to the polar headgroups, which interacted electrostatically with the titratable residues of the peptide, depending on their protonation state, using the Gouy−Chapman potential. A more detailed computational protocol is available in the Supporting Information.

Materials and Methods

Peptides. The peptide NKCS and its derivatives were synthesized by Biosyntan (Berlin, Germany). All three peptides carry a net charge of +10 (calculated by counting the N-terminus, lysine, histidine, and arginine as positive charges and counting aspartate as a negative charge; the C-termini are amidated). The sequences are shown in Table 1. The choice of peptides is explicated in Discussion. The purity of 95% was guaranteed by analytical RP-HPLC (Lichrospher 100 RP 18, 5 μm columns, Merck, Darmstadt, Germany) and MALDI-TOF (Bruker Daltonik GmbH, Bremen, Germany) performed by the company.

Melittin was purchased from Sigma-Aldrich (Deisenhofen, Germany). It was used to compare its known hemolytic activity with that of the investigated peptides.[51]

The peptides were stored at −20 °C. Directly before use they were dissolved in double distilled water to a final concentration of 1 mM. Between the experiments the peptide solutions were also stored at −20 °C.

Lipid. The phospholipid POPE was purchased from Sigma-Aldrich (Deisenhofen, Germany) and stored airtight in the freezer at −20 °C.

Circular Dichroism (CD). CD data were acquired with a JASCO CD spectrophotometer (JASCO, Gross-Umstadt, Germany) using quartz cuvettes with an optical path length of 0.1 cm. The CD was measured between 260 and 185 nm with a 0.5 nm step resolution and a 1 nm bandwidth. The counting rate was 50 nm/min with 4 s response time. Each spectrum was a sum of at least three scans to improve the signal/noise ratio. The detergent, sodium dodecyl sulfate (SDS) (Fluka, St. Louis, MO), which mimics some characteristics of biological membranes, was added to the cuvette with final concentrations of 1 and 10 mM in double distilled water before the peptides were added. As references, the spectra of double distilled water and SDS at the respective concentration were subtracted from the measurements with peptides. All spectra were collected for a concentration of 60 μM peptide in double distilled water. The molar ratio of peptide to SDS was 1:17 (for 1 mM SDS) and 1:167 (10 mM SDS).

Surface Plasmon Resonance (SPR). Surface plasmon resonance phenomenon allows performing the real-time measurements of the adhesion of molecules to the biomimetic surfaces. The SPR detector detects the changes in optical properties at the sensor surface coated with the ligand due to the adsorption and desorption of the solute.[52]

The SPR apparatus BIAcore X (GE Healthcare, Freiburg, Germany) was equipped with an internal injection system (500 μL Hamilton syringe). The running buffer was a 10 mM sodium phosphate buffer (pH 7.4), and the flow rate was 5 μL/min for all experiments. We used the BIAcore L1 chip, which was composed of a thin dextran matrix modified by lipophilic compounds on a gold surface where the lipid vesicles could be captured.[53] All solutions were freshly prepared, degassed, and filtered through 0.22 μm pores. The experiments were done at the room temperature (RT). After the system was cleaned according to the manufacturer's instructions, the BIAcore X apparatus was left running overnight using Milli-Q water as eluent to thoroughly wash all liquid-handling parts of the instrument. The L1 chip was then installed, and the surface was cleaned by an injection of the nonionic detergent *N*-octyl β-D-glucopyranoside (50 μL, 40 mM).

The phospholipid POPE was dissolved in a methanol/chloroform (Merck, Darmstadt, Germany) (1/2, v/v) solution. The solvent was slowly removed by a constant stream of nitrogen. The resulting lipid film was dried in a vacuum oven at 40 °C overnight. Just before the experiments, the lipid films were hydrated in buffer. To form multilamellar vesicles of POPE, sodium phosphate buffer (Merck, Darmstadt, Germany) was added at the room temperature to the lipid films and a small amount of glass beads was put into the vials. After vortexing for 1 min, the solution was incubated for 2 h at 28 °C, while every 30 min the sample was vortexed. Then the solution was cooled to RT and POPE vesicles (100 μL, 1 mM) were applied to the chip surface. To remove artifacts, NaOH (5 μL, 10 mM) was injected, which resulted in a stable baseline corresponding to the lipid bilayer linked to the chip surface. The thickness of

TABLE 2: Average Binding Free Energy and Fraction of All, "Inner" and "Outer" Conformations of NKCS, NKCS-[LP], and NKCS-[AA] Predicted by the MC Simulations[a]

peptide	conformations	calculated membrane-association energy (kT)	fraction (%)	measured membrane-association energy (kT)
NKCS	inner	-21.6 ± 1.8	85 ± 3	
	outer	-6.5 ± 0.7	15 ± 3	
	all	-20.5 ± 1.9	100	-18.5 ± 1.1 ($n = 6$)
NKCS-[LP]	inner	-17.3 ± 1.6	64 ± 2	
	outer	-10.9 ± 1.0	36 ± 2	
	all	-16.0 ± 1.0	100	-16.1 ± 0.3 ($n = 5$)
NKCS-[AA]	inner	-34.3 ± 0.4	99.8 ± 0.2	
	outer	38.9 ± 19.0	0.2 ± 0.2	
	all	-34.3 ± 0.4	100	-25.7 ± 0.3 ($n = 5$)

[a] For comparison, the average binding energies of the peptides to POPE measured using SPR are presented in the last column. The number of experiments, n, is indicated in parentheses. All values are shown as average $\pm$ standard deviation.

the bilayer was calculated by assuming that 1000 RU (response units) correspond to 1 nm layer thickness.[54] This bilayer was subsequently used as a model membrane surface to study the peptide−membrane interactions. For all peptides, 50 μL of a 1 μM solution was injected while the adsorption and desorption of the peptide was observed until it resulted in a stable signal. Finally, NaOH was injected to wash all unbound compounds away. All measurements were performed in triplicates.

Small Angle X-ray Scattering (SAXS). The POPE vesicles were prepared as described above with a final concentration of 25 mg/mL. After 30 min at room temperature, mixing with the appropriate peptide solution followed. The measurements were performed at the A2 beamline at HASYLAB, DESY. It ran with a wavelength $\lambda = 0.15$ nm and covered a scattering vector $s = 1/d = (2 \sin \theta)/\lambda$ (2θ = scattering angle, d = lattice spacing) from 1×10^{-2} to 0.5 nm^{-1}. The calibration for the SAXS pattern was done by measuring rat tail tendon (repeat distance 65 nm, standard at beamline A2) in addition to silver behenate ([$CH_3(CH_2)_2OCOO-Ag$], repeat distance 5.838 nm, made available at beamline A2). The samples were measured in a temperature-controlled sample holder, where the temperature was varied with an increase of 2 °C/min and the data were collected for 10 s per measurement.

The data were normalized with respect to the primary beam and the background (buffer measurement). The positions of the diffraction peaks were determined using the OTOKO software.[55] The repeat distances were calculated from the peak positions based on the rat tail tendon and silver behenate calibration.

Antibacterial Assay. The *Escherichia coli* strain K12 (ATCC 23716), the *Staphylococcus carnosus* strain (ATCC 51365), and the *Bacillus subtilis* strain (ATCC 6051) (all bacteria were obtained from DSMZ, Braunschweig, Germany) were cultivated in the respective medium at 37 °C with shaking at 160 rpm to reach the log-phase. The peptides were 2-fold serial diluted and 10 μL of the log-phase bacteria suspension containing 100 colony forming units (CFU) was added to 90 μL of the peptide solution to measure the antibacterial activity by a microdilution susceptibility test. The density of the bacteria suspension was measured photometrically at 620 nm wavelength with a microplate reader (Tecan, Crailsheim, Germany). Values of the minimal inhibitory concentration (MIC) were defined as the concentration of the highest dilution of the peptides at which the bacteria growth was completely suppressed.

Hemolysis. To measure the hemolytic activity of the peptides, fresh (maximum storage time was 2 days) human blood (group 0 rhesus positive), was centrifuged for 3 min at 2000 rpm. The supernatant was discarded and the pellet washed with phosphate buffered saline (PBS) three times. The erythrocytes pellet was subsequently diluted with MES buffer (20 mM morpholinoethanesulfonic acid, 140 mM NaCL, pH 5.5 (Merck, Darmstadt, Germany)) until 20 μL of this suspension added to 980 μL of double distilled water gave the absorbance 1.4 at the wavelength of 412 nm, which equaled 5×10^8 cells/mL. The peptides were diluted in MES buffer to the desired concentrations before 20 μL of the erythrocyte suspension was added to 80 μL of peptide solution. As the control, 20 μL of erythrocyte suspension was mixed with 80 μL of double distilled water, expecting 100% lysis of the erythrocytes. The negative control was made by mixing 20 μL of erythrocyte suspension and 80 μL of MES buffer. After all samples were carefully mixed, the suspensions were incubated for 30 min at 37 °C. Directly after incubation the samples were stored on ice and MES buffer (900 μL) was added. All suspensions were centrifuged for 10 min at 2000 rpm to separate intact erythrocytes. Finally, the absorbance was measured with a spectrometer (Tecan, Crailsheim, Germany) at 412 nm wavelength.

Simulation Results

We conducted preliminary MC simulations of NKCS in the aqueous phase and within a POPE membrane and analyzed the structural and free energy determinants of the membrane association. The peptide adsorbed on the membrane surface with an association free energy of -20.5 kT (Table 2). A close look at the predicted conformations of the peptide showed a mixture of two main groups (Figure 1A). In the first (Figure 1A), which we called "the inner group of conformations", the peptide was partially dissolved in the membrane. The nonpolar residues were immersed in the hydrophobic region of the membrane, whereas the polar and charged residues were located in water, in close proximity to the membrane surface charge. Most of the conformations were helical with a distortion (hinge) in residues Thr-13 and Phe-14 (Figure 1B). In the second, outer, group of NKCS conformations, the peptide was randomly coiled and located, in essence, outside the membrane. This group of conformations resembled in its low helix content the conformations that were observed in the aqueous phase. The lysine and arginine residues pointed toward the slightly negatively charged membrane surface, whereas the nonpolar residues of the peptide faced the aqueous phase and did not interact with the membrane.

The free energy of membrane-association of the NKCS "inner" conformations was significantly lower (i.e., more favorable) than that of the "outer" ones (Table 2). Free energy decomposition suggested that the difference is mainly due to desolvation of the nonpolar residues (Supporting Information Table S1). These were embedded in the membrane in the inner conformations and interacted favorably with the hydrocarbon region whereas in the outer conformations they faced the solvent.

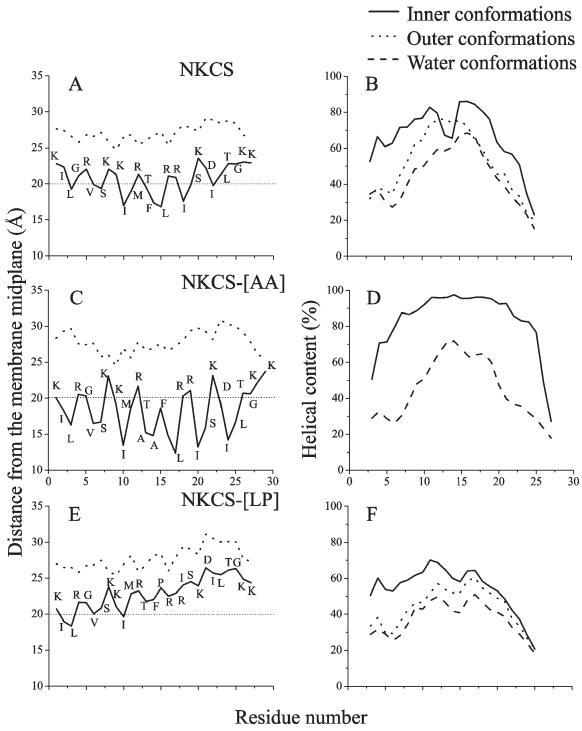

Figure 1. Location of the inner and outer conformations of (A) NKCS, (C) NKCS-[AA], and (E) NKCS-[LP] near the membrane. The average distance of the α-carbon atoms from the membrane midplane in the MC simulations is shown for each residue. The horizontal dotted line marks the location of the lipids polar heads. The calculated helical content of (B) NKCS, (D) NKCS-[AA], and (F) NKCS-[LP] in the aqueous phase and near the membrane. Inner, outer, and water conformations are represented with different curves, as indicated. The helical content of the outer group of NKCS-[AA] is not shown since there were only 6 conformations (out of 3600). In all cases the helical content of the water conformations was the lowest and that of the inner conformations highest.

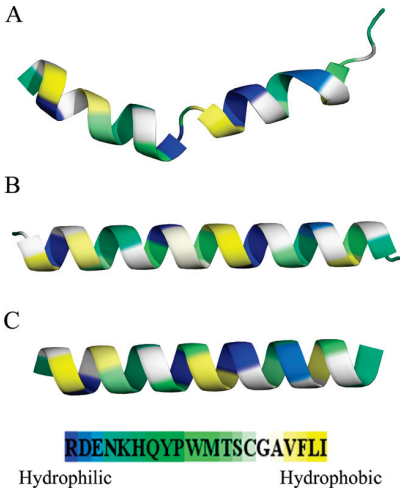

Figure 2. Compatibility of the peptide sequence with an amphipathic helical structure. The peptide is represented as ribbons colored according to the hydrophobicity scale in the bar. (A) Representative structure of NKCS in an "inner" conformation, obtained from the MC simulations in the membrane. The view is from the membrane surface upward, and the structure features two short amphipathic helices, connected by a hinge. (B) NKCS-[AA], constructed as a canonical α-helix. In contrast to NKCS, the sequence of NKCS-[AA] is consistent with the amphipathic helix structure. This is indeed the predominant conformation of the peptide in association with the membrane. The view is from the membrane plan upward, as in "A". (C) NKCS in a (hypothetical) canonical α-helix conformation. It is evident from the picture that the hydrophobic and polar/charged amino acids are spread in all directions and the conformation is not amphipathic. That is, NKCS's amino acid sequence is not compatible with an amphipathic helix structure.

Additionally, the membrane-induced helix formation, as well as close electrostatic interactions between positively charged residues and the negatively charged membrane surface, made the "inner" group of conformations more favorable (Supporting Information Table S1).

On the basis of the preliminary simulations, we hypothesized that the membrane affinity depends on the compatibility of NKCS's sequence with an amphipathic helix structure and designed two peptides to examine this possibility (Table 1). In the first (NKCS-[AA]) we added two consecutive Ala residues into the hinge region of NKCS. With this, the polypeptide sequence becomes compatible with an amphipathic helix structure (Figure 2B) and the anticipation was that its membrane affinity would increase. Indeed, the simulations showed that the vast majority of the conformations, above 99% of total (Table 2), were embedded in the membrane with nonpolar residues within the hydrophobic core and the polar residues in the aqueous phase (Figure 1C). The helical content of these conformations was much higher than that of the original peptide and the only distortions were in the termini (Figure 1D). Reassuringly, the membrane affinity of NKCS-[AA] was much stronger than that of the original peptide (Table 2), as we hoped.

As a negative control experiment, we also designed a second variant (NKCS-[LP]) in which Leu-15 was replaced with a Pro. The idea was to interfere further with the helical structure of the peptide, thereby reducing its membrane affinity. Indeed, the NKCS-[LP] peptide associated with the membrane with less negative free energy than the original peptide NKCS (Table 2). Also here it was possible to distinguish between two groups of conformations. The outer group resembled that of NKCS in orientation and helical content. In both, the N-terminus up to Thr-13 was on average adsorbed on the surface of the membrane (Figure 1A,E) with quite high helical content (Figure 1B,F). The C-terminal region of NKCS-[LP], however, was located in the aqueous phase, and somewhat distorted, by design, due to the presence of Pro-15. Besides disruption of the α-helix, Pro-15 lowered the kink's flexibility, making the amphipathic arrangement of the peptide even less plausible than that of the original peptide.

To summarize, the conformations of the three peptides investigated in the simulations could be divided into two groups. The inner conformations were helical to various degrees, and amphipathic, with nonpolar residues facing the membrane. The outer conformations were much less helical and the interaction of the peptide with the membrane was maintained only by the Coulombic attraction between the positively charged Arg and Lys residues of the peptide with the membrane surface charge. According to the simulations, the membrane affinity of the peptide depended on the compatibility of its sequence with the amphipathic helix structure, in agreement with our hypothesis. Next we describe experiments that characterize the helicity of the three peptides and examine their membrane affinity and activity.

Experimental Results

CD Spectroscopy. To characterize the structure of NKCS, NKCS-[LP], and NKCS-[AA], we carried out CD experiments in the presence and absence of SDS. According to our results,

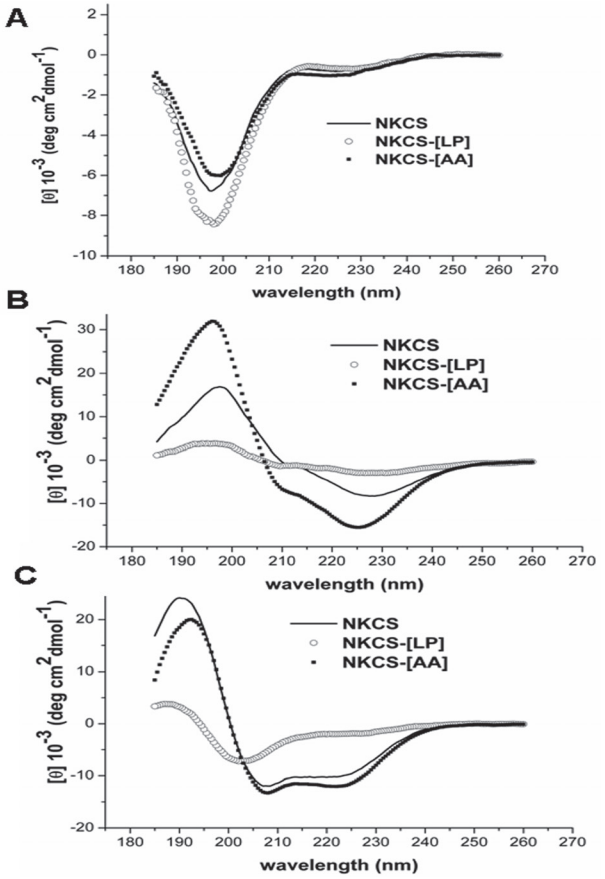

Figure 3. (A) CD measurements of NKCS and its derivatives in double distilled water. Negative bands in the region 198−200 nm and positive bands in the range 216−218 nm indicate disordered peptide structures. CD measurements of NKCS and its derivatives mixed with 1 mM (B) and 10 mM (C) SDS. The low concentration of detergent induced the adoption of ordered structures. At 10 mM SDS, NKCS and NKCS-[AA] clearly fold into α-helices (positive bands at 190−192 nm, negative bands at 208 and 222 nm). NKCS-[LP] is a mixture of β-sheet and random coils.

the three peptides were randomly coiled in water (Figure 3A). After the addition of the negatively charged SDS detergent, the adoption of a secondary structure was visible. Below the critical micelle concentration (CMC) of SDS, which is 8 mM, the peptides showed a preference toward the α-helical conformation (Figure 3B). The strong signal of NKCS-[AA] indicated a higher helical content in comparison with the two other peptides. At an SDS concentration above the CMC (10 mM), the helicity of NKCS and NKCS-[AA] increased (Figure 3C), but NKCS-[LP] seemed to adopt a mixture of random coils and β structures.

SPR. The interaction between the peptides and the lipid bilayer was investigated using the SPR method. The successful coating of the BIACore L1 chip by POPE was documented by the increase in the response units from 18200 to 24000 after rinsing with NaOH to wash away the unbound lipids (Figure 4A). The increase corresponded to a layer of thickness of 58 Å, similar to the thickness of a hydrated membrane obtained on the basis of SAXS measurements.

After injection of NKCS, a strong adsorption of the peptide was visible followed by a very slow desorption (Figure 4A). Such a behavior suggested a strong interaction between the peptide and POPE bilayers. The thickness of the peptide layer was estimated as 14 Å, corresponding to the diameter of an α-helix.[56,57] A different picture was observed after injection of

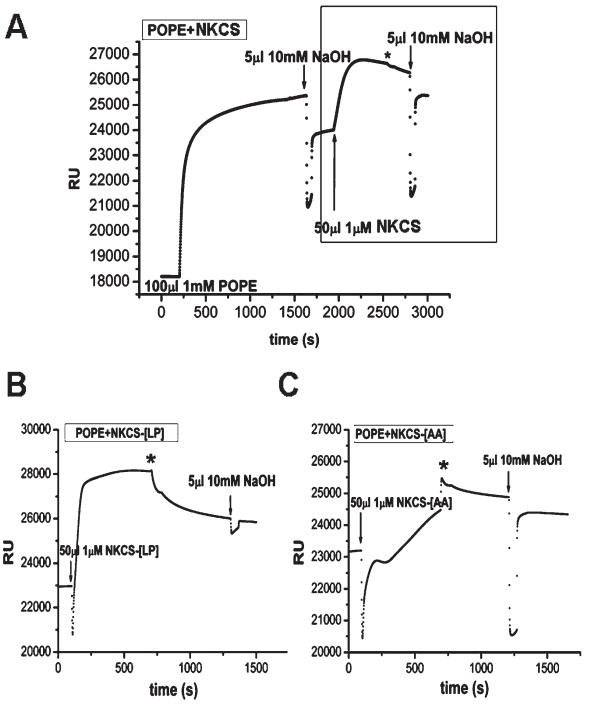

Figure 4. SPR measurements of the (A) NKCS, (B) NKCS-[LP], and (C) NKCS-[AA] peptides. Injections of POPE, NaOH, and peptides are indicated. The frame highlights the time range of the peptide−membrane interaction of NKCS with POPE. The onset was normalized to zero for NKCS-[LP] and NKCS-[AA]. The asterisks mark the end of the peptide injection and the beginning of peptide desorption. RU = response units.

NKCS-[LP] (Figure 4B). The peptide also adsorbed quickly. However, its desorption was very fast, which is indicative of a weaker affinity to the membrane than NKCS. The measurement allowed to estimate the peptide layer thickness as 29 Å.

The interaction of NKCS-[AA] with the POPE bilayer was more complicated (Figure 4C). After the injection of the peptide, its adsorption was very fast and strong but turned into a short desorption after 100 s. After an additional 80 s, a peptide adsorption occurred again. When the injection ended a slow desorption was observed. From the reference units (RU) one could approximate a peptide layer thickness of 12 Å, which corresponds to a single peptide layer. However, it should be stated that the determination of layer thickness from RU is a very difficult task and the reported values should be taken only as approximations.

For comparison, we determined the peptides' membrane affinity from the SPR sensograms, following previous studies.[22,58] The obtained values were similar to the computationally predicted ones, i.e., $-18.5kT$, $-16.1kT$, and $-25.7kT$ for NKCS, NKCS-[LP], and NKCS-[AA], respectively (Table 2).

SAXS Measurements. SAXS measurements were performed to investigate the influence of the peptides on the repeat distance (sum of lipid bilayer thickness and water layer between two lipid bilayers) and the inverse hexagonal phase transitions of POPE. All peptides changed the inverse hexagonal phase transition temperature of POPE liposomes (Supporting Information Figure S1 and Table 3) whereas the repeat distance, which was determined to be 55 ± 9 Å at 37 °C for POPE, remained the same within the error for all experiments (data not shown). All tested peptides shifted the transition temperature to higher values in a concentration dependent manner (Table 3). There

TABLE 3: Increase of the Inverse Hexagonal Phase Transition Temperature of a POPE Vesicles upon Interaction with NKCS Derivatives, Expressed as ΔT (°C)[a]

molar ratio [lipid/peptide]	NKCS	NKCS-[AA]	NKCS-[LP]
1000:1	4	3	4
300:1	10	5	5
100:1		9	6

[a] The aggregation of the sample POPE + NKCS in the molar ratio of 100:1 was so strong that the transfer into the measurement capillary was not possible.

TABLE 4: Antibacterial Activity of NKCS, NKCS-[AA], and NKCS-[LP] against *E. coli*, *S. carnosus*, and *B. subtilis* Determined as MIC (Minimal Inhibitory Concentration, μM)

peptide	*E. coli*	*S. carnosus*	*B. subtilis*
NKCS	0.63	2.5	1.25
NKCS-[AA]	1.25	2.5	2.5
NKCS-[LP]	2.5	5	5
melittin	2.5	0.63	0.63

was no effect on the pretransition between the gel and liquid crystalline phase for any of the peptides (data not shown).

Antibacterial and Hemolytic Activity. The three peptides NKCS, NKCS-[LP], and NKCS-[AA] and melittin (as a control) were tested against one Gram-negative and two Gram-positive bacteria strains and human erythrocytes. NKCS and its derivatives exhibited a good antibacterial activity against both types of bacteria, though they were slightly more active against the Gram-negative *E. coli* (Table 4). NKCS-[LP] showed an activity similar to that of melittin against *E. coli*, while NKCS and NKCS-[AA] were more potent. For the Gram-positive strains the minimal inhibitory concentration (MIC) of the three NKCS-based peptides was higher than the MIC of melittin. The peptides showed low hemolytic activity in comparison to melittin. At the very high concentration of 100 μM, the NKCS-[LP] and NKCS-[AA] derivatives caused lysis of 44.5% and 36.9% of red blood cells, respectively. The hemolytic activity of NKCS reached only 19.6% (Supporting Information Figure S2).

Discussion

In the present study we designed two cationic peptides based on NKCS, the 27-amino-acid fragment encompassing the membrane-active core region of NK-lysin. Their antibacterial and hemolytic activities, secondary structure, and interactions with model POPE membranes were investigated. The experiments were inspired by MC simulations.

Despite the overall good agreement between calculations and experiments in this study, it should be noted that our computational model has inherent limitations owing to its simplification of the complexity of the peptide−membrane interaction. First, the model treats the interaction of a single peptide molecule with the lipid bilayer and is not suitable (in its current form) for the study of peptide concentration effects, which are key to the understanding of antimicrobial peptide's membranolysis. Thus, the simulations are suitable only for results obtained at low peptide concentration. Second, the model membrane is planar (although free to change its width). Thus, membrane curvature effects, which are anticipated in the presence of POPE lipids, cannot be simulated. Third, both the peptide and membrane are described using a reduced representation, providing a procedure that is computationally feasible. However, it does not allow studies of specific peptide−lipid interactions in atomic details. Hydrogen bonds and salt bridges between the peptide and lipid, as well as the exact stereochemistry of the interaction, are not taken into account explicitly.

According to previous studies,[16] our CD measurements, and the MC simulations, NKCS was mostly unstructured in water but adopted an α-helical conformation in the membrane-mimetic environment. Moreover, the simulations of the peptide in POPE membranes showed a helix disruption at residues Thr-13 and Leu-14. The origin of this break in the helicity becomes clear when the peptide was presented as a canonical α-helix (Figure 2C). Two distinct hydrophobic faces, of the N- and C-termini, are oriented in different directions; i.e., the hydrophobic moments of the termini do not point in the same direction. Upon membrane interaction, this would not be a favorable conformation. However, the analysis of the computationally predicted inner conformations revealed that the kink in the middle allowed a deviation from a regular α-helix to a conformation with an improved amphipathic organization of the peptide. The kink enabled the helices in the N- and C-termini to align their hydrophobic moments so that the hydrophobic regions of both were oriented toward the membrane (Figure 2A).

The replacement of Leu-15 with Pro in NKCS-[LP] was assumed to perturb the α-helix even further, and both the CD measurements and the simulations supported this notion. NKCS-[LP] was found to be significantly less helical than NKCS, which can explain the reduced membrane affinity of this peptide in comparison to NKCS (Table 2). The weaker helicity of NKCS-[LP] can be correlated with the lower impact on the inverse hexagonal phase transition of POPE. Moreover, the SPR experiment showed a peptide layer of 29 Å, which is larger than the diameter of an α-helix.[56,57] This result can be correlated with the MC simulations that showed that while NKCS-[LP]'s N-terminus was embedded in the membrane, the C-terminus fluctuated above the surface (Figure 1E), resulting in an apparent thicker peptide layer.

The addition of two Ala residues into the sequence of NKCS was surmised to increase the α-helicity and improve the amphipathicity of the peptide, creating a single uninterrupted hydrophobic face (NKCS-[AA]; Figure 2B). The SPR experiments showed an association of NKCS-[AA] with the POPE membrane. The measured peptide layer thickness of 12 Å corresponds, approximately, to the average diameter of an α-helix, in agreement with the MC simulations. The computed and measured membrane-association free energy of NKCS-[AA] was much more negative (favorable) than that of NKCS (Table 2). Thus, we expected NKCS-[AA] to interfere more strongly with the membrane structure and to be more active against bacteria. However, the SAXS studies at various lipid−peptide ratios revealed consistently that the impact of NKCS-[AA] on the POPE bilayer structure was weaker than that of NKCS. The results also showed that NKCS-[AA] was slightly less active against bacteria than NKCS.

The three peptides shifted the temperature of inverse hexagonal phase transition to higher values. Observations of the peptide-induced lipids phase behavior can give an indication about membrane disruption. A temperature reduction suggests the generation of a negative membrane curvature whereas a high transition temperature indicates stiffening of the membrane and the induction of a positive curvature. The POPE lipid promotes spontaneous negative curvature,[59] and the adsorption of NKCS and its derivatives balanced this tendency and stabilized the bilayer. When the threshold concentration of the peptide was reached, a strong perturbation of the membrane occurred, leading eventually to lysis.[17,60]

This study was performed to examine the hypothesis that α-helicity and amphipathicity are the major structural features determining the membrane affinity of cationic antimicrobial peptides. We designed two peptides, based on the primary structure of NKCS. By exchanging (NKCS-[LP]) or inserting amino acids (NKCS-[AA]), we altered the α-helical content and amphipathicity of the peptide. Our CD and SPR measurements were in keeping with the Monte Carlo simulations regarding the secondary structure and membrane affinity of the peptides. Moreover, NKCS-[LP] showed a decreased antimicrobial activity and weak influence on POPE's hexagonal phase transition temperature, in comparison to NKCS, which correlated well with its lower (calculated and measured) membrane affinity. In contrast, the increase in the membrane affinity of the NKCS-[AA] peptide in comparison to that of NKCS did not result in increased membrane-lytic potency. Quite the contrary, the peptide was slightly less active than the original NKCS (Tables 3 and 4).

Antimicrobial and membranolytic activity correlate with membrane affinity; the affinity must be high enough for the peptide to associate with the membrane. Indeed, NKCS-[LP], which showed a reduced membrane affinity in comparison to NKCS also exhibited a reduced activity. However, NKCS-[AA] demonstrated approximately the same activity as NKCS in spite of its increased membrane affinity, implying that activity depends also on other factors. Perhaps the membrane adsorption of a kinked peptide, such as NKCS, can cause more significant membrane disruption than a perfect α-helix, such as NKCS-[AA]. In this respect, it is noteworthy that a cyclic analog of melittin (which retained the overall helical structure) showed reduced membrane affinity but increased activity.[61]

Conclusions

Overall, the present study demonstrates how the interplay between simulations and experiments can be combined to provide a molecular picture of the membrane interaction of NKCS. The next challenge is to understand the mechanism of membrane lysis. For that, it is necessary to replace the crude representation of the membrane that was used here by a molecular (perhaps even atomistic) model.

Acknowledgment. We gratefully acknowledge the assistance of Sadasivam Jeganathan (Max-Planck-Arbeitsgruppe "Zytoskelett" of Prof. Dr. E. Mandelkow in Hamburg) for CD measurements. We thank Prof. Dr. P. Dubruel from the Department of Organic Chemistry at Ghent University for supporting us with the SPR knowledge and equipment. This work was financially supported by the European Commission under the sixth Framework Program through the Marie-Curie Action: BIOCONTROL, contract number MCRTN-33439 and German-Israeli Foundation for Scientific Research and Development, grant number 831/2004.

Supporting Information Available: Detailed description of computational methods, a table of energy decomposition data, and two figures showing SAXS patterns and hemolytic activity diagram are provided. This material is available free of charge via the Internet at http://pubs.acs.org.

References and Notes

(1) Cohen, M. L. *Science* **1992**, *257*, 1050–5.
(2) Hamilton-Miller, J. M. *Int. J. Antimicrob. Agents* **2004**, *23*, 209–12.
(3) Powers, J. P.; Hancock, R. E. *Peptides* **2003**, *24*, 1681–91.
(4) Bush, K.; Macielag, M.; Weidner-Wells, M. *Curr. Opin. Microbiol.* **2004**, *7*, 466–76.
(5) Shai, Y. *Curr. Pharm. Des.* **2002**, *8*, 715–25.
(6) Zasloff, M. *Nature* **2002**, *415*, 389–95.
(7) Epand, R. M.; Shai, Y.; Segrest, J. P.; Anantharamaiah, G. M. *Biopolymers* **1995**, *37*, 319–38.
(8) Shai, Y. *Trends Biochem. Sci.* **1995**, *20*, 460–4.
(9) Shai, Y.; Oren, Z. *Peptides* **2001**, *22*, 1629–41.
(10) Matsuzaki, K. *Biochim. Biophys. Acta* **1999**, *1462*, 1–10.
(11) Andra, J.; Leippe, M. *Med. Microbiol. Immunol.* **1999**, *188*, 117–24.
(12) Jacobs, T.; Bruhn, H.; Gaworski, I.; Fleischer, B.; Leippe, M. *Antimicrob. Agents Chemother.* **2003**, *47*, 607–13.
(13) Olak, C.; Muenter, A.; Andra, J.; Brezesinski, G. *J. Pept. Sci.* **2008**, *14*, 510–7.
(14) Schroder-Borm, H.; Bakalova, R.; Andra, J. *FEBS Lett.* **2005**, *579*, 6128–34.
(15) Willumeit, R.; Kumpugdee, M.; Funari, S. S.; Lohner, K.; Navas, B. P.; Brandenburg, K.; Linser, S.; Andra, J. *Biochim. Biophys. Acta* **2005**, *1669*, 125–34.
(16) Andra, J.; Monreal, D.; Martinez de Tejada, G.; Olak, C.; Brezesinski, G.; Gomez, S. S.; Goldmann, T.; Bartels, R.; Brandenburg, K.; Moriyon, I. *J. Biol. Chem.* **2007**, *282*, 14719–28.
(17) Lohner, K.; Prenner, E. J. *Biochim. Biophys. Acta* **1999**, *1462*, 141–56.
(18) Haris, P. I.; Chapman, D. *Biopolymers* **1995**, *37*, 251–63.
(19) Ladokhin, A. S.; Selsted, M. E.; White, S. H. *Biophys. J.* **1997**, *72*, 794–805.
(20) Salditt, T.; Li, C.; Spaar, A. *Biochim. Biophys. Acta* **2006**, *1758*, 1483–98.
(21) Bechinger, B. *Biochim. Biophys. Acta* **1999**, *1462*, 157–83.
(22) Papo, N.; Shai, Y. *Biochemistry* **2003**, *42*, 458–66.
(23) La Rocca, P.; Biggin, P. C.; Tieleman, D. P.; Sansom, M. S. *Biochim. Biophys. Acta* **1999**, *1462*, 185–200.
(24) Forrest, L. R.; Sansom, M. S. *Curr. Opin. Struct. Biol.* **2000**, *10*, 174–81.
(25) Kessel, A.; Cafiso, D. S.; Ben-Tal, N. *Biophys. J.* **2000**, *78*, 571–83.
(26) Kessel, A.; Haliloglu, T.; Ben-Tal, N. *Biophys. J.* **2003**, *85*, 3687–95.
(27) Milik, M.; Skolnick, J. *Proteins* **1993**, *15*, 10–25.
(28) Baumgartner, A. *Biophys. J.* **1996**, *71*, 1248–55.
(29) Efremov, R. G.; Nolde, D. E.; Vergoten, G.; Arseniev, A. S. *Biophys. J.* **1999**, *76*, 2448–59.
(30) Ducarme, P.; Rahman, M.; Brasseur, R. *Proteins* **1998**, *30*, 357–71.
(31) Maddox, M. W.; Longo, M. L. *Biophys. J.* **2002**, *82*, 244–63.
(32) Veresov, V. G.; Davidovskii, A. I. *Eur Biophys J* **2007**, *37*, 19–33.
(33) Tzlil, S.; Murray, D.; Ben-Shaul, A. *Biophys. J.* **2008**, *95*, 1745–57.
(34) Wee, C. L.; Sansom, M. S.; Reich, S.; Akhmatskaya, E. *J. Phys. Chem. B* **2008**, *112*, 5710–7.
(35) Kessel, A.; Shental-Bechor, D.; Haliloglu, T.; Ben-Tal, N. *Biophys. J.* **2003**, *85*, 3431–44.
(36) Shental-Bechor, D.; Kirca, S.; Ben-Tal, N.; Haliloglu, T. *Biophys. J.* **2005**, *88*, 2391–402.
(37) Shental-Bechor, D.; Haliloglu, T.; Ben-Tal, N. *Biophys. J.* **2007**, *93*, 1858–71.
(38) Gordon-Grossman, M.; Gofman, Y.; Zimmermann, H.; Frydman, V.; Shai, Y.; Ben-Tal, N.; Goldfarb, D. *J. Phys. Chem. B* **2009**, *113*, 12687–95.
(39) Wang, X.; Quinn, P. J. *Biochim. Biophys. Acta* **2002**, *1564*, 66–72.
(40) Siegel, D. P. *Biophys. J.* **2006**, *91*, 608–18.
(41) van den Brink-van der Laan, E.; Killian, J. A.; de Kruijff, B *Biochim. Biophys. Acta* **2004**, *1666*, 275–88.
(42) Ames, G. F. *J. Bacteriol.* **1968**, *95*, 833–43.
(43) Bishop, D. G.; Rutberg, L.; Samuelsson, B. *Eur. J. Biochem.* **1967**, *2*, 448–53.
(44) Koch, H. U.; Haas, R.; Fischer, W. *Eur. J. Biochem.* **1984**, *138*, 357–63.
(45) Matsuzaki, K.; Sugishita, K.; Ishibe, N.; Ueha, M.; Nakata, S.; Miyajima, K.; Epand, R. M. *Biochemistry* **1998**, *37*, 11856–63.
(46) Hallock, K. J.; Lee, D. K.; Ramamoorthy, A. *Biophys. J.* **2003**, *84*, 3052–60.
(47) Szule, J. A.; Rand, R. P. *Biophys. J.* **2003**, *85*, 1702–12.
(48) Angelova, A.; Ionov, R.; Koch, M. H.; Rapp, G. *Arch. Biochem. Biophys.* **2000**, *378*, 93–106.
(49) Tytler, E. M.; Segrest, J. P.; Epand, R. M.; Nie, S. Q.; Epand, R. F.; Mishra, V. K.; Venkatachalapathi, Y. V.; Anantharamaiah, G. M. *J. Biol. Chem.* **1993**, *268*, 22112–8.

(50) Petrey, D.; Xiang, Z.; Tang, C. L.; Xie, L.; Gimpelev, M.; Mitros, T.; Soto, C. S.; Goldsmith-Fischman, S.; Kernytsky, A.; Schlessinger, A.; Koh, I. Y.; Alexov, E.; Honig, B. *Proteins* **2003**, *53*, 430–5.
(51) Blondelle, S. E.; Houghten, R. A. *Pept. Res.* **1991**, *4*, 12–8.
(52) Hall, K.; Mozsolits, H.; Aguilar, M. I. *Lett. Pept. Sci.* **2003**, *10*, 475–485.
(53) Cooper, M. A.; Hansson, A.; Lofas, S.; Williams, D. H. *Anal. Biochem.* **2000**, *277*, 196–205.
(54) *Real-Time Analysis of biomolecular interactions: applications of BIACORE*; Nagata, K., Handa, H., Eds.; Springer Publishing Co.: New York, 2000.
(55) Boulin, C.; Kempf, R.; Koch, M. H. J.; McLaughlin, S. M. *Nucl. Instrum. Methods.* **1986**, *249*, 399–407.
(56) Vie, V.; Van Mau, N.; Chaloin, L.; Lesniewska, E.; Le Grimellec, C.; Heitz, F. *Biophys. J.* **2000**, *78*, 846–56.
(57) Ambroggio, E. E.; Separovic, F.; Bowie, J.; Fidelio, G. D. *Biochim. Biophys. Acta* **2004**, *1664*, 31–7.
(58) Mozsolits, H.; Thomas, W. G.; Aguilar, M. I. *J. Pept. Sci.* **2003**, *9*, 77–89.
(59) Fuller, N.; Rand, R. P. *Biophys. J.* **2001**, *81*, 243–54.
(60) Bechinger, B.; Lohner, K. *Biochim. Biophys. Acta* **2006**, *1758*, 1529–39.
(61) Unger, T.; Oren, Z.; Shai, Y. *Biochemistry* **2001**, *40*, 6388–97.

JP909154Y

CHAPTER SIX

Antimicrobial Peptides and Their Interactions with Model Membranes

Agnieszka Rzeszutek *and* Regine Willumeit*

Contents

Abstract

Natural and synthetic antimicrobial peptides (AMPs) show interesting features, and they are considered possible alternatives to common antibiotics which might induce resistance in bacteria. We present a comparative study of the interaction of two homologous AMPs with lipids mimicking the cytoplasmic membrane of prokaryotic and eukaryotic cells. The peptides were derived from the membranolytic protein NK-lysin. Phosphatidylcholine (PC) was used as a representative of human erythrocytes and phosphatidylethanolamine (PE) was chosen to build the model cytoplasmic membrane of *Escherichia coli*. Although the sequences of the investigated peptides vary only in one position, they show a difference in activity against *E. coli*. The results of small angle X-ray scattering and differential scanning calorimetry revealed that these two analogs behaved differently upon interaction with PE liposomes. One of the peptides significantly decreased the temperature of the hexagonal phase transition,

* Corresponding author. Tel: +49 4152 871291; Fax: +49 4152 871356.
E-mail address: regine.willumeit@gkss.de

GKSS Research Center, Max-Planck-Str. 1, Geesthacht, Germany

Advances in Planar Lipid Bilayers and Liposomes, Volume 12
ISSN 1554-4516, DOI: 10.1016/S1554-4516(10)12006-7

© 2010 Elsevier Inc.
All rights reserved.

inducing a negative membrane curvature, whereas the second one shifted the phase transition temperature to higher values. No influence on the lipid phase behavior or the bilayer structure was detected after mixing the peptides with PC vesicles. This observation completed the results of the hemolytic assay, where the toxic effect of the peptides on the red blood cells was not found.

1. Antimicrobial Peptides

The contemporary health care is facing an alarming increase of resistance of pathogenic bacteria to antibiotic therapies [1,2]. The studies show that development of methicillin and vancomycin resistance in hospitals follows an exponential behavior while on the other hand, the number of new antibiotics decreased significantly during the last 20 years [3,4]. For this reason, a worldwide effort is made to acquire the potent alternatives for conventional antibiotics. As the nature has always been giving the best solutions, the naturally occurring antimicrobial peptides (AMPs) arose as promising candidates [5–7].

The AMPs constitute a component of the innate immune system of all higher organisms [8–11]. They can act as immunomodulators or by direct killing of invading pathogens [12,13]. Moreover, they can be also produced by bacteria to fight other prokaryotes present in the same environmental niche [14]. The AMPs were found very active against the broad spectrum of Gram-positive and Gram-negative bacteria, fungi, parasites, and viruses and some of them display an activity also against tumor cells [15,16]. They present various structures and it is very difficult to categorize them on the basis of their secondary conformation only [5,17]. In general, they can be characterized as short (12–50 amino acids), positively charged, and amphipathic peptides. The two last features are considered to be crucial for the antimicrobial activity of AMPs.

Although hundreds of peptides have been identified, the mechanism of action has been deeply investigated only for a few of them. Most of AMPs act by direct physical interaction with phospholipids present in a cytoplasmic membrane of pathogens without exploitation of any receptors [18]. The accumulation of peptides on the surface of target bacterial cell occurs via electrostatic interaction between positively charged AMPs and negatively charged residues of lipopolysaccharide in Gram-negative bacteria or teichoic and lipoteichoic acids in Gram-positive bacteria. In Gram-negative microorganisms, the peptides pass the outer membrane using the "self-promoted uptake" system and interact with the phospholipids of the cytoplasmic membrane [19]. Several models have been developed to describe these interactions followed by the disruption of lipid bilayer, namely barrel-stave, toroidal pore, and carpet models [9,20] (Fig. 1).

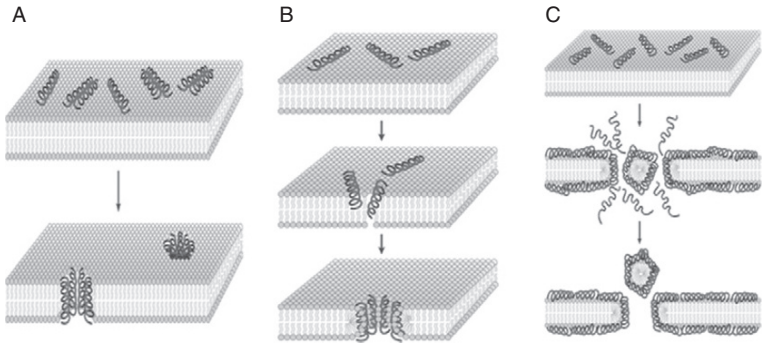

Figure 1 **The model mechanisms of interactions between antimicrobial peptides and membrane bilayer: (A) barrel-stave, (B) toroidal, and (C) carpet model. Reprinted from Ref. [20], copyright 2005, with permission from Macmillan Publishers Ltd.**

Upon the peptide–membrane interaction, the amphipathic structure of AMPs, where the polar amino acid residues are localized on one side and the hydrophobic residues on the other side of a peptide, is very meaningful. The cytoplasmic membrane of bacteria is enriched in negatively charged lipids and the peptide–membrane association is possible because of the attractive forces between the anionic lipid head groups and cationic side chains of AMPs. On the other hand, the interaction of peptides with the nonpolar interior of the bilayer is enabled by the hydrophobic side of AMPs. Although the peptide–membrane interactions at a high peptide:lipid molar ratio eventually lead to the membrane lysis, the intracellular activity of AMPs cannot be excluded [20,21].

2. Cytoplasmic Membrane and Phase Behavior of Lipids

The cytoplasmic membrane plays a very important role as a permeability barrier of a cell. It is composed mainly of lipids and proteins. The mass ratio of these two components can vary from 4:1 to 1:4 in different organisms [22]. The cytoplasmic membrane is a very dynamic and fluid structure. In the famous "fluid mosaic model" presented in 1972 by Singer and Nicolson [23], the membrane was shown as a two-dimensional (2D) solution of lipids and proteins. However, it is important to underline that the role of lipids is not limited only to support the proteins, but they are also involved in many biological functions [24,25].

The phospholipids constitute the major class of lipids present in a cytoplasmic membrane. The most interesting feature of these molecules, which also decides about the functionality of membrane, is an ability to

adopt different polymorphic structures [26]. Under the physiological conditions, the membrane resembles a lamellar liquid crystalline phase. The phospholipids are organized in a lattice which is represented by the bilayer with the hydrophobic core (Fig. 2). The acyl chains are disordered and fluid. Moreover there is no order in the lattice and the head groups are randomly organized. Lipids in this state are able to effect rather fast lateral diffusion. The fluidity of the membrane decides about many processes, for example, transport and the activity of enzymes [27,28]. It depends on the membrane composition and can be regulated by the organisms in response to the environmental changes. In bacterial cells, the viscosity of membrane increases proportionally to the amount of phospholipids with the long and saturated acyl chains. Such phospholipids favor a rigid state in which the hydrocarbon chains interact with each other. Such a structure is known as a lamellar gel phase. Except the high order in the hydrophobic core, this phase is also characterized by the crystalline order of the head groups, which are arranged in a triangular lattice. In animals, the fluidity of membrane is modulated also by cholesterol [29,30].

The other two lipid phases, which can be formed within the biological membranes, are nonlamellar structures: inverse hexagonal phase and three-dimensional (3D) cubic phases (Fig. 3). These forms appear in a very short time scale in living systems, for example, during the cell division or fusion processes [31]. In the inverse hexagonal phase (H_{II}), lipids form elongated cylindrical structures with the acyl chains directed to the outside [32]. To avoid the contact with water, these tubular structures arrange themselves in 2D hexagonal crystals. The cubic phases formed by membrane lipids are mostly bicontinuous, which means that they consist of two coexisting water

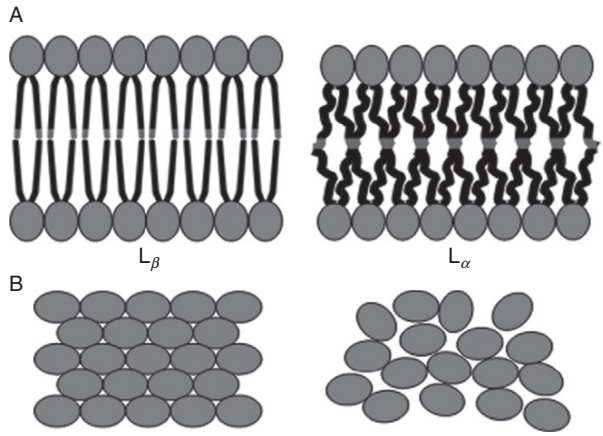

Figure 2 The lipid bilayer in a gel (L_β) and liquid crystalline (L_α) phase; view from the side (A) and from the top (B).

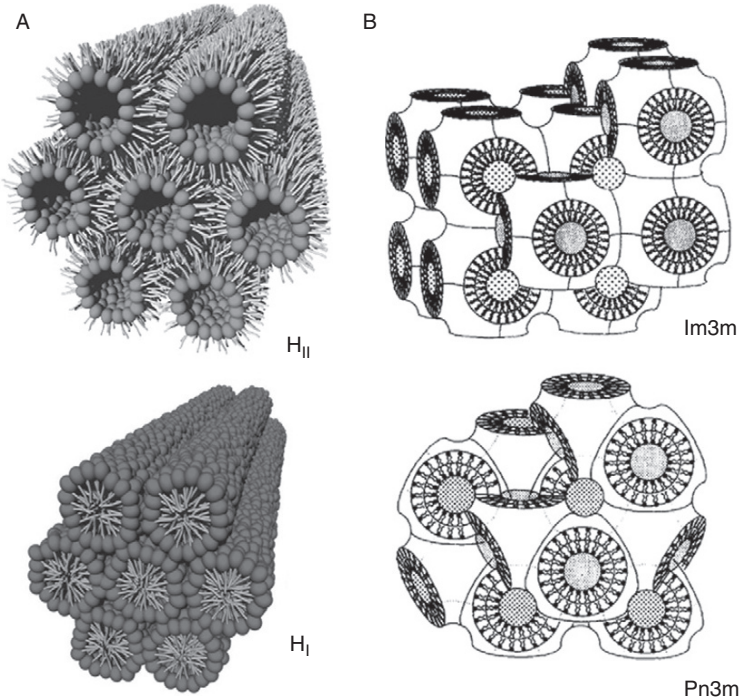

Figure 3 (A) Inverse hexagonal (H_{II}) and normal hexagonal (H_I) phases. Reprinted from Ref. [32], copyright 2009, with permission. (B) Cubic structures formed in biological systems. Reprinted from Ref. [33], copyright 1991, with permission from Elsevier.

regions separated by a single lipid bilayer [33]. Although many types of cubic phases have been identified and described, only two of them are relevant for biological systems as they can exist in an excess of water [34]. These phases are characterized by Pn3m and Im3m space groups and are known also as Q^{224} and Q^{227}, respectively [35,36]. The normal hexagonal phase (H_I) can be formed by the detergents and single chain phospholipids in artificial mixtures; however, usually it is not adopted by biologically relevant molecules.

The ability of membrane to adopt one of these structures depends strongly on the type of lipids and their molecular shape [37,38]. When an area occupied by a lipid head group is the same as a cross-sectional area of acyl chains, the lipid can be envisioned as a cylinder (Fig. 4). Such lipids favor planar bilayers and stabilize the lamellar phase. This group includes phosphatidylcholine (PC), phosphatidylglycerol, phosphatidylserine, phosphatidylinositol, phosphatidic acid, cardiolipin, and sphingomyelin. The lipids with a small head group and much larger area of acyl chains can be

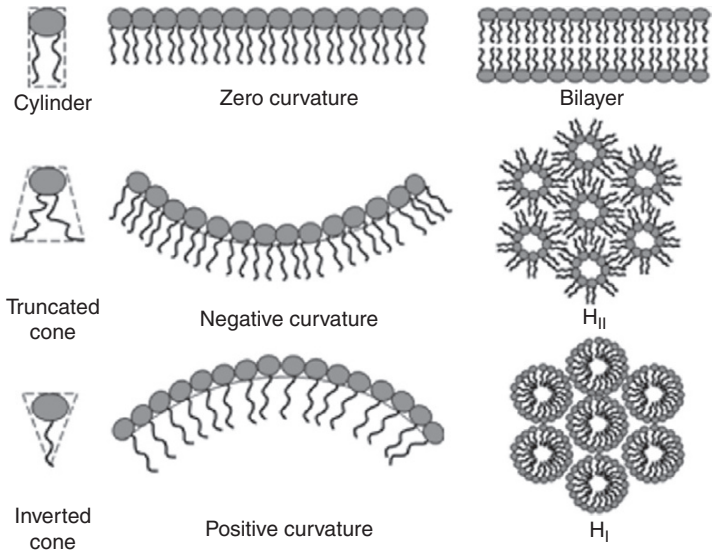

Figure 4 **The relationship between the molecular shape of lipids and polymorphic structures.**

shown as a truncated cone. They have a very strong tendency to induce a negative membrane curvature. This feature imposes the formation of nonlamellar structures: an inverse hexagonal phase, cubic phases, or inverted micelles. This class is represented by phosphatidylethanolamine (PE)—the most prominent bacterial phospholipid. The third group comprises molecules resembling an inverted cone—they are characterized by a relatively big head group and a small acyl chain volume. The detergents and single chain lysophospholipids can be assigned here. These molecules favor a positive curvature and tend to form a normal hexagonal phase or micelles. However, it is important to underline that the presentation of lipids in a molecular shape of truncated or inverted cone is an approximation. The lipid molecules are asymmetric with respect to the axis perpendicular to the monolayer surface and consequently can be characterized as anisotropic. The geometry of inverted or truncated cone can be assigned to isotropic molecules, favoring spherical or inverted spherical micellar shapes, respectively. In case of highly anisotropic elongated aggregates, typical for normal, or inverted hexagonal phases, the anisotropy of molecules should be taken into account and the lipids should be considered as wedge shaped [39,40].

The ratio of lamellar and nonlamellar prone lipids in a cytoplasmic membrane is crucial for many processes. It decides about the membrane permeability, transport, cell division and fusion, folding, and functionality of membrane proteins [31,41–44].

As an activity of AMPs requires interactions with a cytoplasmic membrane, the AMPs must influence the structure of phospholipid bilayer. The peptide–membrane association includes the changes in the curvature stress and the formation of nonlamellar phases. This can be directly linked to the mechanism of interactions [45].

The AMPs, upon the binding to the lipid bilayers, very often shift the temperature of the inverse hexagonal phase transition (T_H). The decrease of T_H is correlated with the promotion of a negative curvature, which consists in the bending of the bilayer around the lipid head groups. The peptides which affect the membrane in such a way can be considered as the catalysts of nonlamellar structures. It is suggested that this type of interaction can lead to the creation of transient nonbilayer intermediates and allows the translocation of a peptide across the membrane, as in the case of polyphemusins [46]. On the other hand, the formation of nonlamellar phases supports the supramolecular reorganization of a bilayer and eventually brings to the perturbation of membrane integrity. The peptides inducing a negative membrane curvature include, for example, alamethicin, which at low concentrations decreases T_H of dioleoylphosphoethanolamine [47], nisin [48], and gramicidin A [49,50].

The second group of peptides modulating the membrane curvature comprises the AMPs able to shift T_H to higher values. These peptides promote the positive curvature strain within a lipid bilayer and inhibit the formation of nonlamellar structures. The positive curvature leads to building a toroidal pore across the membrane. Such behavior was observed for magainin-2 [51], LL-37 [52], and δ-lysin [53]. Very often, the high concentrations of AMPs cause the micellarization of a lipid bilayer, which in fact can be considered as an extreme example of a positive curvature [45,54].

3. NK-Lysin, NK-2, and NKCS

NK-lysin is a polypeptide isolated from natural killer [31] cells found in a porcine small intestine [55]. It belongs to the family of SAPOSIN-like proteins (SAPLIPs), which comprise structurally conserved, but functionally diverse group of small (8–9 Da) polypeptides [56,57]. NK-lysin displays a cytotoxic and antimicrobial activity—it kills the cells involving the lytic mode of action. It is composed of 78 amino acids organized in five α-helices [58]. The detailed studies of structure–function dependence revealed that the membranolytic activity can be caused in particular by the third and forth α-helices. This fragment, embracing 27 amino acids (39–65 residues of NK-lysin), was synthesized with three substitutions and named NK-2 [59].

NK-2 exhibits a very good activity against Gram-positive and Gram-negative bacteria, pathologic fungus *Candida albicans*, protozoan parasite *Trypanosoma cruzi*, and malaria parasite *Plasmodium falciparum* [59–61]. The studies revealed that NK-2 selectively kills several cancer cell lines [62]. Moreover, the peptide is nontoxic toward human cells, which makes it a good candidate for therapeutic applications [59,62,63]. NK-2 is randomly coiled in aqueous solutions, but adopts amphipathic α-helical structure in a hydrophobic environment [59]. The 3D structure of NK-lysin region corresponding to NK-2 allows to assume that the peptide does not resemble a rigid α-helical rod, but rather presents a helix-hinge-helix fold [64] (Fig. 5).

NKCS is an analog of NK-2, derived by the substitution of cysteine at the position 7 by serine [65]. This modification was dedicated to enhance the stability of the peptide. The presence of thiol group in cysteine was connected with the high susceptibility to oxidation and formation of disulfide bridges. NK-2 dimers were found as a result of peptide aging and appeared inactive (detected by MS, unpublished data). The amino acid serine was chosen to keep the same net charge (+10), to minimize possible conformational changes, and to maintain the hydrophobicity of the peptide. NKCS displays an activity comparable to NK-2—it is very active against Gram-positive and Gram-negative bacteria and does not display toxic activity against human cells [64,65]. NKCS was used as a template to design several analog peptides (Table 1). The aim of their synthesis consisted in establishing the importance of particular fragments of NKCS as well as single amino acids for the antibacterial activity. The analysis of membrane interaction of the newly derived peptides showed close analogy to the behavior of parental NKCS. Interestingly, a very striking difference was observed between NKCS and NK-2. Although these two peptides differ only at one position, they behave in very different ways upon the interaction with the bacterial membrane.

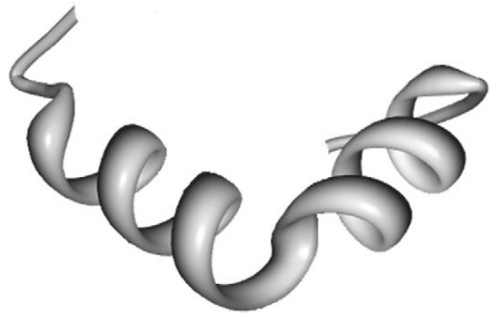

Figure 5 Structure model of peptide NK-2 extracted from the NMR structure of NK-lysin deposited at the PDB (1NKL).

Table 1 The minimal inhibitory concentrations (MIC) of NK-2, NKCS, and NKCS-derived peptides against Gram-negative *Escherichia coli* and Gram-positive *Bacillus subtilis* and *Staphylococcus carnosus*

		MIC (μM)		
Peptide	Sequence	*E. coli*	*B. subtilis*	*S. carnosus*
NK-2	KILRGVCKKIMRTFLRRISKDILTGKK	2.50	0.62	2.50
NKCS	KILRGV*S*KKIMRTFLRRISKDILTGKK	0.62	1.25	2.50
NKCS-DA	KILRGV*S*KKIMRTFLRRISK*A*ILTGKK	1.25	0.62	1.25
NKCS-DK	KILRGV*S*KKIMRTFLRRISK*K*ILTGKK	0.62	0.62	0.62
NKCS-FW	KILRGV*S*KKIMRT*W*LRRISKDILTGKK	1.25	0.62	1.25
NKCS-K17	*K*KILRGV*S*KKIMRTFLRR	2.50	0.62	1.25
NKCS-VMKR	KILRG*MSR*KIMRTFLRR	2.50	0.62	0.62
NKCS-14_2	KILRGV*S*KKIMRTFKI LRGV*S*KKIMRTF	0.62	0.62	1.25

MIC is determined as the minimal concentration of a peptide at which the growth of bacteria is suppressed by at least 90%.

4. Interactions of NK-2 and NKCS with the Liposomes Mimicking Eukaryotic and Prokaryotic Cytoplasmic Membranes

NKCS and its parental peptide NK-2 show virtually no hemolytic activity [63,64]. Their toxicity toward human red blood cells was compared to that of melittin. This AMP, isolated from the venom of honey bee *Apis mellifera*, is very toxic toward both bacterial and human cells [66]. At a very high concentration of 100 μM melittin causes the total lysis of erythrocytes, whereas NKCS and NK-2 lyse less than 20% of red blood cells. At this point, it is necessary to underline that 100 μM concentration is extremely high, as NK-2 inhibits the growth of *Escherichia coli* at 2.5 μM and NKCS at 0.6 μM. To gain insight into the structural and biophysical details of peptide–membrane interactions, small angle X-ray scattering (SAXS) and differential scanning calorimetry (DSC) are often applied. The former technique allows the identification of structures induced by the peptides, whereas the latter one can be used for the thermodynamic description of these changes. Moreover, these two methods enable the use

of liposomes suspended in an aqueous solution. Such conditions closely resemble the native environment, in which peptide antibiotics can target the pathogens.

4.1. Interactions with the Membrane of Erythrocytes

The liposomes composed of 1-palmitoyl-2-oleoyl-*sn*-glycero-3-phosphocholine (POPC) are usually chosen to mimic the membrane of human red blood cells. PC is the main component of the outer leaflet of human erythrocyte membrane and is not present in the bacterial cells [67,68] (Table 2). SAXS of POPC shows the typical diffraction pattern for a lamellar liquid crystalline phase with a repeat distance of 6.5 nm at 20 °C (Fig. 6A). In the course of heating, the intensity of reflections decreased, which was connected with the decomposition of liposomes. Above 60 °C, the position of the first order peak is already very difficult to determine. The addition of NK-2 or NKCS does not influence the structure of POPC bilayers. The only change is observed in the repeat distance, which is defined as a sum of lipid bilayer thickness and a water layer between two lipid bilayers. After the addition of NK-2, the repeat distance increases, but this can be assigned to a hydration of lipid bilayers enhanced by the presence of peptide (Fig. 6B). The similar behavior was observed for NKCS (data not shown).

The lack of interaction between the peptides and POPC can be explained by the nature of PC. The liposomes composed of this zwitterionic lipid do not possess the surface negative charges accessible for interaction with cationic NK-2 and NKCS. The headgroup of POPC consists of a nitrogen atom surrounded by three methyl groups, which shade the negative charge of the phosphate like an umbrella. Such a voluminous headgroup decides about a cylindrical shape of the molecule. As the electrostatic interaction constitutes the force attracting the peptides to the bacterial surface, the lack of anionic molecules on the surface of human erythrocytes makes NK-2 and NKCS harmless for the red blood cells and indicates a very good selectivity.

Table 2 The lipid composition of human red blood cells [68] and the inner membrane of *E. coli* [67]

	Phospholipid (%)							
Membrane	PC	SM	PE	PS	PI	PA	PG	CL
Erythrocyte—outer leaflet	44.8	42.1	11.1	–	–	–	–	–
Erythrocyte—inner leaflet	14.0	9.1	43.9	29.6	1.2	2.2	–	–
E. coli	–	–	69.0	–	–		19.0	6.5

PC, phosphatidylcholine; SM, sphingomyelin; PE, phosphatidylethanolamine; PS, phosphatidylserine; PI, phosphatidylinositol; PA, phosphatidic acid; PG, phosphatidylglycerol; CL, cardiolipin.

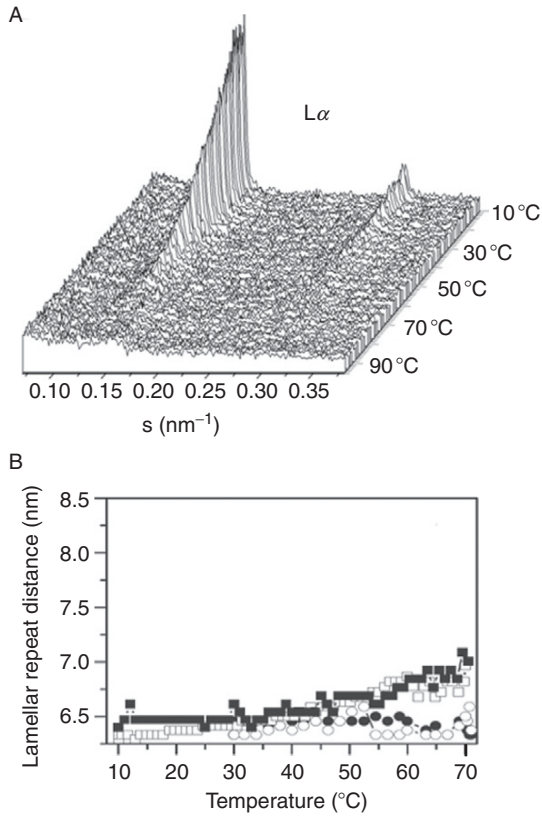

Figure 6 (A) The scattering pattern of POPC liposomes. $s = 1/d = 2\sin(\theta)/\lambda$, where λ is the wavelength of the X-ray beam and 2θ is the scattering angle. (B) The influence of NK-2 on the lamellar structure of POPC at different lipid:peptide molar ratios: pure lipid (●), 1000:1 (○), 300:1 (□), and 100:1 (■). Reprinted from Ref. [69], copyright 2005, with permission from Elsevier.

4.2. Interactions with the Membrane of *E. coli*

The lipid 1-palmitoyl-2-oleoyl-*sn*-glycero-3-phosphoethanolamine (POPE) is used very often to build an artificial system mimicking the cytoplasmatic membrane of *E. coli*. Both POPE and POPC are defined as zwitterionic lipids, but in contrast to the cylindrical PC, PE has a different molecular shape. POPE headgroup has only three hydrogen atoms bound to the nitrogen. Together with the space consuming acyl chains, which are the same for POPC, POPE has a truncated conical shape which allows the lipids to convert into nonlamellar structures. As both lipids are zwitterionic, one would expect the same behavior under the peptide–membrane interactions. Such comparison results in a fast assumption that interactions are not

possible between POPE and peptides. However, the results of SAXS and DSC show that this conclusion is not correct. The possibility of binding NKCS to PE membrane indicates that the surface of the liposomes must carry the negative charge. This hypothesis is confirmed by the Zeta-potential measurements. The results reveal that the surface of PE vesicles has a potential of -32.4 ± 3.4 mV, whereas the potential of PC is determined as -2.3 ± 2.0 mV [69].

POPE is characterized by two phase transitions. At 25.1 °C, the melting of acyl chains occurs and the lipid bilayer undergoes the change from ordered solid (defined also as a gel phase) to liquid crystalline phase. The addition of NK-2 and NKCS does not affect this phase transition (Table 3).

The second phase transition typical for POPE is the formation of non-lamellar structures, identified on the basis of SAXS diffraction patterns as an inverse hexagonal phase (Fig. 7). According to DSC results, pure POPE undergoes this transition at 66.4 °C [69]. The addition of peptides has an interesting and unexpected effect. NK-2 lowers the temperature of hexagonal phase transition in a concentration dependent manner. The lipid: peptide molar ratio 100:1 causes the decrease to 61.1 °C, and at the ratio 30:1 the temperature drops to 52.3 °C. NK-2 induces the negative curvature strain in the bilayer, which favors the formation of nonlamellar structures and leads eventually to the membrane disruption.

A dramatically different behavior is observed for NKCS [64]. Although the peptides differ only at one amino acid position, NKCS acts in the opposite way. The lipid:peptide molar mixture 1000:1 increases the temperature of the phase transition by 4 °C. At the ratio 300:1 the influence on

Table 3 Thermodynamic details of acyl chain melting of pure POPE and changes induced after the addition of NK-2 and NKCS at different lipid:peptide molar ratios, determined on the basis of DSC data

Lipid:peptide (molar ratio)	T_m (°C)	$\Delta T_{1/2}$ (°C)	ΔH (kJ/mol)
POPE	*25.1*	*1.1*	*24.7*
	ΔT_m (°C)	$\Delta T_{1/2}$ (°C)	$\%\Delta H$
NK-2			
3000:1	0	1.2	63.2
1000:1	0	0.9	86.2
300:1	0	1.0	61.1
100:1	−0.5	1.9	55.9
NKCS			
3000:1	0	0.9	94.7
1000:1	−0.1	1.2	96.2
300:1	0.1	1.2	97.3
100:1	0	1.0	108.8

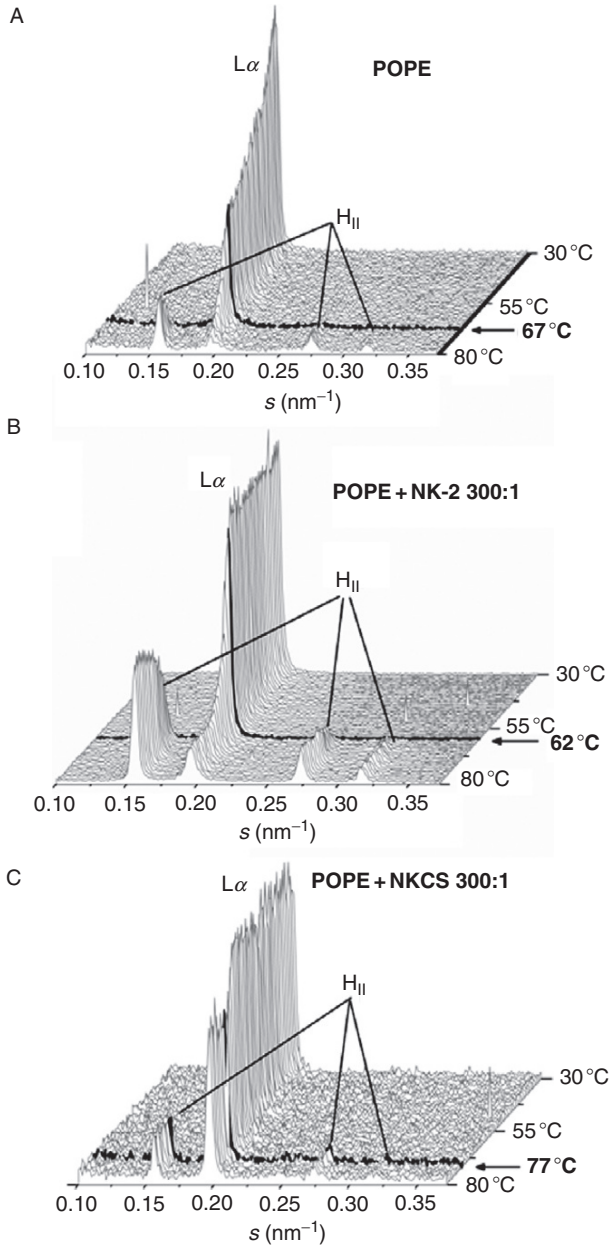

Figure 7 The scattering pattern of POPE (A), and POPE after the addition of NK-2 (B) and NKCS (C) at lipid:peptide molar ratio 300:1. Liquid crystalline (L_α) and inverse hexagonal (H_{II}) phases are indicated. Additionally H_{II} transition is highlighted. (A) and (C) reprinted from Ref. [64], copyright 2010, with permission from American Chemical Society.

the bilayer structure is even more pronounced: the temperature is shifted to 77 °C. The results suggest an inhibition of nonlamellar structures as a result of positive curvature induced in the membrane. As mentioned before, the positive curvature can be linked with the formation of toroidal pores in the bilayer. This mechanism requires, however, the membrane thinning as a prerequisite [70]. According to the results of SAXS, NKCS—similarly to NK-2—does not change the thickness. The repeat distance, established for pure POPE as 5.5 ± 0.9 nm at 37 °C, remains the same also after the addition of peptides.

Interesting results are obtained for the peptides interacting with PE liposomes composed of different acyl chains. The great example of how the hydrocarbon chains influence the biophysical properties of lipids is the temperature of transition from gel to liquid crystalline phase (T_m). According to SAXS results, the liquid disordered structure of POPE (acyl chain composition: 16:0–18:1) is visible already at 25 °C. The lipid DiPoPE (1,2-dipalmitoleoyl-*sn*-glycero-3-phosphoethanolamine), characterized by two identical unsaturated chains (16:1–16:1), undergoes this transition at −33.5 °C [71], whereas the lipid DOPE-*trans* (1,2-dielaidoyl-*sn*-glycero-3-phosphoethanolamine; 18:1–18:1) undergoes the same at 38 °C. The addition of peptides has an interesting effect and reveals that their influence on a bilayer structure strongly depends on the state of lipids at which the peptides are added. This effect is very pronounced for one of NKCS-derived peptides, namely NKCS-K17. When NKCS-K17 is added to DiPoPE at the room temperature (∼24 °C), at which the lipid exists in the liquid crystalline phase, the significant influence on the hexagonal phase transition is observed—the peptide shifts the temperature of this transition by 13 °C. A similar effect is observed for POPE. The peptide added on the edge of T_m also here causes the shift of 13 °C. Much lower influence is, however, observed in case of DOPE-*trans* (Table 4). At the room temperature, at which the peptide is mixed with the lipid, DOPE-*trans* remains in the gel phase. This state does not seem to facilitate the peptide–membrane interactions, which is reflected by lower influence of NKCS-K17 on the hexagonal phase transition.

AMPs usually remain randomly coiled in a hydrophilic aqueous solution, but adopt an ordered secondary structure in a membrane-mimetic environment. NK-2 and NKCS also behave in this way. These peptides adopt an α-helical conformation upon the interaction with the negatively charged phosphatidylglycerol (PG) liposomes mimicking the cytoplasmic membrane of *E. coli* [65]. However, they remain randomly coiled in the buffer and in the presence of zwitterionic POPC vesicles, chosen to build the cytoplasmic membrane of human erythrocytes. The circular dichroism (CD) spectroscopy results additionally underline the different behavior of NK-2 and NKCS toward the bacterial and human cytoplasmic membranes, proved already by SAXS measurements.

Table 4 The influence of NKCS-derived peptide (NKCS-K17) on the hexagonal phase transition of phosphatidylethanolamine lipids depends on the state of acyl chains at which the peptide is added

	Lipid		
	DiPoPE	POPE	DOPE-trans
T_m of pure lipids (°C)	−33.5	25.1	44.0
ΔT_H after the addition of NKCS-K17 (°C)	+13	+13	+5

The presented results were obtained for peptide:lipid molar mixtures 1:100, prepared at the room temperature, where DiPoPE exists in the liquid crystalline phase and POPE is on the edge of the phase transition.

5. Conclusions

The described case of NK-lysin derived peptides presents a fascinating example of two closely related molecules which exhibit completely different modes of action under interactions with the bacterial membrane. In their behavior, NK-2 and NKCS can be compared to the analogs of trichogin GA IV, lipopeptide isolated from the fungus *Trichoderma longibrachiatum* [72]. The two analogs, namely trichogin ST and trichogin BT, differ from each other at four amino acid positions. The changes influence their antimicrobial activity. Moreover, trichogin ST shifts the hexagonal phase transition temperature to higher values inducing the positive curvature in dipalmitoleoylphosphoethanolamine (DiPoPE) bilayers. In contrast, trichogin BT enhances the formation of negative curvature [73]. Although the mode of action of NK-2 and NKCS can be compared to the altered membrane interaction induced by trichogin ST and BT, the difference between these two NK-lysin derived peptides is even more subtle. Their 27 amino acid sequences differ only at one position. This seemingly insignificant change has the dramatic consequences on their interactions with *E. coli* membrane and the way they kill this bacterium. NK-2, promoting the negative curvature in the PE-enriched regions of the lipid bilayer, induces the changes in the membrane tension which eventually leads to the membrane disruption. NKCS stabilizes the bilayer structure, inhibiting the formation of nonlamellar forms. This may disturb the cell division process and functions of the membrane proteins and consequently lead to the suppression of bacterial growth. Such different modes of action of these two closely related peptides can be assigned to the high tendency of NK-2 to form aggregates. NK-2 and NKCS deliver the evidence that the mode of action can depend on very small changes within the sequence of peptides and it is very difficult to predict.

ACKNOWLEDGMENTS

We thank our former colleague Dr. Sebastian Linser for his assistance in the experimental part of this work and Dr. Dagmar Zweytick from the Institute of Biophysics and Nanosystems Research, Austrian Academy of Sciences in Graz for her help with DSC measurements.
This work was financially supported by the European Commission under the 6th Framework Program through the Marie-Curie Action: BIOCONTROL, contract number MCRTN–33439.

REFERENCES

[1] M.-C. Roghmann, L. McGrail, Novel ways of preventing antibiotic-resistant infections: what might the future hold? Am. J. Infect. Control 34 (2006) 469–475.
[2] S.B. Levy, Antibiotic resistance—the problem intensifies, Adv. Drug Deliv. Rev. 57 (2005) 1446–1450.
[3] M. Leeb, Antibiotics: a shot in the arm, Nature 431 (2004) 892–893.
[4] C. Nathan, Antibiotics at the crossroads, Nature 431 (2004) 899–902.
[5] H.G. Boman, Peptide antibiotics and their role in innate immunity, Annu. Rev. Immunol. 13 (1995) 61–92.
[6] R.E.W. Hancock, R. Lehrer, Cationic peptides: a new source of antibiotics, Trends Biotechnol. 16 (1998) 82–88.
[7] M. Zaiou, Multifunctional antimicrobial peptides: therapeutic targets in several human diseases, J. Mol. Med. 85 (2007) 317–329.
[8] R.E.W. Hancock, G. Diamond, The role of cationic antimicrobial peptides in innate host defences, Trends Microbiol. 8 (2000) 402–410.
[9] A. Tossi, L. Sandri, A. Giangaspero, Amphipathic, alpha-helical antimicrobial peptides, Pept. Sci. 55 (2000) 4–30.
[10] M. Zasloff, Antimicrobial peptides of multicellular organisms, Nature 415 (2002) 389–395.
[11] P. Bulet, R. Stöcklin, L. Menin, Anti-microbial peptides: from invertebrates to vertebrates, Immunol. Rev. 198 (2004) 169–184.
[12] T. Ganz, Defensins and host defense, Science 286 (1999) 420–421.
[13] K.L. Brown, R.E.W. Hancock, Cationic host defense (antimicrobial) peptides, Curr. Opin. Immunol. 18 (2006) 24–30.
[14] T. Baba, O. Schneewind, Instruments of microbial warfare: bacteriocin synthesis, toxicity and immunity, Trends Microbiol. 6 (1998) 66–71.
[15] H. Jenssen, P. Hamill, R.E.W. Hancock, Peptide antimicrobial agents, Clin. Microbiol. Rev. 19 (2006) 491–511.
[16] A. Giuliani, G. Pirri, S. Nicoletto, Antimicrobial peptides: an overview of a promising class of therapeutics, Cent. Eur. J. Biol. 2 (2007) 1–33.
[17] R.M. Epand, H.J. Vogel, Diversity of antimicrobial peptides and their mechanisms of action, Biochim. Biophys. Acta (BBA)—Biomembr. 1462 (1999) 11–28.
[18] M.R. Yeaman, N.Y. Yount, Mechanisms of antimicrobial peptide action and resistance, Pharmacol. Rev. 55 (2003) 27–55.
[19] R.E.W. Hancock, Peptide antibiotics, Lancet 349 (1997) 418–422.
[20] K.A. Brogden, Antimicrobial peptides: pore formers or metabolic inhibitors in bacteria? Nat. Rev. Microbiol. 3 (2005) 238–250.
[21] J.D.F. Hale, R.E.W. Hancock, Alternative mechanisms of action of cationic antimicrobial peptides on bacteria, Expert Rev. Anti Infect. Ther. 5 (2007) 951–959.

[22] J.M. Berg, J.L. Tymoczko, L. Stryer, Biochemistry, 5th ed., W. H. Freeman and Co, New York, 2002.
[23] S.J. Singer, G. Nicolson, The fluid mosaic model of the structure of cell membranes, Science 175 (1972) 720–731.
[24] A.G. Lee, How lipids affect the activities of integral membrane proteins, Biochim. Biophys. Acta (BBA)—Biomembr. 1666 (2004) 62–87.
[25] J.A. Killian, T.K.M. Nyholm, Peptides in lipid bilayers: the power of simple models, Curr. Opin. Struct. Biol. 16 (2006) 473–479.
[26] R.M. Epand, Membrane lipid polymorphism, Methods Membr. Lipids 400 (2007) 15–26.
[27] E. Sutherland, B.S. Dixon, H.L. Leffert, H. Skally, L. Zaccaro, F.R. Simon, Biochemical localization of hepatic surface-membrane Na+, K+-ATPase activity depends on membrane lipid fluidity, Proc. Natl. Acad. Sci. USA 85 (1988) 8673–8677.
[28] C. Le Grimellec, G. Friedlander, E.H.E. Yandouzi, P. Zlatkine, M.-C. Giocondi, Membrane fluidity and transport properties in epithelia, Kidney Int. 42 (1992) 825–836.
[29] R.A. Cooper, Influence of increased membrane cholesterol on membrane fluidity and cell function in human red blood cells, J. Supramol. Struct. 8 (1978) 413–430.
[30] O. Mouritsen, M. Zuckermann, What's so special about cholesterol? Lipids 39 (2004) 1101–1113.
[31] E. van den Brink-van der Laan, J. Antoinette Killian, B. de Kruijff, Nonbilayer lipids affect peripheral and integral membrane proteins via changes in the lateral pressure profile, Biochim. Biophys. Acta (BBA)—Biomembr. 1666 (2004) 275–288.
[32] G. Tresset, The multiple faces of self-assembled lipidic systems, PMC Biophys. 2 (2009) 3.
[33] M.W. Tate, E.F. Eikenberry, D.C. Turner, E. Shyamsunder, S.M. Gruner, Nonbilayer phases of membrane lipids, Chem. Phys. Lipids 57 (1991) 147–164.
[34] M. Luckey, Membrane Structural Biology: With Biochemical and Biophysical Foundations, Cambridge University Press, New York, 2008.
[35] G. Lindblom, L. Rilfors, Cubic phases and isotropic structures formed by membrane lipids—possible biological relevance, Biochim. Biophys. Acta (BBA)—Rev. Biomembr. 988 (1989) 221–256.
[36] K. Brandenburg, W. Richter, M.H.J. Koch, H.W. Meyer, U. Seydel, Characterization of the nonlamellar cubic and HII structures of lipid A from *Salmonella enterica* serovar Minnesota by X-ray diffraction and freeze-fracture electron microscopy, Chem. Phys. Lipids 91 (1998) 53–69.
[37] P.R. Cullis, B. De Kruijff, Lipid polymorphism and the functional roles of lipids in biological membranes, Biochim. Biophys. Acta (BBA)—Rev. Biomembr. 559 (1979) 399–420.
[38] W. Dowhan, M. Bogdanov, E. Mileykovskaya, E.V. Dennis, E.V. Jean, Functional roles of lipids in membranes, in: D.E. Vance, J.E. Vance (Eds.), Biochemistry of Lipids, Lipoproteins and Membranes. 5th ed., Elsevier, San Diego, 2008, pp. 1–37.
[39] T. Mares, M. Daniel, S. Perutkova, A. Perne, G. Dolinar, A. Iglic, M. Rappolt, V. Kralj-Iglic, Role of phospholipid asymmetry in the stability of inverted hexagonal mesoscopic phases, J. Phys. Chem. B 112 (2008) 16575–16584.
[40] S. Perutková, M. Daniel, G. Dolinar, M. Rappolt, V. Kralj-Iglic, A. Iglic, Stability of the inverted hexagonal phase, in: A. Leitmannova Liu (Ed.), Advances in Planar Lipid Bilayers and Liposomes, Vol. 9, Academic Press, Oxford, UK, 2009, pp. 237–278; Chapter 9.
[41] P.C. Noordam, C.J.A. van Echteld, B. de Kruijff, A.J. Verkleij, J. de Gier, Barrier characteristics of membrane model systems containing unsaturated phosphatidylethanolamines, Chem. Phys. Lipids 27 (1980) 221–232.
[42] M. Bogdanov, J. Sun, H.R. Kaback, W. Dowhan, A phospholipid acts as a chaperone in assembly of a membrane transport protein, J. Biol. Chem. 271 (1996) 11615–11618.

[43] B.d. Kruijff, Lipid polymorphism and biomembrane function, Curr. Opin. Chem. Biol. 1 (1997) 564–569.
[44] D.P. Siegel, R.M. Epand, The mechanism of lamellar-to-inverted hexagonal phase transitions in phosphatidylethanolamine: implications for membrane fusion mechanisms, Biophys. J. 73 (1997) 3089–3111.
[45] E.F. Haney, S. Nathoo, H.J. Vogel, E.J. Prenner, Induction of non-lamellar lipid phases by antimicrobial peptides: a potential link to mode of action, Chem. Phys. Lipids 163 (2010) 82–93.
[46] J.-P.S. Powers, A. Tan, A. Ramamoorthy, R.E.W. Hancock, Solution structure and interaction of the antimicrobial polyphemusins with lipid membranes, Biochemistry 44 (2005) 15504–15513.
[47] A. Angelova, R. Ionov, M.H.J. Koch, G. Rapp, Interaction of the peptide antibiotic alamethicin with bilayer- and non-bilayer-forming lipids: influence of increasing alamethicin concentration on the lipids supramolecular structures, Arch. Biochem. Biophys. 378 (2000) 93–106.
[48] R. El Jastimi, M. Lafleur, Nisin promotes the formation of non-lamellar inverted phases in unsaturated phosphatidylethanolamines, Biochim. Biophys. Acta (BBA)—Biomembr. 1418 (1999) 97–105.
[49] C.J.A. Van Echteld, R. Van Stigt, B. De Kruijff, J. Leunissen-Bijvelt, A.J. Verkleij, J. De Gier, Gramicidin promotes formation of the hexagonal HII phase in aqueous dispersions of phosphatidylethanolamine and phosphatidylcholine, Biochim. Biophys. Acta (BBA)—Biomembr. 648 (1981) 287–291.
[50] J.A. Szule, R.P. Rand, The effects of gramicidin on the structure of phospholipid assemblies, Biophys. J. 85 (2003) 1702–1712.
[51] K. Matsuzaki, K.-i. Sugishita, N. Ishibe, M. Ueha, S. Nakata, K. Miyajima, R.M. Epand, Relationship of membrane curvature to the formation of pores by magainin 2, Biochemistry 37 (1998) 11856–11863.
[52] K.A. Henzler Wildman, D.-K. Lee, A. Ramamoorthy, Mechanism of lipid bilayer disruption by the human antimicrobial peptide, LL-37, Biochemistry 42 (2003) 6545–6558.
[53] K. Lohner, E.J. Prenner, Differential scanning calorimetry and X-ray diffraction studies of the specificity of the interaction of antimicrobial peptides with membrane-mimetic systems, Biochim. Biophys. Acta (BBA)—Biomembr. 1462 (1999) 141–156.
[54] Y. Shai, Mechanism of the binding, insertion and destabilization of phospholipid bilayer membranes by [alpha]-helical antimicrobial and cell non-selective membranelytic peptides, Biochim. Biophys. Acta (BBA)—Biomembr. 1462 (1999) 55–70.
[55] M. Andersson, H. Gunne, B. Agerberth, A. Boman, T. Bergman, R. Sillard, H. Jornvall, V. Mutt, B. Olsson, H. Wigzell, A. Dagerlind, H.G. Boman, et al., NK-lysin, a novel effector peptide of cytotoxic T-cells and NK-cells—structure and cDNA cloning of the porcine form, induction by interleukin-2, antibacterial and antitumour activity, EMBO J. 14 (1995) 1615–1625.
[56] R.S. Munford, P.O. Sheppard, P.J. O'Hara, Saposin-like proteins (SAPLIP) carry out diverse functions on a common backbone structure, J. Lipid Res. 36 (1995) 1653–1663.
[57] C.M.A. Linde, S. Grundstrom, E. Nordling, E. Refai, P.J. Brennan, M. Andersson, Conserved structure and function in the granulysin and NK-lysin peptide family, Infect. Immun. 73 (2005) 6332–6339.
[58] E. Liepinsh, M. Andersson, J.-M. Ruysschaert, G. Otting, Saposin fold revealed by the NMR structure of NK-lysin, Nat. Struct. Mol. Biol. 4 (1997) 793–795.
[59] J. Andra, M. Leippe, Candidacidal activity of shortened synthetic analogs of amoebapores and NK-lysin, Med. Microbiol. Immunol. 188 (1999) 117–124.

[60] T. Jacobs, H. Bruhn, I. Gaworski, B. Fleischer, M. Leippe, NK-Lysin and its shortened analog NK-2 exhibit potent activities against *Trypanosoma cruzi*, Antimicrob. Agents Chemother. 47 (2003) 607–613.
[61] C. Gelhaus, T. Jacobs, J. Andra, M. Leippe, The antimicrobial peptide NK-2, the core region of mammalian NK-Lysin, kills intraerythrocytic *Plasmodium falciparum*, Antimicrob. Agents Chemother. 52 (2008) 1713–1720.
[62] H. Schröder-Borm, R. Bakalova, J. Andrä, The NK-lysin derived peptide NK-2 preferentially kills cancer cells with increased surface levels of negatively charged phosphatidylserine, FEBS Lett. 579 (2005) 6128–6134.
[63] H. Schröder-Borm, R. Willumeit, K. Brandenburg, J. Andrä, Molecular basis for membrane selectivity of NK-2, a potent peptide antibiotic derived from NK-lysin, Biochim. Biophys. Acta (BBA)—Biomembr. 1612 (2003) 164–171.
[64] Y. Gofman, S. Linser, A. Rzeszutek, D. Shental-Bechor, S.S. Funari, N. Ben-Tal, R. Willumeit, Interaction of an antimicrobial peptide with membranes: experiments and simulations with NKCS, J. Phys. Chem. B 114 (2010) 4230–4237.
[65] J. Andra, D. Monreal, G.M. de Tejada, C. Olak, G. Brezesinski, S.S. Gomez, T. Goldmann, R. Bartels, K. Brandenburg, I. Moriyon, Rationale for the design of shortened derivatives of the NK-lysin-derived antimicrobial peptide NK-2 with improved activity against Gram-negative pathogens, J. Biol. Chem. 282 (2007) 14719–14728.
[66] H. Raghuraman, A. Chattopadhyay, Melittin: a membrane-active peptide with diverse functions, Biosci. Rep. 27 (2007) 189–223.
[67] G.F. Ames, Lipids of *Salmonella typhimurium* and *Escherichia coli*: structure and metabolism, J. Bacteriol. 95 (1968) 833–843.
[68] J.A. Virtanen, K.H. Cheng, P. Somerharju, Phospholipid composition of the mammalian red cell membrane can be rationalized by a superlattice model, Proc. Natl. Acad. Sci. USA 95 (1998) 4964–4969.
[69] R. Willumeit, M. Kumpugdee, S.S. Funari, K. Lohner, B.P. Navas, K. Brandenburg, S. Linser, J. Andrä, Structural rearrangement of model membranes by the peptide antibiotic NK-2, Biochim. Biophys. Acta (BBA)—Biomembr. 1669 (2005) 125–134.
[70] K. Lohner, E. Sevcsik, G. Pabst, Liposome-based biomembrane mimetic systems: implications for lipid–peptide interactions, in: A. Leitmannova Liu (Ed.), Advances in Planar Lipid Bilayers and Liposomes, Vol. 6, Academic Press, 2008, pp. 103–137; Chapter 5.
[71] P.W.M. Van Dijck, B. De Kruijff, L.L.M. Van Deenen, J. De Gier, R.A. Demel, The preference of cholesterol for phosphatidylcholine in mixed phosphatidylcholine-phosphatidylethanolamine bilayers, Biochim. Biophys. Acta (BBA)—Biomembr. 455 (1976) 576–587.
[72] C. Auvin-Guette, S. Rebuffat, Y. Prigent, B. Bodo, Trichogin A IV, an 11-residue lipopeptaibol from *Trichoderma longibrachiatum*, J. Am. Chem. Soc. 114 (1992) 2170–2174.
[73] R.F. Epand, R.M. Epand, F. Formaggio, M. Crisma, H. Wu, R.I. Lehrer, C. Toniolo, Analogs of the antimicrobial peptide trichogin having opposite membrane properties, Eur. J. Biochem. 268 (2001) 703–712.

Acknowledgements

I am very grateful to Prof. Regine Willumeit for her supervision and for giving me the opportunity to work in the interesting field of peptide-membrane interactions. I want to thank her for her guidance, advice and all constructive discussions.

I want to thank Dr. Sebastian Linser for the introduction to the topic of antimicrobial peptides and biophysical techniques, for his patience and encouragement.

I thank Dr. Frank Feyerabend for promoting friendly work atmosphere in the lab, for his support and invaluable feedback.

I sincerely appreciate scientific and mental support from Dr. Vasyl Haramus, especially his help with the small angle scattering techniques.

I give a special thank to Dr. Anna Schuster for her friendliness, suggestions and encouragement.

Many of the results were obtained with the collaboration with other institutes. I want to express my gratitude to

- Prof. Vincent Raussens from Université Libre de Bruxelles for the help with FTIR measurements, for all the discussions and friendly support
- Prof. Beate Klösgen from Southern University of Denmark for the help with SAXS measurements and valuable advices regarding the DSC experiments
- Dr. Karl Lohner from Austrian Academy of Science in Graz for the inspiring discussions concerning my SAXS and DSC results
- Dr. Sergio S. Funari from HASYLAB/DESY in Hamburg for the support during my work at the beamline, for his patience and help with all my questions.

Without the support and motivating atmosphere in the group of Structural Research on Macromolecules at HZG this work would not have been possible. I owe my thanks to all current and former colleagues: Farida Ali, Dr. Borislav Angelov, Kevin Brown, Anna Burmester, Axel Deing, Tie Di, Dr. Artem Feoktystov, Janine Fischer, Yana Gofman, Maksym Golub, Plamen Iliev, Nadège Lambert-Benoit, Daniela Lange, Sandra Lazaroski, Tao Li, Dr. Bérengère Luthringer, Birte Mucha, Wilhelm Müller, Rama Nunberg, Ravi Ramchal, Jessica Rutz, Elżbieta Rzeszutek, Gabriele Salamon, Lili Wu and Lei Yang.

I want to give also a special acknowledgement to Marie Curie Research Training Network BIOCONTROL for a friendly and inspiring atmosphere during all our workshops and assemblies.

I thank my family and friends for their patience and support during my studies. I want to express my deep gratitude to Claudio, because his encouragement helped me to finish this thesis.